The copyright of this thesis vests in the author. No quotation from it or information derived from it is to be published without full acknowledgement of the source. The thesis is to be used for private study or non-commercial research purposes only.

Published by the University of Cape Town (UCT) in terms of the non-exclusive license granted to UCT by the author.

University of Cape Town

A Thermo-Mechanical Finite Element Simulation of Hot Rolling for the Prediction of Roll Forces

By Gareth Floweday

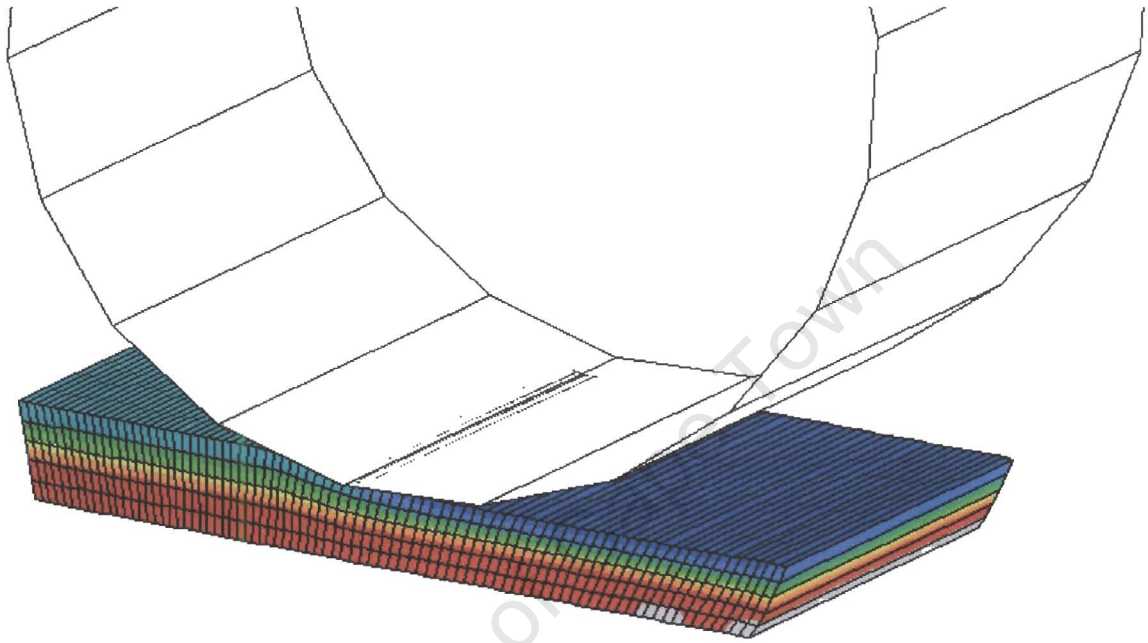

A thesis submitted to the Faculty of Engineering and the Built Environment of the University of Cape Town, in partial fulfilment of the degree of Master of Science in Mechanical Engineering.

University of Cape Town

Centre for Materials Engineering
Department of Mechanical Engineering
University of Cape Town

September 2001

Declaration

I, Gareth Floweday, hereby declare that the work in this thesis project is essentially my own work and that no part of it has been submitted for a degree at any other university.

I further declare that this work is presented with full integrity with regard to the presentation of its results and that values obtained have not been altered in any way.

I empower the University of Cape Town to reproduce for the purpose of research, either the whole, or any portion of this contents in any manner whatsoever.

Signed .....

Date: .....

University of Cape Town

Dedication

I would like to dedicate this work to my father, who died of cancer during these studies. He was the one who inspired my interest in engineering as a child and worked hard to ensure that my studies were paid for even before I started engineering. He was never scared of hard work and I know that he would have been proud to see this work come to completion.

University of Cape Town

Acknowledgements

I would like to thank the following people for their help and support in producing this thesis project:

Professor Robert Knutsen, for his materials expertise, solid guidance with the materials science of the project and for his organisation of the opportunity to do the material testing at Birmingham University.

Mr Hellmut Bowles, for his patience and help with the numerical work in the project.

Doctor Claire Davis from the School of Metallurgy at the University of Birmingham, for her willingness to host and oversee the material testing and for her help in overcoming the many problems encountered with the Gleeble 3500.

Mr Len Watkins and Glen Newins, for their hard work in the workshops to produce the specimens for use in the compression testing.

Dr Janet Basson, for her support and help with mechanical and electro-polishing, as well as the electron microscope.

Columbus Stainless (Mpumalanga, RSA) for initiating and sponsoring the project.

The National Research Foundation (Pretoria, RSA) and the University of Cape Town Research Committee (UCT-URC) for the provision of financial support.

My wife Clare for her unfailing support and help with the testing in Birmingham.

God, the creator of heaven and earth, for His grace in giving me the opportunity to study and for His wisdom and perspective in issues of life.

University of Cape Town

Abstract

The main objective of this project was to provide Columbus Stainless (Mpumalanga, RSA) with a numerical simulation model that would be able to accurately predict roll forces in the roughing mill. The material used in the model is AISI 304 stainless steel.

In order to model the material flow stress accurately, uniaxial compression testing was conducted in the temperature range of 800-1250°C at intervals of 50°C. The strain rates tested were 35, 10, 3.5, 1.0, 0.35, 0.1, 0.01s^{-1} and each temperature was tested within each strain rate. Stress curves were fitted to an equation to give stress as a function of strain, strain rate and temperature.

The model was constructed as a 2D, seven pass thermo-mechanical model using Abaqus Explicit version 6.2.1. The billet was modelled using *6250*, 4 noded plane strain elements. The model used a basic Coulomb Friction model with a specified maximum value of friction before shearing of the billet material took place. The roller was modelled as a rigid body.

The rolling simulation took into account the through thickness distribution of temperature, strain and strain rate in the roll gap in order to accurately model the flow stress of the material. In order to define the temperature in the roll gap, the convection, conduction and radiation heat transfer to rollers, coolants, descaler sprays and general environment was taken into account throughout the simulation. Heat generated by plastic work and heat generation due to sliding friction between the roller and billet was also included.

The effects of variation of parameters in the simulation was shown and roll forces compared to those obtained on the rougher mill at Columbus Stainless. Microstructural changes such as static recovery and recrystallisation were not taken into account in this project.

The sensitivity of the roll force prediction to many of the physical sub-models (e.g. friction and contact algorithms) and variables within the model, mean that at this stage, the model is not in itself a reliably accurate tool for roll force prediction in the development of new roll schedules. However, the simulation does demonstrate an ability to accurately model the physical behaviour of the material and with further research into some of the physical phenomena affecting roll force prediction, should become a vital tool in the understanding and prediction of many aspects of the hot rolling process.

University of Cape Town

Table of Contents

University of Cape Town

List of Tables and Figures

Page

University of Cape Town

University of Cape Town

Chapter 1: Introduction

With the increasing development of software used in mechanical modelling, rolling simulations have become a valuable tool to steel producers for prediction of material behaviour, roll forces, coolant requirements, as well as geometry control systems.

At the time of commencement of this project, Columbus did not have an accurate method for predicting the forces on rollers in the rougher mill. They merely used a progression of empirically based equations and experience from rolling schedules as a guide for force prediction.

The main objective of this project was to provide Columbus Stainless Steel with a numerical simulation model (using Abaqus Explicit version 6.2.1) that would be able to accurately predict roll forces in the rougher mill. This would aid the control of roll bending in order to produce more steel within required specification and lower the average geometric gauge toward the lower bound of the specification, thereby reducing cost. Further aims are to refine this model to include data output of thermal, strain and strain rate histories that could be used as input into a microstructure prediction model.

University of Cape Town

The rolling simulation takes into account the through thickness distribution of temperature, strain (see figure below) and strain rate in the roll gap in order to accurately model the flow stress of the material. The material used in the model is AISI 304 stainless steel. In order to define the temperature in the roll gap, the convection, conduction and radiation heat transfer to rollers, coolants, descaler sprays and general environment is taken into account throughout the simulation. Once the thermal and mechanical properties of the material have been accurately modelled and validated, the simulation can be used as the foundation for microstructural evolution research.

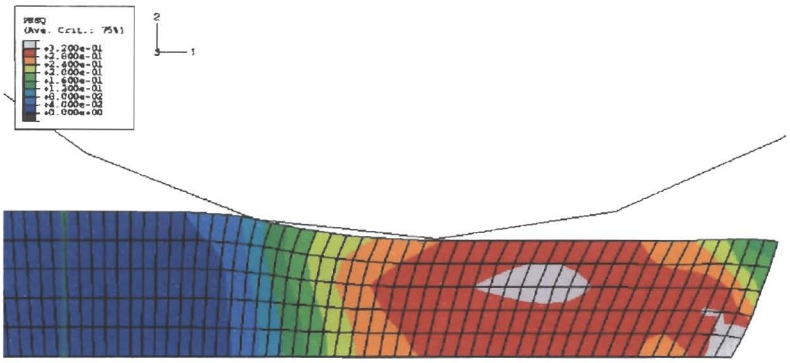

Fig 1.1: Plot showing strain distribution during hot rolling

Note: The roller is mathematically circular although Abaqus 6.2.1 does not render it as such.

Chapter 2: Process Description

In order to accurately model an industrial process, it is important to have a good understanding of the process practice. Columbus Stainless do both hot and cold rolling processes to produce a wide range of austenitic and ferritic stainless steels.

The hot rolling process begins with the melting of the raw material (scrap iron, ferro-chrome, nitrogen , ferro-silicon, ferro-molybdenum, manganese, lime etc) in the electric arc furnace. At this stage some liquid metal is allowed to solidify and is analysed in the chemical laboratory.

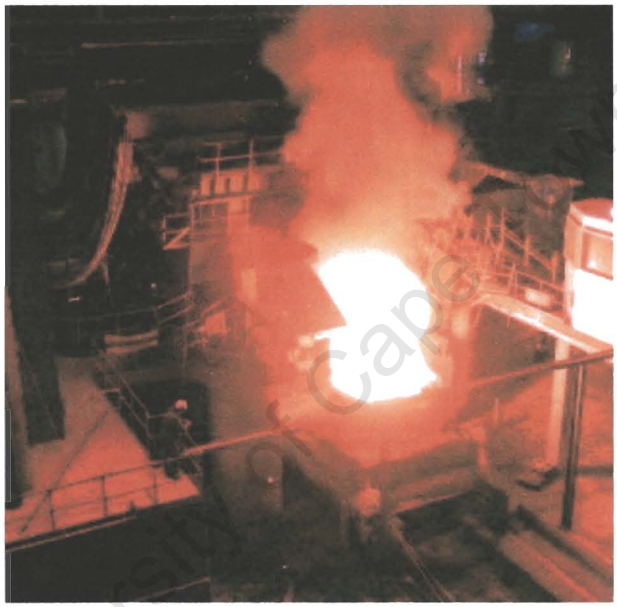

Fig 2.1: Tapping an Arc Furnace

University of Cape Town

The molten metal is then taken through a CLU (Cruessot, Loire, Uddeholm) converter. In the CLU super heated steam is used as a source of oxygen. The steam is blown into the CLU via openings situated in the floor of the CLU vessel. The oxygen reacts with the carbon in the steel and forms carbon monoxide and carbon dioxide. By doing this the carbon in the steel is lowered to the required levels. This is an exothermic reaction and the bath heats up during blowing. During this process, more raw material will be added to bring the chemistry closer to the aim ranges. After blowing, levels of chromium in the slag are high, having oxidised during the oxygen blowing. Once the carbon is at the required level the slag is reduced by adding silicon, which releases chromium from the slag. After this, blowing is completed using pure argon to remove oxides and to adjust the carbon levels.

From here it is sent through the rinse station. At the rinse station argon is bubbled through the steel from an opening in the bottom. This is a gentle process to float out any inclusions (pieces of metal oxides which are solid at high temperature). The secondary function is to bring the temperature within a range of super heat just above the solidification point (i.e. cooling the steel). Final raw material additions in very pure form are made to make final adjustments to the chemistry.

The molten metal is poured into a vertical continuous caster. The caster is a water cooled copper mould which cools the metal, forming a slab. As the outer shell of the slab solidifies (with the middle still molten), the slab is bent through 90 degrees and rolls onto the roller table where it is cut by the crop shear into manageable lengths, cools further and is surface ground by the slab grinder.

When an AISI 304 stainless slab is needed for rolling, it is first heated to 1240^0C in the reheat furnace, before passing through descaling sprayers. The slab is then fed into the two-high rougher mill, which reduces the gauge thickness from 202mm to approximately 23mm in seven passes. Edge rollers are also used on the first and third passes to introduce an edge profile that minimises alligator cracking of the edges.

The strip is then fed into the Steckel mill which reduces the gauge thickness required (2.5mm minimum). This mill coils the strip between passes and has front and back tension to help control wrinkling. The strip is then cooled and coiled, and is either sent to the packing line, annealed, cleaned and cut, or sent to the cold rolling process line.

University of Cape Town

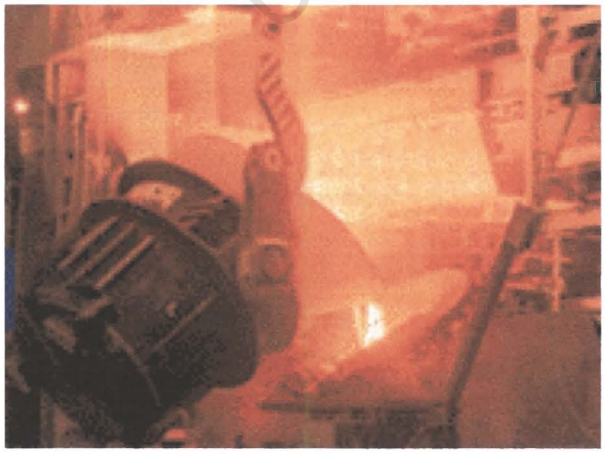

Fig 2.2: Pouring into the Continuous Castor

Fig 2.3: Columbus' Hot Rougher Mill

Chapter 3: Explanation of Finite Element Method

The Finite Element Method is a numerical technique used for analysing structures and continua. It is often used to obtain an approximate solution in cases far too complicated to analyse analytically.

Finite element methods have been used for numerical work for many years and have grown in application, effectiveness and complexity, along with the technological advances allowing more computationally expensive problem solving. They are traditionally used for complex stress analysis, but have also been used to solve problems involving heat transfer and fluid flow problems.

The basic steps in the Finite Element Method used for stress analysis are as follows:

1. The domain is divided or discretised into a mesh of small blocks or elements. If the object is studied in 3 dimensions, these elements may be brick, tetrahedral, shell, beam or truss elements. If the object is studied only in two dimensions, these elements may be rectangular, triangular, beam or truss elements.

2. The equations relating force to acceleration, velocity and displacement are formulated for each element in each degree of freedom. This requires knowledge of the geometry of the element and the constitutive laws governing the behaviour of the material under the general type of loading conditions.

   The basic element equation is the Hooke's Law expression

   $$\underline{dF} = [K_{elm}]\,\underline{dx}$$

   where $\underline{F}$ is the vector containing the loads and forces on the element for each degree of freedom, $\underline{x}$ is the displacement vector, and $[K_{elm}]$ is the element stiffness matrix, given by the equation:

   $$[K_{elm}] = \int [B]^T [D][B] dV$$

   Where $[D]$ is the material stiffness matrix and $[B]$ is the strain-displacement matrix.

University of Cape Town

3. The equations for all the elements are assembled into a large system of equations in the global co-ordinate system.

4. Boundary and load conditions are applied. These may include pressures, point loads, fixed supports, pivoting supports and reaction forces of various kinds.

5. The system of simultaneous linear equations is then solved numerically. The response may be non-linear, due to non-linear plastic deformation, transient contact conditions or dynamic geometry.

6. Post processing is done to calculate other variables and draw deformed shapes, contour plots and graphs.

University of Cape Town

Since the method was applied to a metal forming process, a numerical elasto-plastic model was used. This model is based on the equation:

$$\dot{\underline{\varepsilon}} = \dot{\underline{\varepsilon}}^{el} + \dot{\underline{\varepsilon}}^{pl}$$

Where the material strain rate ($\dot{\underline{\varepsilon}}$) is decomposed into elastic and plastic contributions.

This equation, when integrated over a time step Δt, gives:

$$\Delta\underline{\varepsilon} = \Delta\underline{\varepsilon}^{el} + \Delta\underline{\varepsilon}^{pl}$$

The numerical plasticity model introduces a yield function, which defines when plastic deformation takes place at a specific material point:

$$f(\sigma,\varepsilon,T) = \sqrt{\frac{1}{3}J_2} - K$$

Where J_2 is the second invariant of the deviatoric stress state, and K defines the current material flow stress state. Note that the yield is a function of stress (σ), strain (ε) and temperature (T).

The increment in plastic strain is computed using the following equation:

$$\Delta\underline{\varepsilon}^{pl} = \Delta\lambda \frac{\delta g}{\delta \underline{\sigma}}$$

Where $\Delta\lambda$ is the scalar equivalent plastic strain increment, g is the flow potential, and $\frac{\delta g}{\delta \underline{\sigma}}$ defines the flow direction.

The stress at the material; point is defined by the elastic strain only, according to the following equation:

$$\underline{\sigma} = [D]\underline{\varepsilon}^{el}$$

This stress is updated at each increment and/or iteration using the equation:

$$\underline{\sigma}_{new} = \underline{\sigma}_{old} + [D]\left(\Delta\underline{\varepsilon} - \Delta\underline{\varepsilon}^{pl}\right)$$

The Finite Element Method can be divided into two approaches:

The Lagrangian Approach, in which the material of the object is meshed and the position of the material is shown by the position of the nodes and elements of the mesh. These positions are updated incrementally with each time step. This approach can be likened to an object constructed from small blocks of differently coloured plasticine. When the object is deformed, the deformation in each area can be studied by the deformation of each plasticine block.

The Eulerian Approach, where the space occupied by the object is meshed with a mesh that is fixed in space. The material is then modelled as a non-Newtonian fluid that flows through the fixed mesh. The velocity field is then calculated at the nodes. This approach is used for steady state analyses. The approach can be likened to pouring mud through a roll of chicken wire mesh.

Finite Element analyses can further be divided into Implicit and Explicit analyses.

Implicit analysis solves the equilibrium equation

$$\Psi = F_{ext} - F_{\text{int}} = 0$$

using Newton Raphson methods in an incremental-iterative procedure. Implicit analysis is unconditionally stable with respect to the time step that may be taken. However, implicit analysis requires convergence (obtained through incremental time stepping) within each time iteration before moving forward to the next time iteration. This produces good accuracy, but in cases of complex, highly non linear response, can cause the time step to become very small, making the analysis very computationally expensive and often failing to converge at all.

University of Cape Town

Explicit analysis can be used in cases where the mass matrix is a lumped mass matrix and the coupled system of equations can be uncoupled, using explicit time integration, and solved separately. This is very efficient computationally, but is only numerically stable for the following time step size:

Stability condition: $\Delta t < \frac{l}{c}$

Where: l = shortest effective element length.

c = Speed of sound in the material.

Note that: $c = \sqrt{\frac{E}{\rho}}$

Where: E = Young's modulus for the material

ρ = Density of the material.

Reducing the time step causes the analysis to become computationally expensive. A fine mesh yields a low value for l, thus making the analysis computationally expensive. A common practice is to artificially increase the density of the material so as to increase the critical time step. This is called mass scaling, and can only be used up to the point where artificial inertia effects start to decrease the accuracy of the analysis. A useful check to monitor the contribution of inertia effects to the solution, is to plot the kinetic and internal energy of the system over the analysis time. If the kinetic energy (which is affected by the density increase) is raised above 5% of the internal energy (which is not affected by the density increase), then inertia effects play a significant role in the solution.

University of Cape Town

Chapter 4: Review of Research in Literature

Conducting a literature review for a subject such as hot rolling is a difficult thing to do for a number of reasons. Firstly, hot rolling has a long history, beginning right at the beginning of the steel industrial revolution where hot rolling took over from the steam hammer which was used from 1850-1860. The first rolling mill was an iron rail mill, built in Port Talbot, Wales, 1851. The first 3 high mill was built in the 1820s, but was only generally used after 1850, when bearings and gear drive technology improved the mill's precision. The first coiling mill was built in 1923 in the U.S.A.

The second reason for complexity is that due to the time and technology that has been poured into this area, the published information on various aspects of hot rolling is vast and diverse. This review tries to give an overview of work on the subject and concentrates on the areas which have particular impact on this project.

The literature reviewed falls into five main categories:

1. Hot rolling as a metallurgical process
2. Numerical modelling of hot rolling in general
3. Material testing, microstructural considerations and empirical models.
4. Thermo-mechanics of hot rolling
5. Friction models in rolling simulations
6. Experimental procedures for validation of modelling
7. Control of rolling systems.

University of Cape Town

1. Hot rolling as a metallurgical process

Because hot rolling has been used as a forming process for many years, review papers give a useful overview. Hartley *et al.* [1] put together a comprehensive review of the 100 odd year history of scientific studies into metal rolling, from the first recorded research by Hollenberg in 1883 to the date of writing in 1989. The paper references some 134 publications and is a significant contribution to rolling knowledge.

The paper discusses the various techniques and procedures used in experimental work to study metal flow, stresses and strain distribution in rolling. Less common techniques such as caustic, photoelastic, visioplastic and pressure pin methods are included.

Theoretical analyses start with plane strain homogeneous models and progress to modelling inhomogeneity. Studies of deformation distribution, slip line fields and upper bound methods are also discussed. Finite element models of various forms are reviewed along with the complexities of thermal modelling, roll deformation, friction conditions and accurate material characterisation.

In concluding the summary of the paper, Hartley *et al* state the following:

> "Both the analytical and numerical methods described here depend on a knowledge of the material constitutive relation (stress-strain curves for different strain rates and temperatures). While there is a large amount of information available, it is rarely for the material under consideration, over the appropriate range of strain rate and temperature, especially for hot rolling. There is then, a large amount of work to be done purely on generating suitable material property data, especially for the more detailed numerical models. These, and other areas such as dynamic effects, are in need of further attention."

Other reviews are far more specific in subject. Guerrero *et al.* [2] did a survey of numerical models for characterising the heat flow to and from the work rolls during hot rolling. The aim of the research was to gain a better understanding in this area for the prediction of thermal fatigue, roll surface wear and the effect of thermal expansion on roll radius and therefore roll gap control.

J.N. Harris' book [3] is an excellent foundational resource on metal working. The author outlines the basics of metallurgy, material behaviour and testing. Deformation under complex stress systems and theories of failure are also covered.

The author claims that the fraction of energy converted to heat during plastic deformation is 95%, and shows that yield stress under plane strain constraint is about 15% greater than the homogeneous yield stress.

Harris summarises the principal mechanical working processes of rolling, deep drawing, pressing, forging, stretch forming, extrusion and wire drawing as well as examining the differences between hot and cold working. The author then examines each process in more

University of Cape Town

detail, deriving basic formulae, giving an overview of history and methods and providing some worked examples with experimental flow stress data from literature.

In the chapter on rolling of steel, the author shows that the coefficient of friction, $\mu = \tan(\theta_{max})$ where θ is the angle of arc of contact. The author also shows that:

$\tan\theta_{max} = \frac{\sqrt{R\Delta h_{max}}}{R - (\Delta h_{max}/2)}$ where R is the roll radius and Δh_{max} is the maximum reduction that the mill can do before rejection occurs.

Harris shows that if the ratio of slab width, $W : \sqrt{R\Delta h}$ is greater than 5:1 , then strain in the width direction is negligible, its effect on the rolling loads is negligible and the process can be assumed to be under plane strain conditions.

Harris shows two formulations of roll load (with and without friction considerations), with the following assumptions:

1. Constant friction coefficient μ.
2. Homogeneous perfectly plastic strain distribution in the roll gap.
3. Plane strain conditions.
4. Ridged rollers

Friction ignored: Roll Load, $F = \sigma_0^* . W\sqrt{R\Delta h}$ where σ_0^* is the constrained yield stress. $\sigma_0^* = \frac{2}{\sqrt{3}}\sigma \approx 1.155\sigma$

Sliding Friction: $F = \sigma_0^* . W\sqrt{R\Delta h}.\left[1 + \frac{\mu\sqrt{R\Delta h}}{2(h_1 - \{\Delta h/2\})}\right]$

Sticking Friction: $F = \sigma_0^* . W\sqrt{R\Delta h}.\left[1 + \frac{\sqrt{R\Delta h}}{4(h_1 - \{h/2\})}\right]$

Where: $h = h_{mean} = h_1 - \Delta h/2$

These equations show that by increasing the coefficient of friction for a given geometry, the rolling load is increased. The author also shows that by including elastic roll flattening effects (Hitchcock approach), the predicted roll load is slightly greater.

University of Cape Town

Many general rolling models have been formulated with different focuses. Zaharoff *et al.* [4] did some work looking at the transverse deformation (spread) of metal in a single stand rolling process. They did a comparison of results obtained using empirical, numerical and experimental methods.

Their Empirical Asymptotic Model assumes homogeneous deformation through thickness and thus deviates from experimental results as the thickness of the slab increases. Friction on the roll – slab interface is assumed to be proportional to relative velocity, i.e. the friction is assumed to be hydrodynamic. The model was simplified by assuming zero entry and exit tension. This model showed that spread is primarily related to the ratio of half width to roll bite length and reduction.

Their Numerical Lateral Flow Model is a basic quasi 3-dimensional finite element rolling model. Only one layer of elements is used through half the sheet thickness and similar kinematic assumptions are used as the empirical model above. In spite of the gross simplification of a single element layer, the model incorporates deformable rolls, some thermal capabilities and various constitutive and interface models.

Their experimental methods consisted of the hot rolling of steel and aluminium, and the cold rolling of pure lead. Different reductions, thickness to width ratios and lubricants were used and then compared to the empirical and numerical models. The agreement was good for thin plate up to reductions of 30%, after which the results diverged.

Since the rolling process is not limited to flat strip rolling, other types of rolling were also considered. Jiang *et al.* [5] formulated a finite element model to simulate the ribbed strip rolling process in order to gain better understanding of the influence of rolling parameters on the "pull down" effect encountered in this type of rolling.

The material (carbon steel) was modelled as a "slightly compressible", rigid visco-plastic type with thermal dependence. The strip was modelled with ½ symmetry and quite coarsely meshed although the friction model was quite intricate.

University of Cape Town

The results from the simulation were compared to measured values and a number of useful conclusions were drawn regarding the parameters which most affect the variation and severity of "pull down" of rib heights. This could lead to better design of rolls used in this operation.

Numerical simulations are often used as tools for predicting roll forces, however this is not the only mathematical method available. S. Nishino *et al.* [6] used an entirely different approach to predicting roll forces. Their method is a purely mathematical model that starts with an educated guess for the yield stress, calculates the roll force for the first pass, compares it to the measured roll force for that pass and then calculates a correction factor with which the yield stress is multiplied before the 2nd pass roll force is calculated. This process is used throughout the rougher and finishing mill, and can be used for an entire lot (batch of slabs of similar alloy), in order to "learn" the yield stresses and roll forces with increasing accuracy.

The rolling load model combines a rule identification method based on a hierarchical clustering analysis and an adaptive method, based on the recursive least squares method.

The paper claims to correct the ratio of actual roll force to predicted roll force, to 1.0, with a standard deviation of 6%, compared to conventional adaptive methods which are typically in the order of 1.1 and 10%. The model seems to work well and does so at very low cost, however it is in a sense a "blind" method, since it has no intrinsic understanding of the details and complexities in the rolling process and therefore cannot be broadened to include shape control, roll bending prediction, ambient conditions effects and microstructural evolution.

Another factor crucial to the whole subject of hot rolling is the emerging technology of thin strip casting. There seems to be an increasing lean towards the implementation of unequal diameter twin roll strip casting, which does the job of the continuous caster and hot rougher mill in one process, at a greatly reduced energy and capital cost. This process works by pouring molten steel between two water cooled rollers which cool the material between them and impose slight deformation, to produce thin sheets. A relatively homogeneous microstructure is produced in steel sheet, which is thin enough to be coiled and sent for descaling before cold rolling.

Raabe [7] studied the texture and microstructure evolution during cold rolling of a strip cast and of a hot rolled stainless steel, and made comparisons of the microstructural aspects of these two processes. The hot rolled steel showed a homogeneous microstructure and a weak

University of Cape Town

orientation distribution with slight texture gradient between centre and surface layers, which was attributed to the profile of shear strains experienced during hot rolling. The cast strip revealed a less homogeneous microstructure and a weak texture fibre close to {100}<UVW>, which was attributed to growth selection. The material used for the study was an 18% Cr, 8.5% Ni austenitic stainless steel.

Numerical models have also been formulated to analyse thin strip casting. Tavares and Guthrie [8] used computational fluid dynamics to simulate the twin roll casting process and used it to analyse one of the crucial aspects of the process - the method of molten metal delivery into the roll castor. The position and shape if the delivery nozzle has a large impact on the solid shell formation, homogeneity, segregation and surface quality. A tubular nozzle and a slot shaped nozzle were analysed along with variation in position and angle. The results of the simulation were compared with experimental results obtained at a pilot caster mill.

In a second paper, Guthrie and Tavares [9] used computational fluid dynamics to analyse the required geometry and cooling capacities needed to make twin roll castors and horizontal belt castors competitive in production, compared to conventional continuous castors and hot roughing rolling mills.

They give a useful overview of the status of research and development in the field of thin strip casting, and outline the trends in production method. Problems and potential solutions were discussed as well as the need for more experimental work in the field.

University of Cape Town

2. Numerical modelling of hot rolling in general

Much work has been done modelling the forming of the metal during hot rolling. Most of the simulations include temperature, strain and strain rate dependence in the material model, for the calculation of flow stress.

Numerical simulations of the rolling process can be divided into those formulated within the bounds of a suitable software package, and those coded in basic Fortran code. Software utilisation has the advantages of saving programming time and runs faster due to the efficient programming of the professional software programmers. However, the power of starting from scratch lies in the greater flexibility in choice and implementation of solution algorithms and saves the significant cost of the software.

J.J.M. Too [10] formulated such a simulation using *METFORM software* to model heat transfer in the billet, with a view to establishing the relationship between skid marks (cooled areas on the underside of the billet from water cooled rail supports) and 'head-end turndown' (downward bending of the end of the billet resulting during rougher rolling).

The cooling effects of the skids was simulated and 'head-end turndown' resulted in the simulation corresponding to the phenomenon found in practice. Effort was made to correct this phenomenon by increasing the speed of the lower work roll fractionally and using a lubricant with a different heat transfer coefficient on the lower work roll. The simulation showed that 'head-end turndown' could be almost totally eliminated by optimising these two preventative measures. Microstructural prediction was not considered in the modelling.

Numerical models of hot rolling coded in Fortran are usually analytical, finite element based, or finite difference based models. Analytical equations are the most computationally efficient and are often used in gauge control systems, while finite element simulations are the most accurate and computationally expensive.

Cherukuri *et al.* [11] formulated a rate dependent, plane strain model for analysing sheet metal rolling. The model comprises of a *series of analytical equations* including an asymptotic scheme that is based on the assumption that the ratio of sheet thickness to roll bite length is small. The model considered both relative slip and zero slip friction models. The deformation was assumed to be plane strain and homogeneous through thickness. Material constitutive behaviour was based on the power law and assumed to be rigid-plastic with no temperature dependence. Work rolls were assumed ridged.

The model was found to be useful in comparing the relative effects of changing parameters in the rolling process, but correlation to experimental values showed error of 20-30%. The models usefulness was in its computational efficiency, enabling it to be used in shape control programming.

Devadas *et al.* (part 2) [12] simulated hot strip rolling at Stelco's Lake Erie Works hot strip mill.

University of Cape Town

The following assumptions were made in the rolling simulation:

1. Plane strain conditions apply due to the small thickness to width ratio and the rolling was thus modelled in 2D.
2. Deformation is homogeneous in the roll gap and vertical sections remain vertical.
3. The coefficient of friction is constant over the contact arc.
4. The roll deformation was taken into account, but assumed to remain circular.
5. Rolling an radial directions were assumed to be principle stress directions and von Mises yield criteria assumed valid.
6. Zero front and back tension.

Friction coefficients for unlubricated rolling were found to vary between 0.3 and 0.35, while lubricated rolling required the use of coefficients around 0.25. Heat transfer coefficient values for lubricated and unlubricated rolling were used as for an earlier paper (part 1) [13]. The paper claims that the incorporation of thermal gradient through the thickness of the billet, as opposed to a constant temperature equal to the core billet temperature, raises the predicted roll forces by 6 to 10%. Note that due to assumption 2, the heat generation due to plastic work is assumed to be distributed evenly in the roll gap and results in inaccurate modelling of the thermal gradient , and therefore flow stress in subsequent passes.

The model was validated by comparing predicted forces with the roll forces measured on the industrial mill. For the first two passes, the roll predictions were within 7% of measured values. The predictions worsened to an under estimate of 28.6% in the 4^{th} pass; the discrepancy being attributed to the retained strain in the billet between passes.

Most of the finite element models are formulated in order to study a particular aspect of the rolling process. Richelsen [14] analysed the rolling process using a plane strain *finite element* model. The model used an elasto-viscoplastic material model incorporating temperature dependence. The contact and friction at the roll/slab interface were enforced using nodal springs of constant high stiffness.

University of Cape Town

The aim of the analysis was to explore the effects of using two different friction models. The first model used was the basic Coulomb friction model, which assumes direct proportion between the maximum frictional force and the normal force, and has no limit on the amount of shear stress that can be imposed. The second model was based on Wanheim and Bay's expression for the variation of frictional stresses with the normal stresses, and included a friction limit due to the shear strength of the material. This limit was linked to the material model and thus made to be rate and temperature dependent.

The two models were compared using a range of roll radius to thickness ratios, friction coefficients, strain hardening coefficients and roll speeds. The results showed the basic Coulomb friction model to be unrealistic in its predictions of neutral point position, sticking zone length and stress levels.

On the other hand, Galantucci *et al.* [15] developed a 2 dimensional (plane strain) coupled thermo-mechanical finite element simulation of the hot rolling process with a view to studying the thermodynamics of rolling and comparing to experimental results.

The material was modelled as an elasto-plastic type with isotropic work hardening. For temperatures lower than the recrystallisation temperature, the yield stress and slope of linear hardening were made functions of temperature and for higher temperatures, the stress was assumed to be a function of strain rate and temperature only. Heat generation due to plastic work and frictional effects was taken into account, and convection and conductive heat transfer was modelled on the slab and roller.

Thermal distribution history predicted by the model compared favourably with experimental results although the model was found to be very sensitive to thermal coefficient values within the range of values suggested by literature.

In finite element models, one of the difficulties lies in trying to determine which effects are significant and thus worth the computational expense of modelling, and which effects can be ignored. These debates are the subject of many heated intellectual discussions.

For instance, Lin and Shen [16] developed a coupled temperature-displacement finite element model of hot and cold rolling. The simulation makes use of a thermo elasto-plastic material

University of Cape Town

model which does not incorporate rate effects in the constitutive equation – a discrepancy which some would judge to make the simulation invalid.

The model does take into account heat transfer through radiation and convection to the environment, film boiling of the coolant sprays, conduction to the work rolls and heat generation due to plastic work, but does not include frictional heating effects. The roller is assumed to be an isothermal rigid body.

Strip spread and profile, strain, strain rate, residual stress and temperature distribution were compared for different reductions. Roll forces were also analysed and compared to literature values, but not published.

Torres *et al.* [17] formulated a *finite difference* model to characterise the heat transfer through the oxide layer formed in hot rolling of steel. The oxide layer was divided into three sub layers of wustite, magnetite and hematite and appropriate thickness given to each sub layer. The oxide layer was assumed to grow in thickness according to a parabolic function fitted to experimental results.

The properties of the steel were characterised as being temperature dependant, but the different thermal coefficients of the three different sub layer oxide materials were assumed to be constant w.r.t. temperature.

The results showed that for oxide thickness less than 6mm, there is no significant difference between modelling the three sub layers, and just modelling the entire oxide thickness as consisting of wustite, which constitutes 90% of the real oxide thickness. For thickness in excess of 6mm (not common in hot rolling) and for modelling the integrity of the oxide layer, the added complexity of the sub layer divisions is warranted and provides useful information.

Another popular approach, is to model the rolling process using a fluid dynamics/steady state/Eulerian approach, where the material is modelled as flowing in one end, between the rollers, and out the other end.

Ashok Kumar *et al.* [18] modelled the steel strip deformation and heat transfer in the roll bite, using a 2D, coupled finite element model based on the *flow formulation (steady state) approach*. The program was coded in Fortran and run at the University. The roll bite zone was

University of Cape Town

discretised into 104, 8 noded (quadratic), iso-parametric elements. Roll flattening, roll chilling and friction effects were taken into account. The model illustrated the strain rate inhomogeneity, with peak strain of 5 – 10 times the nominal strain rate just beneath the surface. The author also showed that the effects of roll flattening account for an 8 – 13% increase in roll force.

He outlined the need for thermo-mechanical simulations in terms of geometric control and microstructural prediction. The author also outlined the issues of material flow stress models used in rolling simulations as well as discussing the thermal dynamics and boundary conditions incorporated in hot rolling.

Heat transfer in the roll gap (conduction only) was modelled using a time dependent heat transfer coefficient, calculated experimentally. Radiation and convection to the environment were also taken into account. Along the arc of contact, material was simply given the roller velocity, i.e. no slip was accounted for. Frictional effects were introduced by incorporating a thin layer of friction elements at the interface and relating the shear stress in this layer, to the coefficient of friction at the interface.

The flow stress was calculated using a version of the Arrhenius hyperbolic sine function to include strain rate and temperature, and the scaling parameters in the equation were made dependent on strain and 3 constants, which were found experimentally.

University of Cape Town

One of the disadvantages of the Eulerian approach, is the fact that a reversing mill cannot be modelled with a single simulation. Thus Nepershin *et al.* [19] formulated six different FORTRAN PC programs to simulate the hot rolling of steel slab and strip of different geometry. The simulations were programmed as steady state plane strain formulations using hyperbolic sine material flow curves. Material elasticity were ignored and friction is modelled as sticking case.

However, the Eulerian approach does have advantages in analysing the flow of material and differences in deformation through the material. Bayoumi [20] did research on the distribution and causes of variation of edge stresses in the hot rolling of wide strip. A *flowline solution* was developed in which the strip was divided into three sections. The middle section was shown to exhibit true plane strain flow behaviour due to the lateral constraints imposed by the

two flanking sections on the outsides of the strip width. These two sections were shown to exhibit some lateral flow due to the lack of constraint at the free edge, and were modelled as such. A finite element model was formulated to model the three zones in order to investigate the nature (including width and direction and magnitude of stresses) of the stresses in the edge zones and their dependence on rolling parameters. The model assumed a strain, strain rate and temperature sensitive rigid-plastic material. Roll bending and flattening was neglected, as were the effects of front and back tension.

Results showed that the maximum value of the longitudinal stress on the strip edge is $1/\sqrt{3}$ times the flow stress, and that this value occurs at the neutral point, where the width of the edge zone is at a maximum. The influences of friction, roll diameter and thickness reduction percentage, were found to have little influence on the magnitude and distribution of edge stresses.

While some papers have subtle errors and discrepancies, others are glaring. Anglov and Nedev [21] developed a finite element model of the hot rolling process with a non-linear friction model. The model was a steady state analysis incorporating a strain rate sensitive rigid-plastic material model. The effects of different friction factors, reductions and velocities were analysed and compared to experimental results. However, the one large discrepancy in the model was that the billet was assumed isothermal and no heat transfer or heat generation was taken into account.

Other models are far more rigorous. Beynon *et al.* [22] formulated a steady state Eulerian Finite Element Model to model the thermal and deformation dynamics in hot strip rolling. They formulated a modified Petrov-Galerkin method to smoothen the numerical instability caused by the addition of convection terms in the partial differential equation. The model actually consisted of two separate models: One to model heat transfer and deformation during rolling and one to model heat transfer between passes. This was done due to the differences in scale of thermal changes, during rolling, and between rolling.

The process was modelled with linear triangular elements in 2 dimensions (plane strain assumed). The strip was assumed to have uniform initial temperature distribution. Heat loss to the environment and rollers was modelled as well as the heat gained due to plastic work.

University of Cape Town

3. Material testing, microstructural considerations and empirical models

Much time has been spent trying to obtain reliable flow stress data for 304 stainless steel, at varying strain rates and high temperatures. Much work seems to have been done developing constitutive empirical data, but due to the lack of expensive testing equipment, most of the publications reference other research for validation and thorough published experimental flow stress data for any particular alloy at these high temperatures has still not been found. The only reliable experimental data has been kindly supplied by P.D. Hodgson at Deakin University after written query regarding his paper [23]. This data is derived from hot torsion tests done at Deakin University. Unfortunately, they only obtained flow curves for a single strain rate of 2.3/s. Since accurate modelling requires extensive characterisation of flow stress behaviour, papers on flow stress testing were reviewed.

Miguel A. Cavaliere *et al.* [24], showed that 'true stress-true strain' data can be produced by using an "upsetting" test, for logarithmic strain values less than 0.8. They used a Gleeble 3500 machine and a cylindrical specimen to produce a force displacement curve at a given temperature and strain rate. The transient cross sectional area was calculated as a function of displacement (assuming zero barrelling) and the corresponding stress–strain curve plotted.

The test procedure was then modelled numerically with METFORM, using a basic Coulomb friction model and two extreme values for the friction coefficient (0.2 and 0.9). The experimental stress strain curve was used as the material flow characterisation in the simulation. Due to the model's incorporation of friction, the associated barrelling phenomenon was accurately modelled and the force–displacement curve generated by the model (for both friction coefficients) matched the experimental result extremely well for strains of less than 0.8. When strained further, the curves diverged.

The result proved was that the effects of barrelling are negligible for strains of less than 0.8 and this is a significant finding since the shape of a typical flow curve usually flattens out by this value of strain. Unfortunately the effects of different specimen aspect ratios, strain rates and temperatures were not investigated.

Devadas *et al.* (part 2) [12] simulated hot strip rolling at Stelco's Lake Erie Works hot strip mill. They conducted compression tests using a cam plastometer and a Gleeble 1500 machine to obtain flow curves for carbon steels, for a range of temperatures and strain rates. The paper discusses the experimental procedure used for both tests, and the suitability of various

University of Cape Town

published empirical models to fit the experimental data. A hyperbolic sine form equation was found to best fit the experimental data, and this formulation was used in the rolling simulation once the necessary constants had been solved.

Baragar [25] determined the stress-strain curves for a plain carbon and an HSLA steel at high temperatures and high strain rates using a cam-plastometer.

Cylindrical specimens, 12.7mm diameter and 18.5mm long were homogenised before the unlubricated tests were conducted. Strain rates of 2, 20 and 120 s^{-1} and temperatures of 900, 1000 and 1100^{0}C were examined. Specimens were strained to a strain of 0.7, and thus the need for lubrication was avoided according to literature.

University of Cape Town

He then compared the experimental results with the empirical relationships:

1. $\exp(\beta\sigma) = A_1\dot{\varepsilon}\exp(Q/RT)$
2. $(\sinh(\alpha\sigma))^n = A_2\dot{\varepsilon}\exp(Q/RT)$
3. $\sigma = b + c\varepsilon^{0.4} + d\varepsilon^{0.8} + e\varepsilon^{1.2}$

Values for flow stress were taken at strains of 0.2, 0.3, 0.4, 0.5 and 0.6 and the "constants" calculated for each strain. Equations 1 and 2 then gave two different methods of finding the stress value for that strain (both with temperature and strain rate dependence), and the curve of equation 3 could be fitted to these values. While the plain carbon steel flow curves could be quite accurately fitted with the equations above, the HSLA steel could not be fitted due to some athermal behaviour in the 900 - 1000^{0}C temperature range.

Dynamic Systems Inc. in their Application note 1 [26] produced a useful document in describing the procedure for performing valid uniaxial compression tests in order to gain flow stress information for a given material.

Thermocouples were used to demonstrate temperature homogeneity through the specimen. Different thickness graphite foil was used as a lubricant to minimise barrelling and the associated strain inhomogeneity.

The document outlines the use of the following parameters to verify the validity of uniaxial compression tests:

1. The Barrelling coefficient, B, defined as:

$$B = \frac{l_f d_f^2}{l_o d_o^2}$$

Where : l_o = initial specimen length

d_o = initial specimen diameter

l_f = deformed specimen length

d_f = deformed specimen diameter

This is the most important coefficient in assessing validity.

For a valid test: $B \geq 0.9$

2. The Ovality coefficient, O_v, defined as: $O_v = d_{f\,max} / d_{f\,min}$

3. The Length coefficient, L, defined as:

$L = Sdl_f / l_f$ Where : Sdl_f = The standard deviation of four measurements of the length of the deformed specimen measured at the centre and at 120^0 intervals on the edge.

l_f = the average of the four measurements.

For a valid test: $L \leq 0.05$

4. The Circularity coefficient, C, defined as:

$C = Sdd_f / d_f$ Where : Sdd_f = The standard deviation of eight equally spaced measurements of the diameter of the deformed specimen.

d_f = the average of the eight measurements.

The microstructure of the tested specimens was also examined for each test to confirm the uniformity of both temperature and deformation, and found to show good uniformity in both cases. Factors influencing barrelling and lubrication efficiency are discussed. It is recommended that 0.1mm or even 0.06mm thick graphite foil be used for lubrication rather than the 0.25mm foil. Smooth contact surfaces also reduce friction.

University of Cape Town

The use of graphite foil may result in a carburised layer when used at high temperatures and cause welding to the anvils due to the drop in melting point. Nickel coating on the ends of the specimens can be used as a diffusion barrier to prevent this problem.

Dynamic Systems Inc. in their Application note 2 [27] provide useful information on flow stress correction for uniaxial compression testing. The document discusses correction for friction (barrelling), test machine compliance and adiabatic heating.

Flow stress correction due to friction is as follows:

$$\sigma = \frac{4F_i}{\pi d_i^2}\left(1+\frac{\mu d_i}{3l_i}\right)^2$$

or $$\sigma = \frac{2F_i}{\pi d_i^2}\left(\frac{\mu d_i}{l_i}\right)^2\left(\exp\left(\frac{\mu d_i}{l_i}\right)-\frac{\mu d_i}{l_i}-1\right)^{-1}$$

Note that provided the barrelling coefficient is not less than 0.9, it is not necessary to correct for friction.

Laasraoui *et al.* [28] analysed techniques in flow stress prediction using four low carbon steels as materials on which the experimental tests were done for training data. Single hit compression tests were conducted in the strain rate range of 0.2 to $50s^{-1}$ and temperatures from 800 to 1200^0C. The flow curves at higher strain rates were corrected for adiabatic heating in the deformation process in order to be able to formulate idealised isothermal constitutive equations. Hyperbolic sine and power law equations were evaluated along with many variations of microstructural constitutive equations used by other researchers, to include dynamic recrystallisation and recovery.

Deformation heating was found to affect the flow stresses in tests of lower relative temperature and high strain rates by up to 11%. The hyperbolic sine function was found to fit the data well and values for the activation energy were calculated. When the power law was used, the values of activation energy were found to be strongly stress dependent.

Schindler *et al.* [29] conducted hot torsion tests and proposed a new method of result interpretation to obtain true stress-true strain curves for the material for a range of

University of Cape Town

temperatures and strain rates. The paper describes the methods used to calculate the representative radius, the equivalent strain and strain rate, equivalent stress and empirical equation forms used to best fit the data.

Results were extrapolated to the strain rate range of the working condition of hot rolling, and average values for strain rate, temperature and strain in the billet were calculated. These values were used in calculating the predicted roll force and compared with the roll force measured at an industrial hot rolling mill.

No attempt was made to compare the interpreted true stress-true strain curves for the material to other test results for that alloy. Prediction of roll forces assumed homogeneous strain, strain rate, stress and temperature, and don't take into account heat generation by plastic work or friction effects. Comparison to measured roll forces to show the accuracy of the material data is not valid in such a case.

J.J.M. Too [10] did experimental tests to determine heat transfer and generation due to plastic working, in the form of 'upsetting' tests. The tests were also modelled numerically and good correlation was shown.

One of the driving forces in rolling research is the need for microstructural prediction models. These models have to be able to model the deformation and thermal history very accurately in order to form the basis for microstructural prediction. However, in addition to this, much experimental work is needed to establish the relationships between the microstructural evolution and strain, strain rate and temperature histories.

H.J. McQueen at Concordia University is very well read (171 references on his paper). His paper[30] is a thorough examination of the current constitutive methods for prediction of flow stress, dynamic recrystallisation and recovery in stainless steels. The author also outlines the usefulness and limitations of various flow stress testing procedures such as 'upsetting', plane strain compression, and torsion testing.

McQueen also outlines a method of calculating the flow curves empirically, using four equations and incorporating grain size as well as the necessary strain, strain rate and temperature variables. The equations make use of a number of constants. Some of these are material constants and some are merely scaling factors. However the values of these constants

University of Cape Town

are either missing or merely referenced to various other papers, making their reliability unsure, since details of testing procedure and data fitting is non existent in any one source.

McQueen *et al.* [31] wrote another paper exploring the mechanical properties and microstructural mechanisms of plastic deformation of austenitic stainless steels. These properties and mechanisms were examined across the range of hot and cold working and compared to common carbon and HSLA steels. The influences of temperature, strain and strain rate on strain hardening, dynamic recovery, dynamic recrystallisation and static recrystallisation were discussed and associated constitutive equations were examined.

Differences in the two temperature domains as well as the "warm" working domain were contrasted to explain their use in forming operations. Different testing procedures and their suitability for forming processes were also discussed.

Park [32] developed a flow stress prediction model to analyse the effects of temperature, strain, strain rate, and in particular, the inter-pass time on dynamic and static recrystallisation. Conventional and interrupted torsion test data formed the basis for the model, which was used in a finite element model for conventional and controlled hot rolling of thick plates.

Controlled rolling was found to yield finer grain sizes than conventional rolling, however the rolling forces in controlled rolling were found to become immensely large, limiting the practical use of this technique. Deviation of grain size and retained strain through the thickness, increased with increasing thickness of the plate.

Kim and Oyo [33] wrote an outstanding paper on the dynamic recrystallisation behaviour of 304 stainless steel. The samples were strained on a hot torsion machine in the temperature range of 900 – 1100 ^{0}C and a strain rate range of 0.05 – 5 s^{-1}. The initiation and evolution of dynamic recrystallisation was investigated using microstructural analysis. The effects of process variables of strain, strain rate and temperature were established on the volume fraction recrystallised, the grain size and the strain at which dynamic recrystallisation initiates. The experimental data was fitted with modified Avrami, Zener-Hollomon and Hyperbolic sine equations.

University of Cape Town

Korczak and Dyja [34] formulated a mathematical model to predict the microstructural dynamics of recrystallisation and precipitation in 15G2Anb niobium carbon steel. The model was formulated according to equations developed by the likes of Hodgson and Sellars. The results were compared to experimental tests and micrographs.

The formation and treatment of the oxide layer developed during hot rolling also affects the microstructure on the billet surface. Fishkis and Lin [35] did some work investigating a subsurface layer that develops in the hot working (in this case hot rolling) of a non heat treatable magnesium containing aluminium alloy. The layer extends 1.5 to 8 μm below the surface and decreases in depth with increase in rolling passes. Changes in grain size and shape, as well as composition were studied with respect to the number of rolling passes.

Experimental results concerning metal grain size stabilisation were compared with the theory of Zener Pinning and composition results were compared to the results of the Monte Carlo computer simulation by M.P. Anderson.

The microstructure of the edge surface has also been shown to have significance in the hot rolling process. Czerwinski *et al.* [36] did a study on the correlation of high concentrations of δ-ferrite and edge cracking in the austenitic stainless steel hot rolling process. The presence of δ-ferrite concentrations along the billet edges reduces the hot ductility of austenitic stainless steels, resulting in increased tendency toward edge cracking during rolling at the ferrite/austenite interface. Specimens from rolled billet edges were etched and examined under optical and TEM microscopes to confirm the theory.

University of Cape Town

However, very few microstructural prediction models have been used in finite element rolling simulations. Dyja *et al.* [37] did work adding the microstructural evolution modelling to an existing thermo-mechanical simulation of the rolling process. This work demonstrates the beginning of technology able to model microstructural evolution through changes in the hot rolling process.

The model used a form of the hyperbolic sine equation to model the flow stress of the material. Recrystallisation and precipitation were modelled using an Avrami equation with some semi empirical equations developed by Dutta, Sellars and Hodgson. Recovery was not modelled and this led to deviations of roll force predictions in later passes due to retained strain.

The results of the simulation were compared to results from the reversing hot plate mill in the Czestochowa steel plant in Poland, for a C-Mn-Nb steel.

4. Thermo-dynamics of hot rolling

Since the material properties of metals are strongly temperature sensitive in the hot working range, accurate modelling of the thermodynamics in the simulation is crucial to solution accuracy. B.K.Chen, P.K.Thomson and S.K.Choi [38], set out to accurately determine the temperature distribution history of aluminium in the roll gap. They paid particular attention to the dominant transfer of heat from the billet to the work rolls. The rolling process was modelled using different values of h_{RS} (heat conduction coefficient), to generate different histories of billet surface temperature. Experimental work was done to establish the actual surface temperature history of the billet by placing thermocouples on the surface of a specimen that was then rolled at around 400^0C.

The experimental thermal history did not correlate to any of those calculated with fixed h_{RS} values, which was expected since it was suspected that it would be mainly dependent on the pressure between surfaces. Thus a profile of roll pressure along the arc of contact was produced using the numerical model and this was compared with the back fitted transient values of h_{RS} along the arc of contact. From the two plots, the deduction was made that the value of h_{RS} is not dominated by pressure and that other effects such as oxide layer growth and thickness, and surface roughness and chemistry must play a significant role in determining the heat transfer coefficient.

The surface thermal history was measured using different lubricant types and it was found that the lubricant type made negligible difference to the value of h_{RS}. However, heat generated through slipping at the roll billet interface was not taken into account in the analysis.

Thermal modelling is a complex task. Not only are the material properties temperature sensitive, but deformation of the material also generates heat which contributes to the heat balance. Devadas *et al.* (part 1) [13] did a series of hot rolling tests with thermocouple fitted samples to measure the thermal response of steel during hot rolling. They used a mathematical heat transfer model to back calculate the roll/strip interface heat transfer coefficients. The effects of lubrication, reduction percentage, roll speed and prerolling were also investigated.

University of Cape Town

The effects found were as follows:

1. For unlubricated (water only), 1st pass rolling at around 1000^0C, and reduction of 35%, htc (heat transfer coefficient) = 50 kW/m^2 ^{0}C
2. For reduction of 50%, htc = 57 kW/m^2 ^{0}C
3. With lubrication, htc = 31 kW/m^2 ^{0}C
4. Increase in rolling speed caused the coefficient value to rise faster but did not change the steady state value.
5. Pre-rolling resulted in a htc value that didn't reach steady state and increased throughout time in the roll gap, reaching a max value of htc = 290 kW/m^2 ^{0}C. This was attributed to the difference in the contact arc pressure distribution of the two passes.

Their paper discusses the dependence of heat transfer coefficient on probable factors such as interface pressure, bulk strain and relative velocity, as well as commenting on the effects of lubricant films in the interface asperity gaps.

Pietrzyk *et al.* [39] also analysed the importance of accurate heat transfer and friction coefficients at the roll/workpiece interface. The effects of these parameters on predictions of roll forces and torque were illustrated using a "one dimensional model" and a "thermal and mechanical model", which were not described in detail.

Hot rolling experiments were conducted using low carbon steels rolled in a lab mill with embedded thermocouples, and cold and warm rolling experiments were conducted using aluminium specimens. Thermal profiles were measured and compared to the mathematical models' prediction when constitutive models for temperature, strain and strain rate sensitive material flow stresses were incorporated in the models. Accuracy of the constitutive models was not discussed.

Most of the thermal simulations and models do not take the scale growth into account. However, Shirizly *et al.* [40] did an investigation into the effects of scale thickness and position of cooling emulsion sprayers on roll forces, torque heat transfer coefficients. They concluded that the position of the sprayers had a very minor effect on the temperature of the slab and roll. The heat loss was higher when rolled with thinner scale and the roll forces were insensitive when interface conditions were varied.

University of Cape Town

The most significant finding was that the heat transfer coefficient increased with increasing pressures and temperatures and decreased with decrease in relative velocity.

The use of coolant and descaling sprayers also has a chilling effect which must be characterised. Rivallin and Viannay [41] formulated a model to simulate the fluid and thermodynamics of cooling hot (800^0C), flat surfaces with water jets. The research was done with the aim of understanding the dynamics of accelerated cooling in order to produce controlled cooling machines capable of cooling requirements (speed and homogeneity and a precise final temperature) needed by hot metallurgical processes like hot rolling and forming.

The model progresses from initial contact, through film boiling, where the water boils sliding on a layer of steam on the surface of the metal, to progressive rewetting and nucleated boiling as the surface cools to the point where the liquid does not boil immediately on contact, through to cooling by the turbulent liquid layer without boiling.

Forced contact during the film boiling regime is modelled to show the increased efficiency of cooling and the results of the model are compared to experiments.

Horski *et al.* [42] did an experimental study on the cooling dynamics of hot rolling products, which are sprayed with coolant while travelling at typical roll table speeds. The experimental rig consisted of a long, horizontal girder, on which a platform containing the thermocouple fitted specimen and coolant sprayers, was rolled at constant speed. The effects of platform speed and sprayer pressure and angle, on the heat transfer coefficient, were investigated.

The rig proved very useful in simulating industrial conditions and determining heat transfer coefficients for different coolants, spray and billet velocities, nozzle shapes and oxide growth times. The rig also proved useful for investigating the effectiveness of descaling sprayer designs.

5. Friction models in rolling simulations

One of the parameters which significantly affects the prediction of roll forces as well as roll surface wear, is the characterisation of friction at the roll/billet interface. Shirizly *et al.* [43] did some thorough and useful work in determining the effects of different lubricants on roll forces, roll torque, heat transfer at the interface and scale formation in the hot rolling of low carbon steel strips. Five different interface conditions were tested: dry rolling, distilled water,

University of Cape Town

a 1:1000 oil:distilled water emulsion, a 1:500 oil:distilled water emulsion, and a commercially available hot forging oil.

Small changes in the oil to water ratio were found to cause significant variations in the effectiveness of the emulsion. The largest reductions in roll force and roll torque were found when using the 1:1000 oil:distilled water emulsion. The largest roll forces and roll torque were found when using the dry rolling technique. The 1:1000 oil:distilled water emulsion also showed the best insulating ability, the lowest scale formation and the softest scale formation. It is also expected that this emulsion will give the longest roll surface life.

In addition to lubricant considerations, the growth of the oxide layer also affects friction conditions. Munther *et al.* [44] conducted oxidation and hot rolling experiments to investigate scale formation dependence on time and temperature, as well as its effect on friction at the roll/slab interface.

The paper reviewed research done on oxide layers and included properties and proportions of the three sub layers of wustite, magnetite and hematite. The paper suggested that in addition to the influences of reduction, temperature and velocity, the most important factor in determining the coefficient of friction, was the scale index at the interface. A thicker scale resulted in lower friction, partly due to its reduced slab adherence capacity. The growth of the scale could be modelled simply with dependence on temperature and time.

Many different models have been proposed in calculating friction and analysing its dependence on normal force, surface roughness, material strength and lubricants. Lagergren [45] evaluated three friction models often used in the simulation of hot rolling, using direct measurement on a model duo mill with acrylate rollers. Waxes of different compositions were formulated to produce flow curves of similar shape to those obtained using hot steel. The flow curves for the waxes were determined using "upsetting" tests.

The model rolling rig was set up to measure normal pressure, shear stress and shear stress angle in the roll gap. Variations in reduction, velocity, lubrication and materials were simulated on the mill and results were compared to the Coulomb, Tresca and Wanheim-Bay friction Models.

University of Cape Town

Neither the Coulomb nor the Tresca friction models could suitably describe the distribution of friction in the roll gap. The Wanheim-Bay model was shown to be the best choice, but the need for an expression for pressure dependent real area was expressed.

6. Experimental procedures for validation of modelling

Any numerical model needs to be validated against real life processes. Simulations aiming to predict roll forces can usually be compared to forces measured at an industrial or test rolling facility. However, it is far more worthwhile to validate the thermal history in addition to the roll forces as this can be helpful in identifying the cause of discrepancies. Thermal validation is however, quite an experimental challenge.

J.J.M. Too [10] formulated such a simulation using METFORM software to model heat transfer in the billet, with a view to establishing the relationship between skid marks (cooled areas on the underside of the billet from water cooled rail supports) and 'head-end turndown' (downward bending of the end of the billet resulting during rougher rolling).

The through thickness profiles of temperature were predicted along the roll gap using the model, These temperature profiles were validated quite well using thermocouples inserted into a specimen that was then rolled at around 800^0C in a test rolling rig.

Rolling validation can also be used to validate strain distribution. Ashok Kumar *et al.* [18] modelled the steel strip deformation and heat transfer in the roll bite, using a 2D, coupled finite element model based on the *flow formulation (steady state) approach.*

Validation of surface temperature rise was done by spot welding Chromel-alumel (type K) thermocouples to the surface of a 304 stainless steel specimen which was heated to 1000^0C and rolled at 2.7cm/s (22% reduction). Temperature rise in the model was verified using thermocouples inserted in a specimen and rolled in a lab test rig. Strain distribution was also validated by inserting a small steel pin into the specimen and examining its deformed longitudinal cross section subsequent to rolling the specimen.

University of Cape Town

7. Control of rolling systems

One of the uses for mathematical models of the rolling process is in the control of roll bending and gauge. Grimble and Hearns [46] developed a continuous-time LQG (Linear Quadratic Gaussian) optimal control system for application to the control of roll position to ensure constant exit thickness in spite of the lack of constant thickness, hardness and friction in industrial hot rolling. Part of the challenge in developing such a system is the fact that the position of the thickness transducers is always some distance from the roll bite, and thus transport delay must be included in the control design.

The system incorporates a Kalman predictor and state estimate feedback. The structure of the control system is similar to that of a Smith predictor.

Okada *et al.* [47] developed a control system for the hot strip finishing mill process. Their model was based on optimal servo theory and the model decoupling method. The control system incorporated the previously independent control systems of the strip gauge, the strip tension, the width control and the looper angle, to produce an integrated system with greatly improved performance.

University of Cape Town

Chapter 5: Approach to Project

Effective and efficient progress in this project required a multi-focus approach to the different areas that influence procedure and outcome of the research. The 1st level approach to this project is shown schematically below:

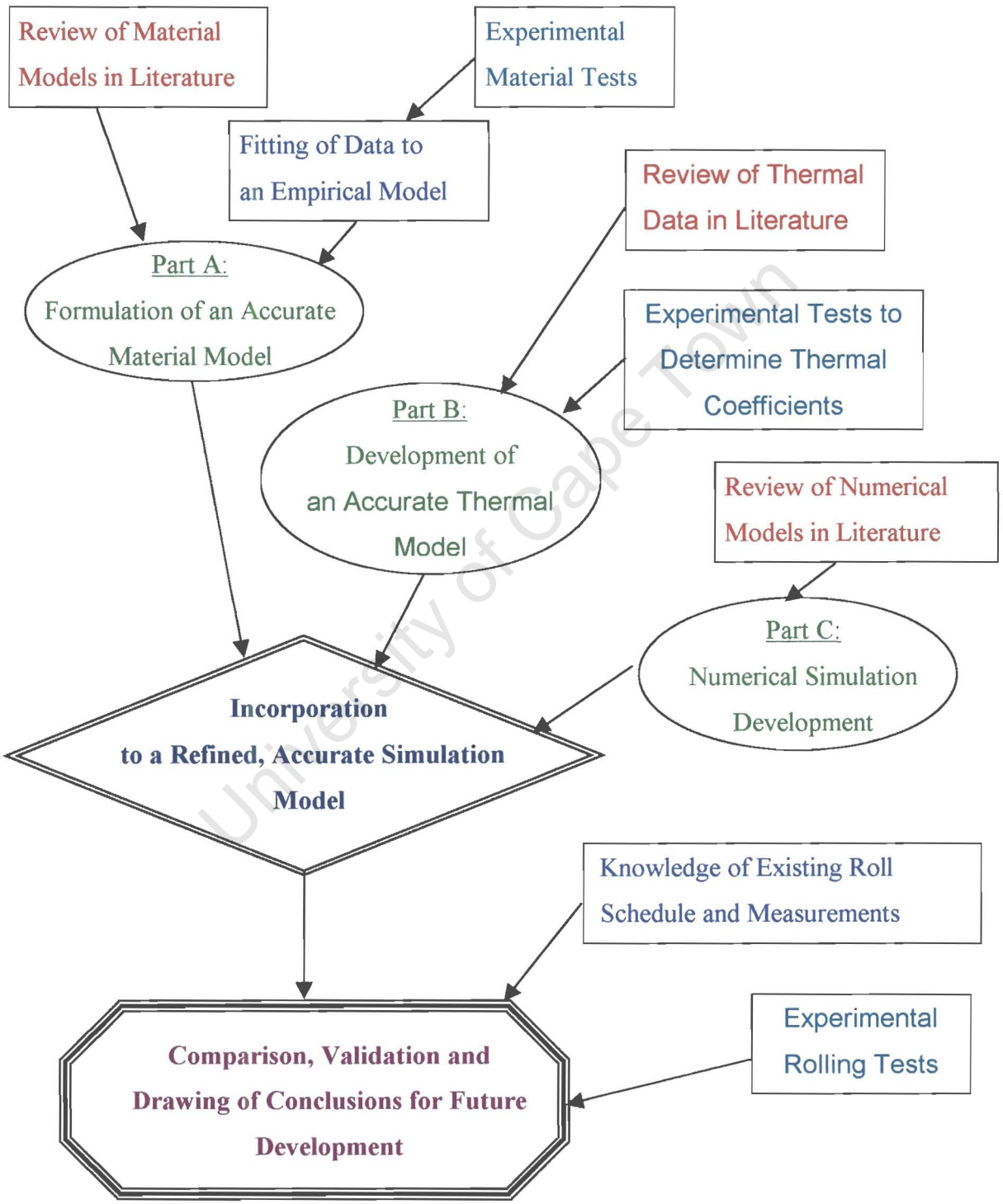

Fig 5: Flowchart Representation of 1st Level Approach to Thesis Project.

University of Cape Town

Chapter 6: Part A: Material Testing

Introduction:

The most important factor influencing the accuracy of a numerical model to calculate roll forces is a thorough knowledge of the material strength characteristics as a function of temperature, strain and strain rate. Unless the material concerned is accurately characterised in terms of its flow stress behaviour, all the numerical accuracy in the world will not yield an accurate roll force prediction model.

Unfortunately, very little thorough flow curve characterisation has been done experimentally for AISI 304 in the necessary ranges of strain, strain rate and temperature, and where empirical models are used, they are based on sparse and inconsistent training data. Many of the rolling simulation models have been constructed in such a way as to make them as generic as possible, enabling the user to address a wide variety of metal alloys, and roll schedules simply by changing a few variables and material constants in the program. However, in order to produce greater accuracy in force prediction, the specification of details in the process and complexity of accurate material description, require a simulation to be limited to a particular alloy at a particular industrial rolling mill.

For this project, the material flow characteristics were comprehensively tested in the appropriate range of strain rates and temperatures. Since the simulation accesses flow stress information as uniaxial flow stress values and because the exact relationship between tension and compression curves does not seem to have been adequately quantified, uniaxial compression testing was chosen as the most suitable for application for the simulation.

University of Cape Town

Preparation of Specimens:

Cylindrical specimens were cut from the rolled material with the length of the specimens corresponding to the rolling direction. The length of the specimens was constrained by the desired maximum strain rate and the maximum compression speed of the DSI GLEEBLE 3500 hot compression machine, and was set to 10mm. The diameter of the specimens was made as large as could be accommodated by the anvil face diameter, and was also set to 10mm.

Specimens were roughed on the lathe before being annealed at 1050°C for 25 minutes and water quenched. The following micrographs were taken of the annealed grain structure:

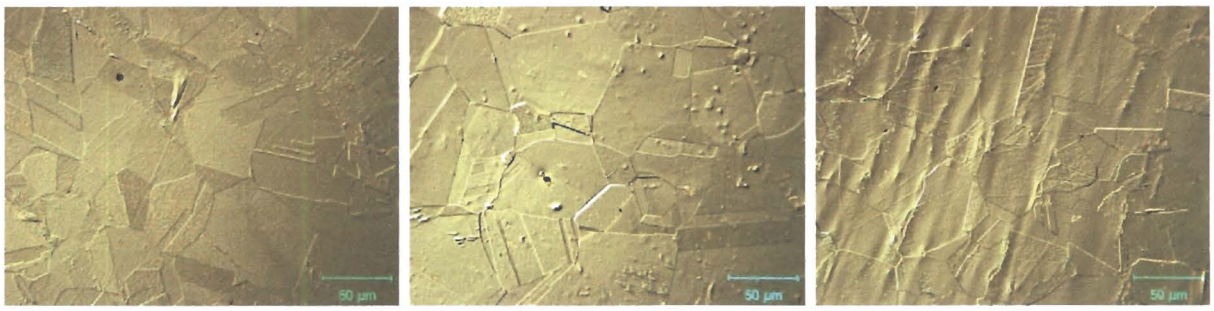

Fig 6.1: Orthographic views of the annealed specimen microstructure

These three micrographs show the typical grain structure in each of the three orthogonal directions of the rolled plate after annealing. From these micrographs, the relatively equiaxed and uniform grain structure can be seen, indicating homogeneous grain structure.

The specimens were then turned to a tolerance within 0.04mm and parted off. The specimen ends were surface ground and polished mechanically down to 1200 grit silicon carbide paper to achieve a tolerance within 0.05mm and an Ra value (as defined in figure 3 below) of 0.02µm.

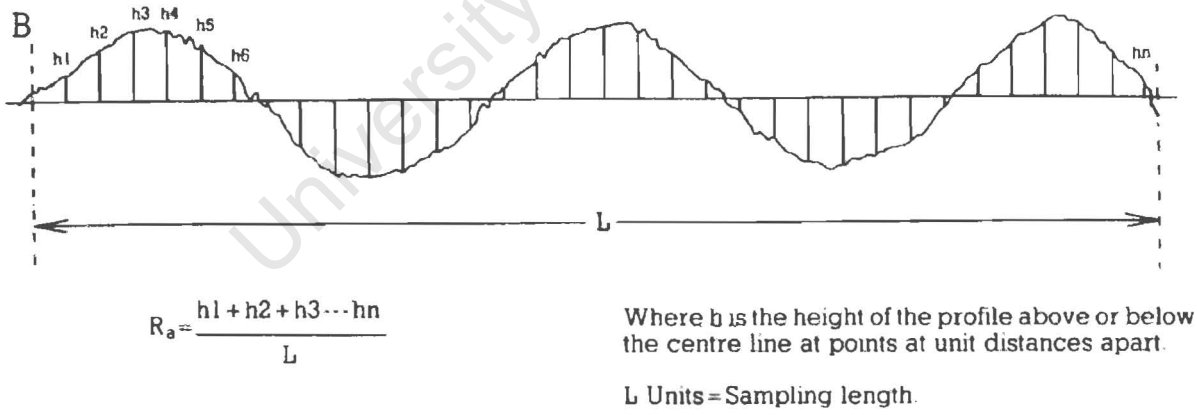

Fig 6.2: The definition of Ra value for surface roughness

This was done in an effort to minimise contact friction and thus reduce barrelling, in order to approximate uniaxial flow as closely as possible. Each specimen was measured to ensure specifications and each specimen's length and diameter was entered into the compression program and used in calculation of true stress and true strain.

University of Cape Town

Testing Procedure:

Unfortunately the software module enabling the Gleeble to perform constant strain rate and multiple hit testing was not available on the machine at Birmingham University where the testing was conducted. In order to closely approximate the constant strain rate, the curves of anvil position vs. time were plotted for each of the chosen constant strain rates. Best fit linear (constant anvil speed) approximations to the curves were then calculated and programmed into the test program. The Cooper-Symonds rate dependence power law was used to show the induced error associated with the divergence from true strain rate, and it was found that the error was within 1.5% for a strain of 1.0 in the strain rate range required.

Compression testing was conducted in the temperature range of 800-1250°C at intervals of 50°C. The strain rates tested were 35, 10, 3.5, 1.0, 0.35, 0.1, 0.01 s^{-1} and each temperature was tested within each strain rate, resulting in a test matrix of 70 flow curves.

A thermocouple was spot welded to the side of each specimen half way along its length. Initially, 0.25mm graphite foil was placed at the specimen/anvil interface to minimise friction and associated barrelling effects. However, the graphite foil tended to break down at high temperatures and cause arcing even with large preloads. This arcing caused pitting in the tungsten carbide anvil inserts and in many cases, caused the specimen to become welded to the anvil insert. This in turn led to severe damage to the face of the anvil insert when the specimen and insert were forcibly separated. To overcome this problem, 0.05mm tantalum foil was used at the specimen interface instead of the graphite foil. This solved the arcing problems, but was not as good a lubricant as the graphite foil.

After positioning the sample, foil and thermocouple between the anvils and setting a slight preload to hold the specimen in place, the chamber was evacuated to a pressure of 0.2 torr.

The compression of samples was preceded by a thermal cycle. The specimens were resistance heated to within 10°C of the test temperature in the first 20 seconds. They were then heated to the test temperature over the next 5 seconds and held at the test temperature for a further 5 seconds to ensure thermal homogeneity, before compression. After compression, the specimens were air cooled in situ with water cooling of the anvils providing a heat sink for the flattened specimens.

University of Cape Town

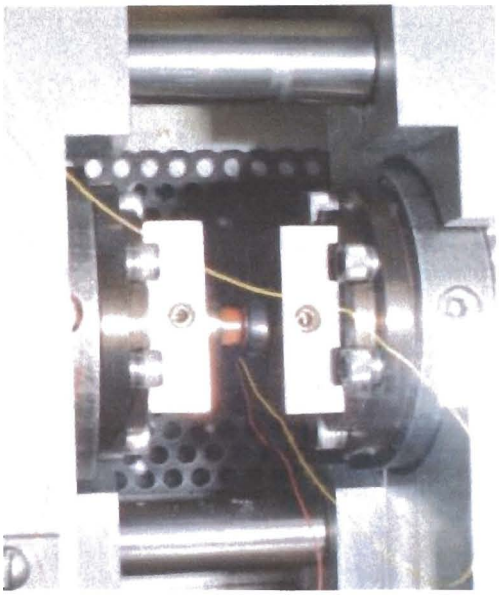

Fig 6.3: A specimen in the Gleeble anvils during testing

University of Cape Town

Processing of Specimens:

Specimens were measured and filed with test details after compression. Barrelling coefficients and length coefficients (See definitions on page 22) were calculated for the deformed specimens to ensure test validity. Length coefficients were typically around 0.007 which is well below the validity value of 0.05. Barrelling coefficients for samples tested using graphite foil were typically around 0.93 while the coefficients for samples tested using tantalum foil were typically around 0.91, both above the validity value of 0.9.

Several deformed specimens were cut in half along the longitudinal plane and the cross-section polished using a Struers RotoPol-22-RotoForce-4 automatic mechanical polisher. The cross-section was electro-polished using an acetic acid solution at 20 volts, for 15 seconds at room temperature. The acetic acid solution was made up as follows: 133ml acetic acid, 25g CrO3, 7ml distilled water. The cross-section was then etched using a 10% solution of oxalic acid at 10 volts, for 5 seconds at room temperature. Specimens were then examined under the Reichert MeF3A microscope using a Nomarski interference contrast to add depth appreciation to the microstructure.

The following micrographs were taken:

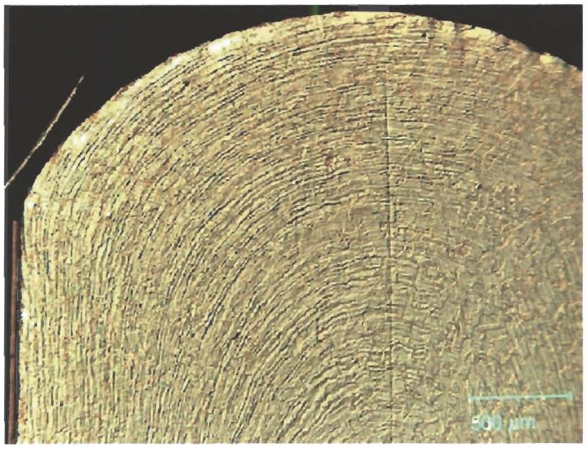

Fig 6.4: Micrograph A: edge barrelling

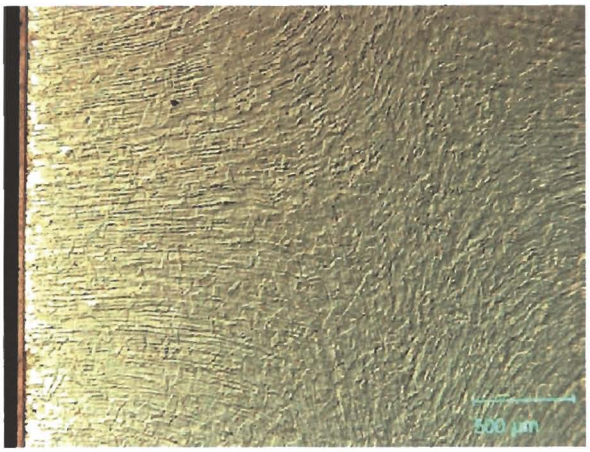

Fig 6.5: Micrograph B: surface centre

From these micrographs the flow of the material can be seen. The point at which the material rolled over the circumferential edge can also be seen in the micrograph below.

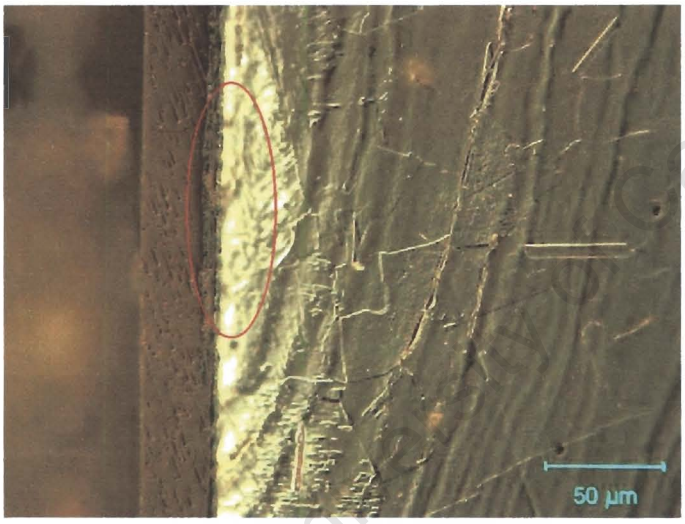

Fig 6.6: Micrograph C: stick/slip interface

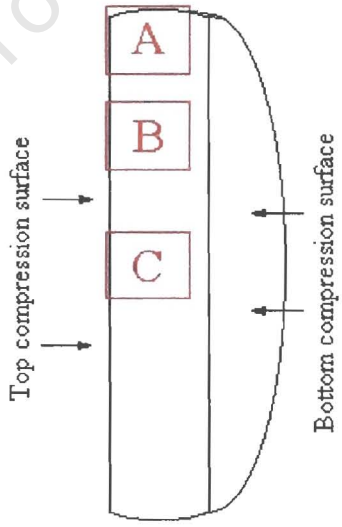

Fig 6.7: Micrograph Positions

University of Cape Town

Processing of Results:

Flow curves obtained for the material can be seen as APPENDIX A. These curves were fitted to an equation to give stress as a function of strain, strain rate and temperature. This was done in order to smooth noise on the curves and irregularity in trends of temperature and rate effects on the positions of the curves. A description of the formulation of this equation is given in the following chapter.

Constitutive Equation Formulation

In order to insert the material data into the Abaqus simulation, it was necessary to fit the data to a function describing the flow stress (σ) as a function of strain (ε), strain rate ($\dot{\varepsilon}$) and temperature (T). The experimental results could have been inserted almost directly into the simulation due to the fact that the range of data needed was almost covered by the experimental data with very little need for extrapolation. However it was felt that if the data could be fitted to a function which accurately fitted the experimental data, trends of the influence of strain rate and temperature would be smoothed out, and noise in each stress-strain flow curve would be removed. The latter was especially important as noise in the flow curves would directly cause numerical instability and noise in the numerical simulation.

However, unless the form of the equation was correct for the data concerned, fitting the test data to a function, and using that function to produce the tabular data for the numerical simulation, would simply result in loss of accuracy of the most crucial aspect of the simulation. Many of the articles in the literature review used equations which try to impart some physical meaning to the constants used in their equations for stress relationships. This seems to be done for two reasons:

Firstly, many of the equations are used for extrapolating the experimental data into the range of strain rate and temperature needed. Thus the use of constants with physical meaning, can debatably, give some assurance of the validity of extrapolation.

Secondly, many of the equations try to include constants such as initial grain size and activation energy and others in an attempt to make the functions compatible with later research on recovery and recrystallisation kinetics.

University of Cape Town

In reviewing stress relationships for steel in the literature, the following forms were investigated.

H.J. McQueen at Concordia University Ref.[30] does a thorough examination of the current constitutive methods for prediction of flow stress. He proposes the following models for predicting flow stress of AISI304 as a function of strain, strain rate and temperature. The table below gives the constants in the equations; some are material constants and others are merely scaling factors.

$$A(\sinh(\alpha\sigma)^n = \dot{\varepsilon}\exp(Qhw/RT) = Z$$

$$\varepsilon_p = BD_o^{-0.75}\, Z^{0.125}$$

$$\sigma_p = (1/\alpha)\sinh^{-1}[\dot{\varepsilon}/\dot{\varepsilon}_n \exp\{Qhw/R[(1/T)-(1/T')]\}^{1/n}$$

$$\sigma/\sigma_p = [(\varepsilon/\varepsilon_p)\exp(1-\varepsilon/\varepsilon_p)]^{C'}$$

Material constants	value	units
grain size, Do =	7.00E-05	m
activation energy, Qhw =	3.63E+05	J/mol
stress exponent, ηhw =	4.6	
Ahw =	14.66	
characteristic temp, T' =	1424	K
a' =	3.30E-03	Pa^-1
b' =	0.24	
C' =	0.216	0.216
B' =	1.80E+00	
R =	8.31	
strn rate n =	1	
α =	0.12	

Miguel A. Cavaliere *et al.* [24], used the following relationship for :

$$\sigma = \sigma_s\sqrt{1-e^{\Omega.\varepsilon}}$$

Where σ_s = 125.36 Mpa

Ω = 12.046

Ashok Kumar *et al.* [18] , used the following relationship:

$$\sigma = \frac{1}{\alpha}\sinh^{-1}\left(\frac{\dot{\varepsilon}\exp(Q/RT)}{A}\right)^{1/n}$$

Where Q, n, and $\mathrm{Ln}(A) = \frac{A_i}{\varepsilon^{B_i}} + C_i$

Devadas *et al.* (part 2) [12] , considered the following relationships:

$$\sigma = a + b\,Ln(\varepsilon) \quad , \quad \sigma = c\,\varepsilon^n$$

& $\sigma = a_0 + b_0\varepsilon^{0.4} + c_0\varepsilon^{0.8} + d_0\varepsilon^{1.2}$ for strain dependence.

$\sigma = C_1\dot{\varepsilon}^m$ for rate dependence, combining to give:

$$\sigma = A\varepsilon^n\dot{\varepsilon}^m\exp(Q/RT)$$

University of Cape Town

Baragar [12], compared the experimental results with the empirical relationships:

1. $\exp(\beta\sigma) = A_1\dot{\varepsilon}\exp(Q/RT)$
2. $(\sinh(\alpha\sigma))^n = A_2\dot{\varepsilon}\exp(Q/RT)$
3. $\sigma = b + c\varepsilon^{0.4} + d\varepsilon^{0.8} + e\varepsilon^{1.2}$

Baragar found that equation 1 fitted better than eqn 2, although even eqn 1 only fitted sections of the data adequately. Eqn 3 worked well for fitting the strain dependence.

\- \- \-

Unfortunately, it was found that many of the relationships used sacrifice accuracy in fitting the training data to accomplish the requirements described at the beginning of the section. Since this project was not concerned with extrapolation, nor static recovery and recrystallisation, use of such equations held none of the benefits described above and imposed the loss of accuracy.

Thus the approach used in this project was to very carefully study the trends and dependencies in the experimental data, and formulate an equation to describe the stress relationship, so as to remain as true to the original data as possible, with the strict consequence of not being able to use the equation for extrapolation.

The Product of Dependencies Approach

The reasonably well known Johnson-Cook Equation is as follows:

$$\sigma(\varepsilon,\dot{\varepsilon},T) = \left[A + B\varepsilon^n\right]\left[1 + C\,\mathrm{Ln}\left(\frac{\dot{\varepsilon}_{pl}}{\dot{\varepsilon}_0}\right)\right]\left[1 - \left(\frac{T - T_{trans}}{T_{melt} - T_{trans}}\right)^m\right]$$

This formula works on the principle of fitting the dependencies of each variable (contained in each square bracket) and multiplying the terms together to obtain a function of all three variables. This "product of dependencies approach" is far easier to understand as it can be broken down and analysed for correctness of form in each variable's part. This approach was used in obtaining the equation used to fit the experimental data in this project.

University of Cape Town

Strain Dependence

The most complex dependence to model accurately was that of strain. Exponential relationships used in many equations did not fit the data well. Natural log relationships were more accurate, but gave negative stress values for low strains when incorporated in the final equation. The best fit obtained from standard equations was given by the following form:

$\sigma = a_0 + b_0\varepsilon^{0.4} + c_0\varepsilon^{0.8} + d_0\varepsilon^{1.2}$ although, since the flow curve should pass through the origin, the constant a_0 could be omitted, and the best fit was found using the powers: 0.38, 0.50 and 0.83 instead of the powers: 0.4, 0.8, 1.2.

Thus the first square bracket took the form:

$$\sigma:(\varepsilon) = \left[A_1\varepsilon^{0.38} + A_2\varepsilon^{0.50} + A_3\varepsilon^{0.83} \right]$$

Strain Rate Dependence

The strain rate dependence of the model was investigated by comparing tests at the same temperature and analysing the effects of strain rate on stress, for given strains. Taking the natural log of the strain rate and plotting it against stress yielded a set of almost straight lines. Adding a constant to the $\mathrm{Ln}(\dot{\varepsilon})$ value shifted the curves so that the fitted curve passed through the origin, thereby reducing the number of constants needed in solving the linear regression. The following plot shows the relationship:

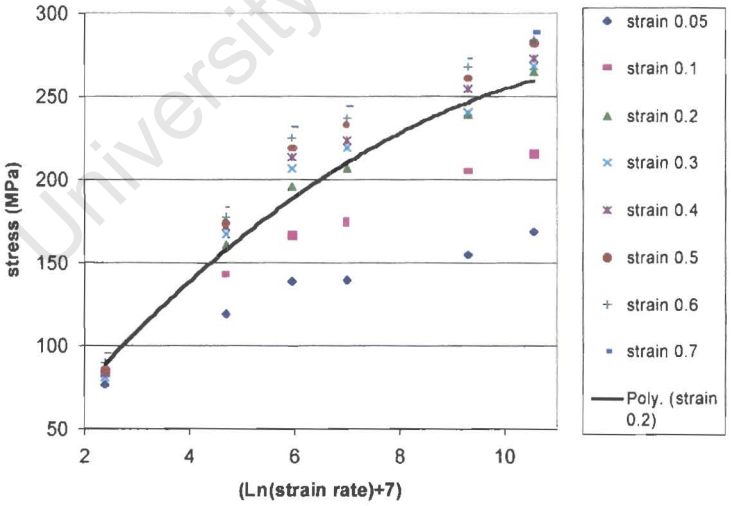

Fig 6.8: Plot showing rate dependence of flow stress at 950^{0}C

Thus the 2nd square bracket took the form:

$$\sigma:(\dot{\varepsilon}) = \left[B_1(\mathrm{Ln}(\dot{\varepsilon}) + 7) + B_2(\mathrm{Ln}(\dot{\varepsilon}) + 7)^2 \right]$$

University of Cape Town

Temperature Dependence

This was analysed similarly to the strain rate dependence. A constant was subtracted from temperature values to obtain curves that passed through the origin. Plotting stress vs. (Temperature-1500) yielded the following set of curves, each of which could be fitted to a quadratic equation such as the one shown below.

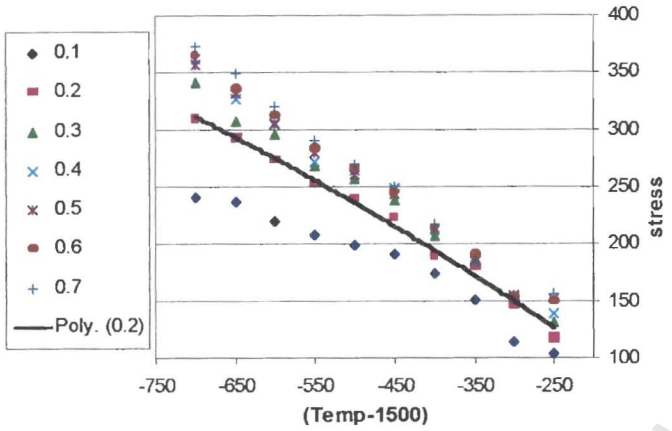

Fig 6.9: Plot showing temperature dependence of flow stress at 950^{0}C

Thus the 3rd square bracket took the form:

$$\sigma:(T)=\left[C_1(T-1500)+C_2(T-1500)^2\right]$$

Final Formulation

The final equation became simply the product of the individual dependencies:

$$\sigma:(\varepsilon,\dot{\varepsilon},T)=\left[A_1\varepsilon^{0.38}+A_2\varepsilon^{0.50}+A_3\varepsilon^{0.83}\right]\left[B_1(\mathrm{Ln}(\dot{\varepsilon})+7)+B_2(\mathrm{Ln}(\dot{\varepsilon})+7)^2\right]\left[C_1(T-1500)+C_2(T-1500)^2\right]$$

Or, by substitution:

$$\sigma:(\varepsilon,\dot{\varepsilon},T)=\left[A_1X_1+A_2X_2+A_3X_3\right]\left[B_1Y_1+B_2Y_2\right]\left[C_1Z_1+C_2Z_2\right]$$

The constants in this equation were solved in Excel using multiple linear regression (see table 6.1). The regression obtained a 98,9% correlation to the original test data. The equation was then used to produce an interpolated data sheet of flow curves for 8 strain rates and 10 temperatures for each rate, within the range of the training data, as well as curves for 1300 ^{0}C. The data sheet was inserted directly into the Abaqus code and together with the specified Young's Modulus, resulted in a temperature and rate sensitive elasto-plastic material model.

coefficient number		17	16	15	14	13	12	11	10
variable product		Y2Z2	Y2Z1	Y1Z2	Y1Z1	X3Z2	X3Z1	X2Z2	X2Z1
coeff value		**-1.715E-05**	**-0.01206**	**0.0001524**	**0.098746**	**-0.01129**	**-8.1649**	**0.017322**	**11.1641**
	9	8	7	6	5	4	3	2	1
	X1Z2	X1Z1	X3Y2	X3Y1	X2Y2	X2Y1	X1Y2	X1Y1	const
	-0.00555	**-2.9629497**	**-61.1385**	**553.41685**	**87.39399**	**-762.541**	**-29.943**	**261.1527**	**-70.8188**

Table 6.1: Coefficients as solved by linear regression

University of Cape Town

Chapter 7: Part B: Thermodynamic Modelling

Modelling of conduction, radiation and convection heat transfer to and from the billet and roller was added to the basic mechanical simulation. Specific heat and thermal expansion were also incorporated in the model. Values for all heat transfer coefficients were taken from literature, mostly from Ref [48].

The roller was assumed isothermal and set at a constant temperature of 100^0C, the boiling point of the water coolant. Although it is well known that the temperature of the roller is far from constant during rolling, modelling of the thermal behaviour would have meant fine meshing of the roller in order to define the curved surface of the roller accurately enough to avoid roll force noise. This would not have made a significant difference to the chilling effect of the rolls and would have greatly increased the computational expense of the simulation, and imposed a much coarser billet mesh in order to achieve realistic run times.

The billet was set to an initial homogenised temperature of 1240^0C due to the fact that the billets are reheated to this temperature in the reheat furnace for several hours before rolling. The billet was then allowed to cool in the simulation due to radiation and convection to the environment until the surface temperature was equal to the surface temperature measured just before the 1st rolling pass. Thus a thermal gradient existed in the billet very similar to the gradient of the billet at the Columbus mill just prior to rougher rolling.

University of Cape Town

Radiation heat transfer to the environment was modelled using the following equation:

$$Q_{radiation} = \varepsilon.\gamma\left[\left(T-T_Z\right)^4-\left(T_0-T_Z\right)^4\right]$$

and Convection heat transfer to the environment was modelled using the following equation:

$$Q_{convection} = -h\left[T-T_0\right]$$

Where: ε = material surface emissivity

γ = Stefan Boltzmann Constant

T = material temperature

T_0 = environment temperature

T_Z = Absolute zero temperature

h = coefficient of convection heat transfer

Gap heat transfer between the billet and roller was modelled as follows:

Clearance & pressure dependent gap conduction:

Because there is heat conducting lubricant in and around the roll gap, heat conduction was modelled with a clearance dependence prior to contact. The value of the conduction coefficient was made zero for clearances greater than 10mm, and increased exponentially to 2/3 of the conductivity of the material on initial contact. After contact the value of the conduction coefficient was dependent on pressure, reaching full conduction at 20 Mpa (an estimate of pressure needed to achieve full face contact). This was done to model the behaviour of asperities and crushable oxide at the billet/roller interface.

Clearance dependent gap radiation:

Radiation heat transfer between the billet and roller was modelled using a clearance dependent scale factor on the value of radiation heat transfer between the billet and roller. The radiation heat transfer was determined by the same equation as radiation to the environment described above, except that the environment was in this case, the roller. This heat transfer was then scaled according to the clearance, due to the interference of lubricant presence in the clearance space. The scale factor therefore decreased exponentially from 95% on contact, to zero at a distance of 10mm.

University of Cape Town

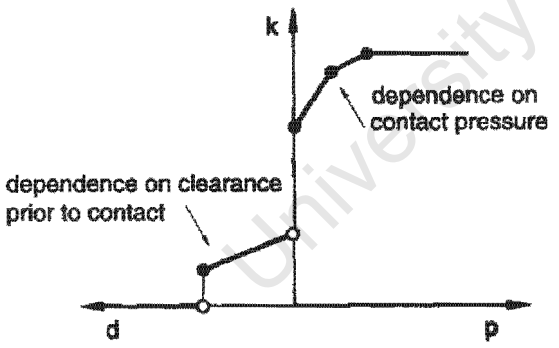

Fig 7.1: e.g. of conduction coefficient dependence on displacement & pressure

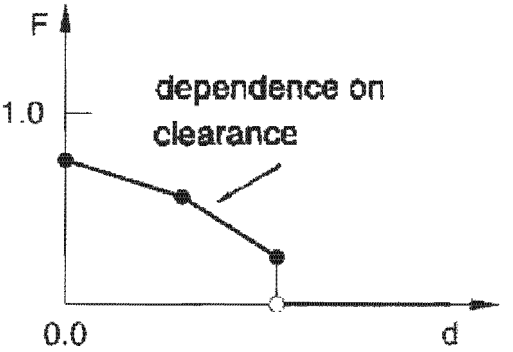

Fig 7.2: e.g. of radiation factor dependence on displacement

Heat generated by plastic work was incorporated into this model using the equation:

$$r^{pl} = \eta\sigma : \dot{\varepsilon}^{pl}$$

Where r^{pl} denotes the heat flux added to the thermal energy balance, σ is the stress matrix, $\dot{\varepsilon}$ is strain rate and η is a coefficient defined by the user. Note that the colon represents the sum of the matrix conjugate products. Specific heat and thermal expansion were also incorporated in the model. Values for coefficients were taken from literature.

Heat generation due to sliding friction between the roller and billet was also included. All energy lost due to slipping at the billet/roller interface was assumed to be converted into heat energy transferred, and divided equally between the billet and roller.

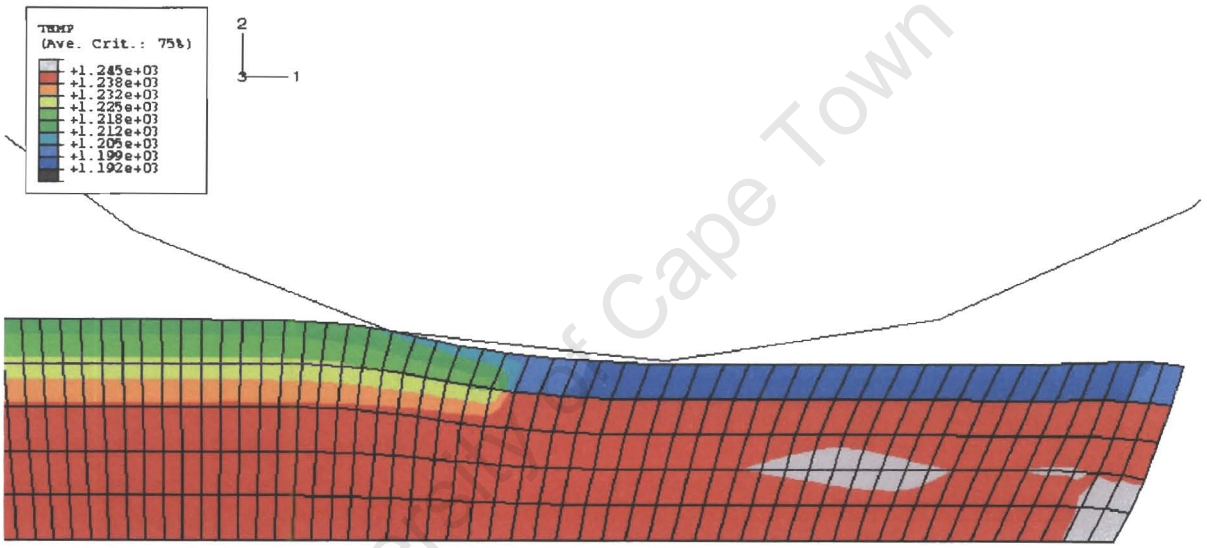

Fig 7.3: Diagram of the temperature distribution in the FEM model

University of Cape Town

Chapter 8: Part C: Mechanical Modelling

The model was constructed as a 2D, seven pass thermo-mechanical model. The billet was modelled using 6250, 4 noded plane strain continuum elements with an extra temperature degree of freedom. These elements use bilinear shape functions with a single (reduced) integration point, and incorporate visco-elastic hourglass control.

The model made use of the fact that the process is symmetrical about the centre of the billet, and so the simulation could be modelled as a ½ model with only the upper roller, and the midline nodes constrained in the y – direction. Elements were given a 1:8 initial aspect ratio to avoid excessive distortion and element locking in later passes. Although the simulation was formulated as a 2D plane strain model, the billet was given a constant width in order to calculate the roll forces, i.e. spread was not taken into account. The specified width was the width of the billet before the 1st pass.

The roll velocity conditions were taken from the existing roll schedule, and the billet was given an initial velocity equal to the x component of the velocity at the point of 1st contact on the roller. This was done to minimise the shock force on the roller and billet when feeding the billet into the 1st pass.

The roller was modelled as a rigid body (analytical ridged surface) as it was felt that the temperature of the billet relative to that of the roller would make the deformation of the roller very small relative to the deformation of the billet.

The model used a basic Coulomb Friction model with a specified maximum value of friction before shearing of the billet material took place.

The elastic properties of the material were included in the simulation, even though they have little significance due to the large plastic deformations during rolling.

The plastic flow curves of the material were calculated from the equation developed earlier, and grouped in sets of strain rate and temperature and strain, in ascending order. The material properties were assumed to be isotropic throughout the simulation.

The value for density was taken from literature as

University of Cape Town

Mass scaling was used to speed up the simulation run time by artificially increasing the mass of the billet elements and thus increasing the stable time increment. The value by which the model was scaled was chosen carefully so as to increase the computational efficiency the most, without causing inertia effects to cause inaccuracy in the solution. This was done by ensuring that the total kinetic energy (strongly affected by mass) remained less than 5% of the total internal energy.

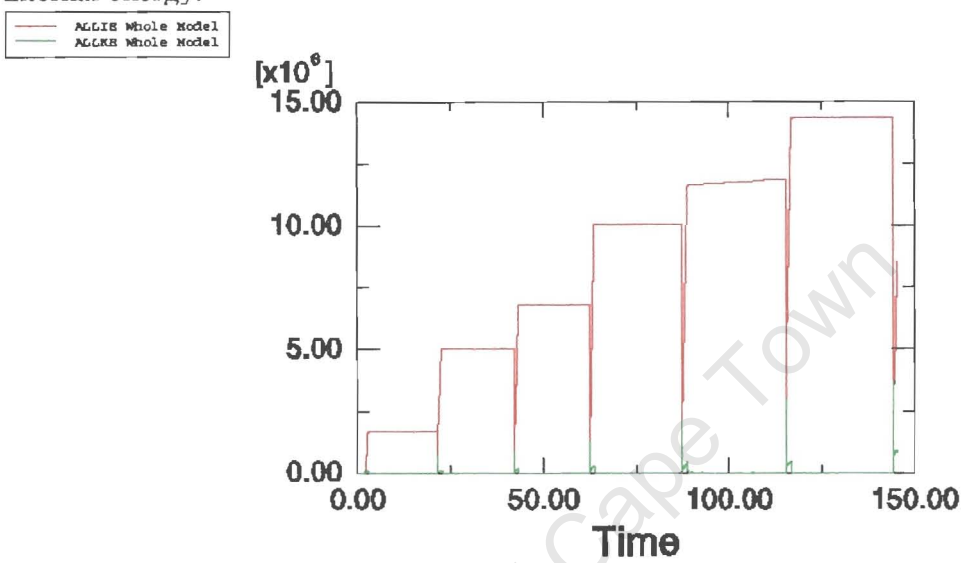

Fig 8.1: Plot of the internal (ALLIE) and kinetic energy (ALLKE) of the model

Due to the large noise generation in the plot of roll forces, a "soft-contact" algorithm was used as an attempt to model the behaviour of progressive loading pressure between two surfaces with asperities which deform as the surfaces come into contact. This required defining the degree of surface roughness (an estimate) and the desired value for pressure on non-penetrating, fully contacting surfaces. The algorithm applied an exponentially increasing corrector force (maximum stiffness equal to Young's Modulus) in cases of predicted penetration (over-closure) of surfaces, and incorporated some damping on the corrector force response.

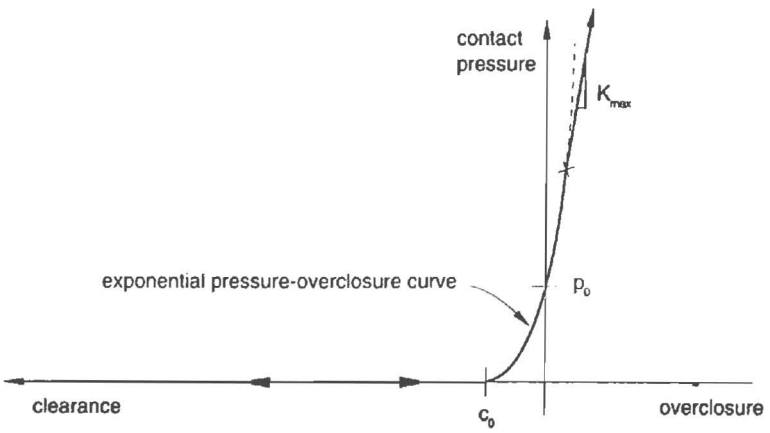

Fig 8.2: Plot showing the "soft contact" pressure vs distance relationship

University of Cape Town

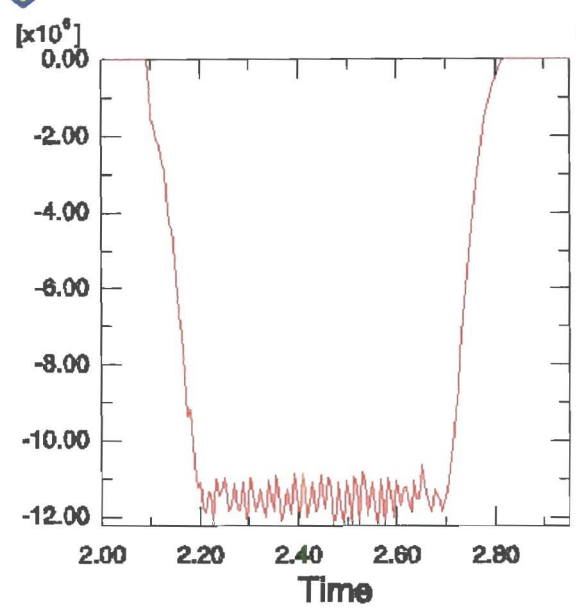

Fig 8.3: Plot of roll forces without soft contact

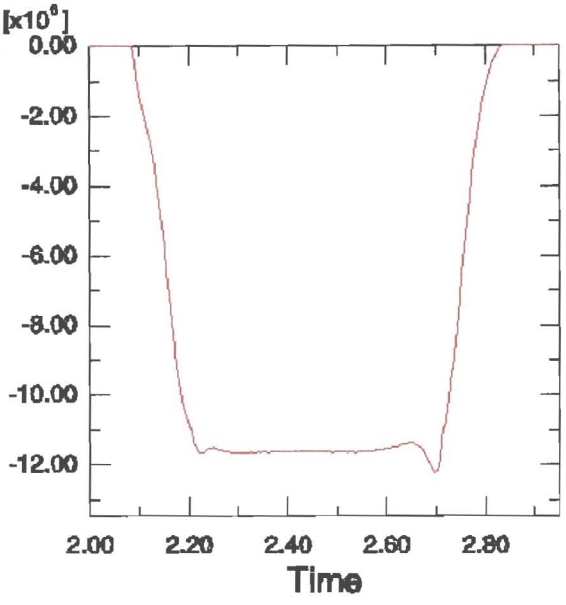

Fig 8.4: Plot of roll forces with soft contact

Work was done investigating the numerical effects of manipulating the value of the coefficient for corrector force damping. This was quite successful in reducing the noise generated in plots of rolling force. The noise seemed to increase dramatically in later passes due to element distortion and increasing numerical instability. However, since static recovery and recrystallisation are not taken into account in this project, the predictions for passes after the first pass would be over estimates due to these softening effects. Thus noise on these plots is not of significant importance.

University of Cape Town

Chapter 9: Results of the Project

Many of the variables in the simulation have been investigated specifically and scientifically, while others are merely drawn from general physical knowledge and engineering judgement. For those variables, whose values have been the subject of research, the results are varied even in each single source, resulting in a range of "acceptable" values. For other variables, whose values have not been directly investigated, there also exists a range of seemingly fair values that could be used, and these are subject to debate, since they have not been proven experimentally. Thus, both the thermal and mechanical results of the simulation are easily manipulated, by changing the values of variables within the "acceptable" range. Some of these effects will be discussed.

PASS NO	SLAB ID	GAUGE IN [mm]	GAUGE OUT [mm]	ROLL FORCE [kN]	ROLL VEL [m/s]	SURF TEMP [°C]
1	3276943	202.4	164.1	14340	1.400	0
2	3276943	164.1	129.5	17779	1.512	969
3	3276943	129.5	94.6	22549	1.994	1037
4	3276943	94.6	60.5	28100	2.500	1044
5	3276943	60.5	39.0	27096	2.909	1089
6	3276943	39.0	25.2	26529	3.399	1073
7	3276943	25.2	20.8	18248	4.811	1044

Table 9.1: Typical rougher mill roll schedule at Columbus Stainless

Effects of Variable changes within the "acceptable" range

Friction Coefficient

The coefficient of friction in a Coulomb friction model has been shown to affect the roll forces quite dramatically [Ref. 43, 44, 45]. Lubricated coefficients range from 0.24 to 0.28, while unlubricated values range from 0.3 to 0.35. Since the rougher mill being modelled uses only water as a coolant of the rollers, the range of 0.26 to 0.34 was investigated.

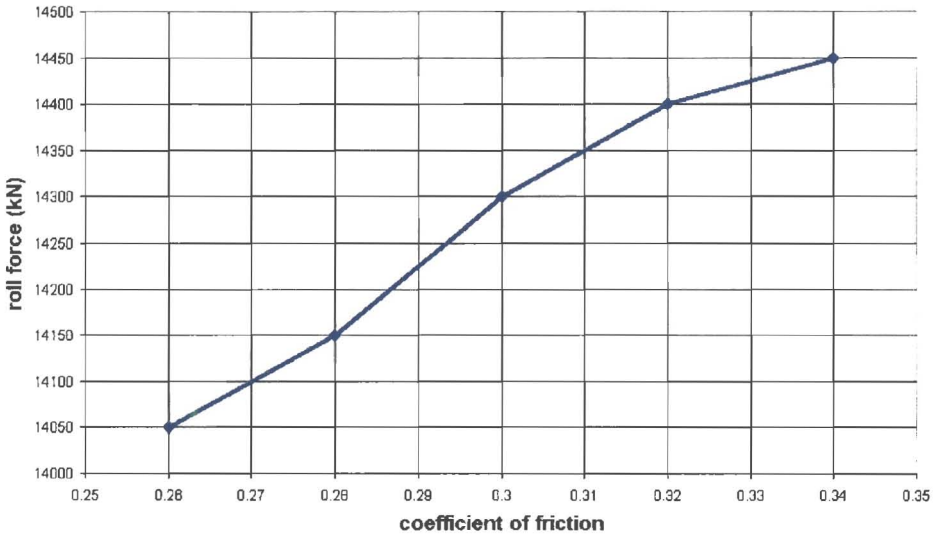

Fig 9.1: Effect of friction coefficient on roll forces for the 1st pass

University of Cape Town

It can be seen from fig 9.1 that the change in the value used during the first pass for the friction coefficient results in a 2.8% variation in roll force prediction. This sensitivity is also related to the billet and roll geometry and thus the friction coefficient sensitivity was also investigated on the seventh pass.

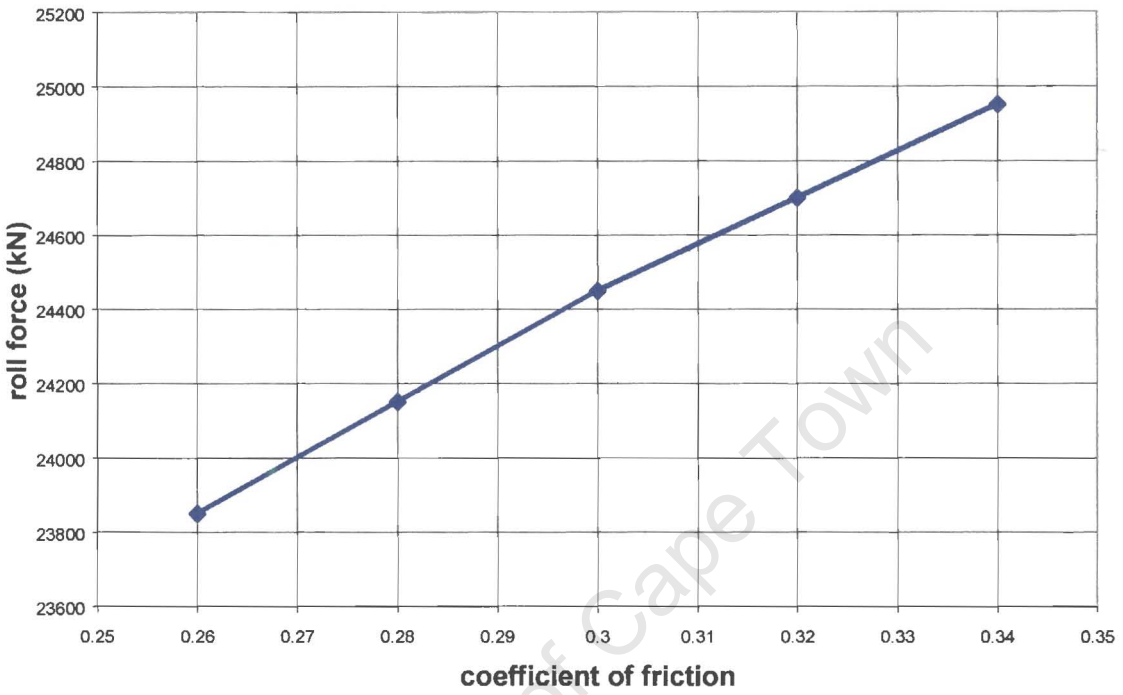

Fig 9.2: Effect of friction coefficient on roll forces for the 7th pass

As would be expected due to the longer contact length, the friction sensitivity is slightly larger at 4.6%. This means that the sensitivities on the friction coefficient for all the passes on the roughing mill should lie between 2.8 and 4.6%.

Friction Limit

The friction model used in the simulation set a maximum frictional force at which the shear yield at the interface was reached. This is an important feature in a simulation where contact forces result in plastic deformation. The shear yield stress was not known. It is not the same as the yield stress of the material as lubricant and oxide is present at the roll/billet interface. It was therefore estimated.

University of Cape Town

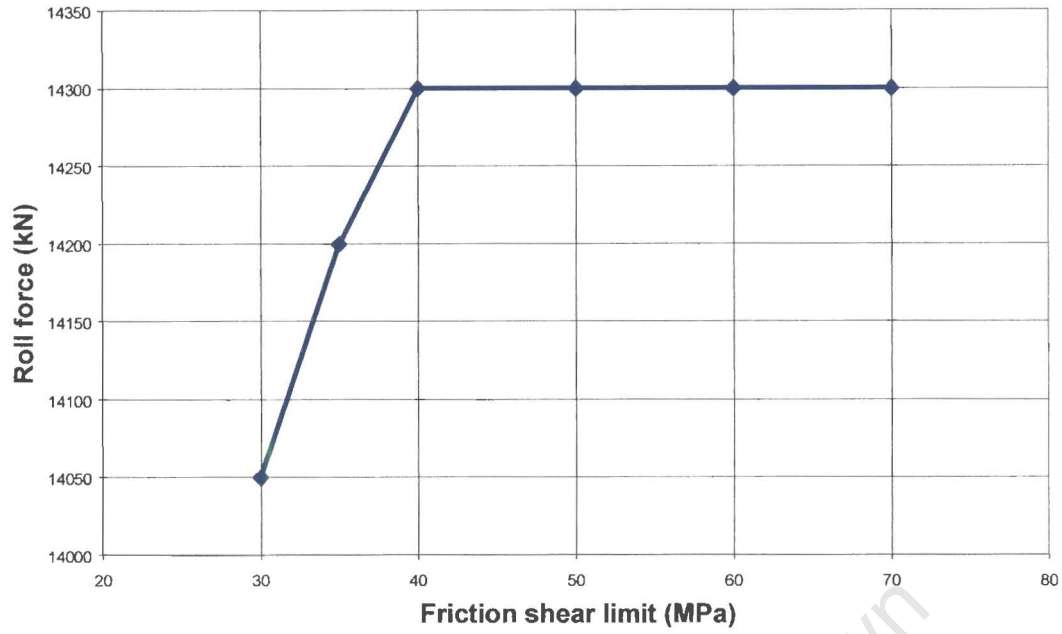

Fig 9.3: Effect of friction limit on roll forces for the 1st pass

From this plot it would seem that the material shear stress at the interface is around 40 MPa, and that setting the friction limit higher than this value makes no difference to the roll forces.

Element mesh refinement

A parametric study showed more effect on the noise on the roll force plot than on the roll force value. This effect was due to the effect of mesh refinement on the definition of the billet surface and the subsequent effect on contact definition used in the prediction of roll forces. This is a significant result, since mesh refinement drastically affects the computational efficiency of the simulation and means that noise smoothing using curve fitting could be used rather than mesh refinement as a means of obtaining an accurate result.

Although aspect ratios of up to 10:1 can be used successfully in some applications, the closer the aspect ratio is to 1:1, the better the accuracy. The internal angles of the elements should also be kept as close to 90^0 as possible. In order to model all 7 passes of the schedule, the original billet was meshed with an aspect ratio of 1:8 which by pass 7 became about 8:1. However, for the parametric study an aspect ratio of 1:2 was used since only the 1^{st} pass was studied.

The effect of mesh refinement on the roll forces was shown by keeping the aspect ratio of the elements the same for all mesh versions. The number of elements in the thickness direction was altered and the number of elements in the length direction was calculated according to the element aspect ratio.

University of Cape Town

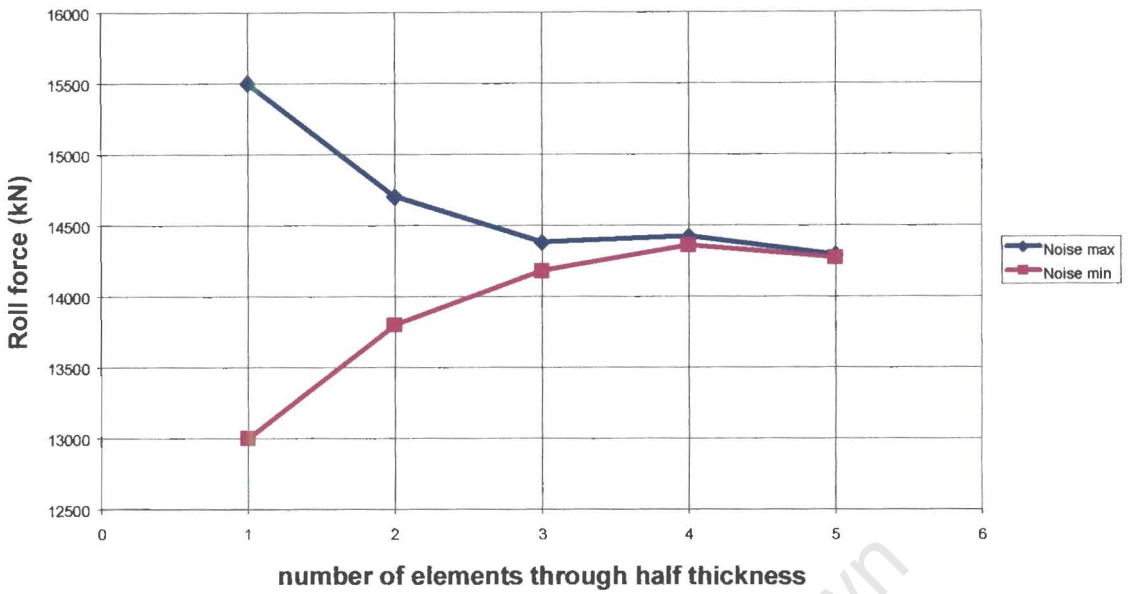

Fig 9.4: Effect of mesh refinement on roll forces for the 1st pass

This plot shows that as far as the noise and accuracy of the roll forces are concerned, 5 or 6 elements through the half thickness of the billet are enough to give an accurate value of roll force for the first pass. However, due to element distortion, the noise increases with each pass and thus more elements are needed for the later passes.

Oxide thickness

In the soft contact algorithm used in the simulation, the distance over which the contact force is applied, must be specified. This may be given physical meaning by the presence and thickness of the oxide layer at the roll/billet interface.

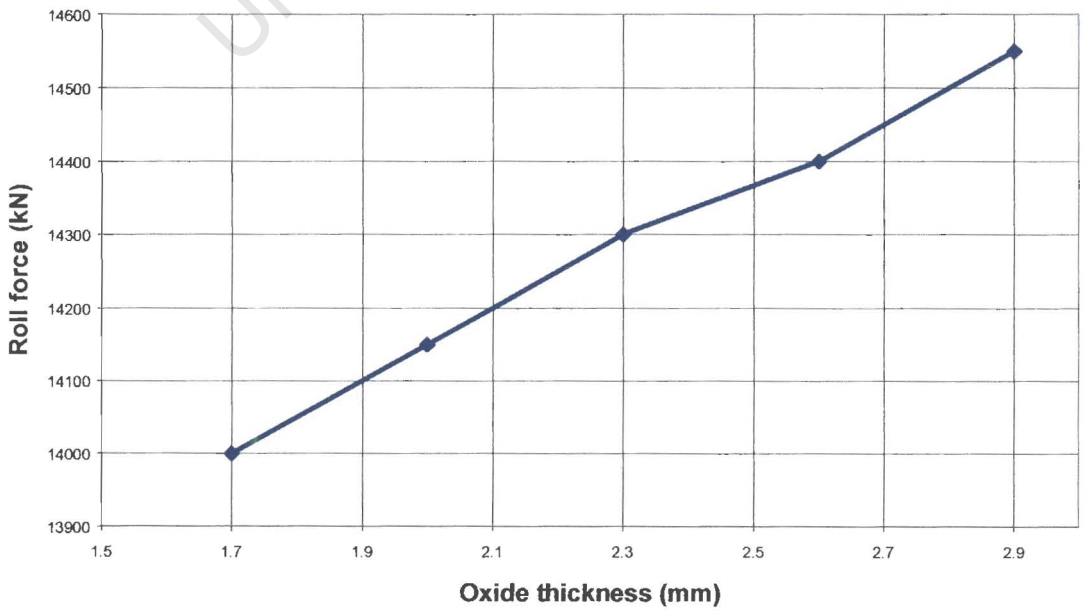

Fig 9.5: Effect of oxide thickness on roll forces for the 1st pass

University of Cape Town

This result is understandable, since increasing the oxide thickness, increases the arc length on the roller over which the normal force is applied, thus increasing the total roll force. The oxide thickness also affects the ratio of steel to oxide and therefore the net compressibility. The variation in oxide layer thickness shows a 3.8% variation in roll force prediction.

Oxide layer yield stress

In the soft contact algorithm used in the simulation, the stress at which full contact occurs must be specified. This may be given physical meaning by the presence and yield stress of the oxide layer at the roll/billet interface.

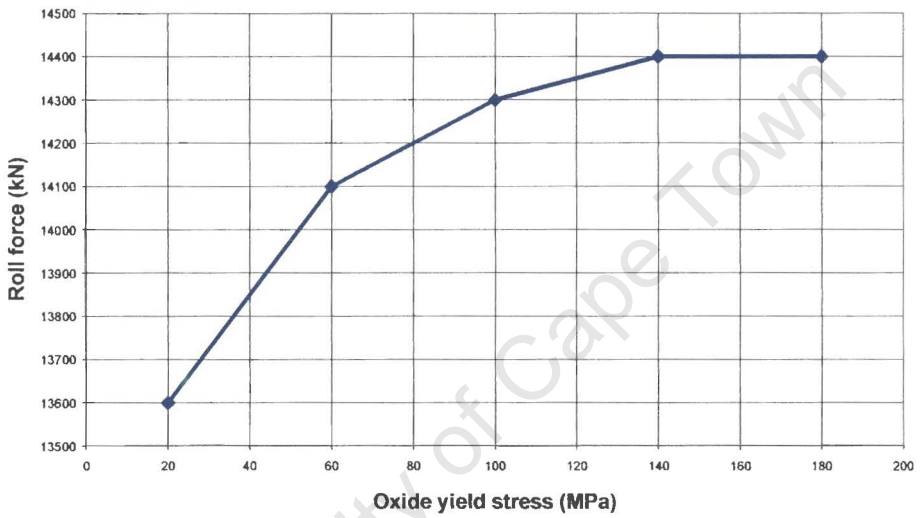

Fig 9.6: Effect of oxide yield stress on roll forces for the 1st pass

This result is understandable, since the roll forces should increase as the yield stress of the oxide approaches the yield stress of the billet material. After this point, increasing the oxide strength will make no difference to the roll force, as the billet material will yield preferentially to the oxide layer. The variation in oxide strength shows a 5.7% variation in roll force prediction.

Comparison of thermal performance

Validating the thermal modelling of the simulation from the roll schedule proved difficult due to the inaccuracy of actual measured values. The surface temperature is quite dynamic. Heat is lost through convection and radiation to the environment and also to the rollers. Heat is gained on the surface due to frictional effects, and through thickness due to plastic work done Thus the surface temperature drops as it passes through the roll gap, and heats up again in the interpass time due to the heat generated in the billet being conducted to the surface.

University of Cape Town

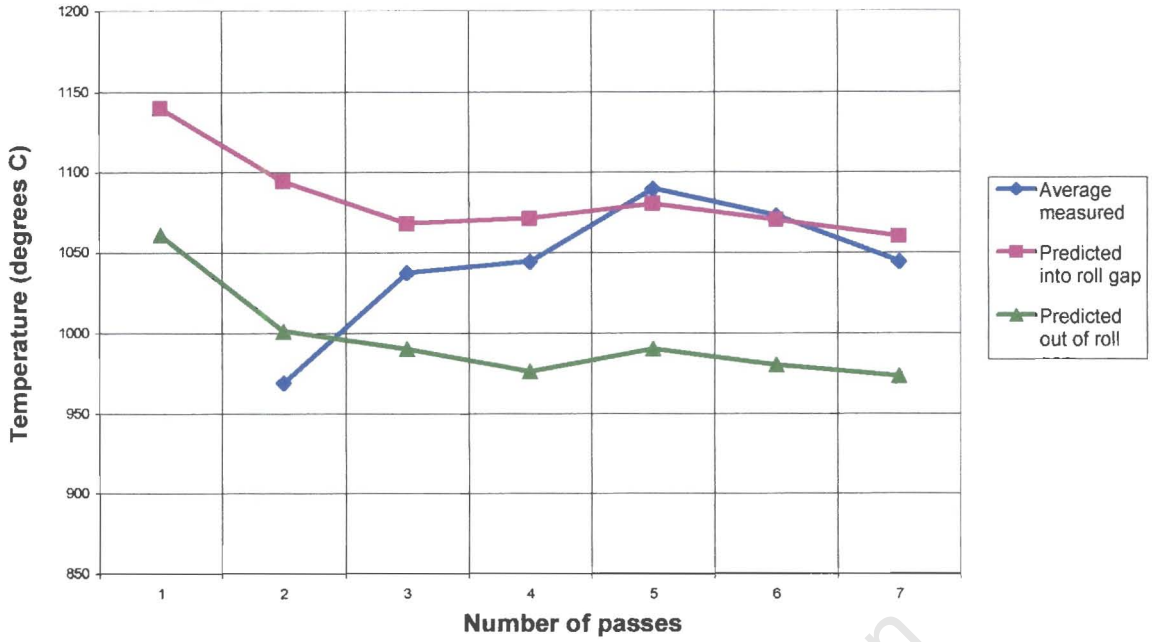

Fig 9.7: Comparison of measured and predicted thermal performance

The above figure shows a fairly consistent drop of around 90^{0}C as the billet passes through the roll gap. The average temperature drops in the early passes due to the higher losses to the environment and smaller % reductions, but increases slightly in later passes due to the reduction in heat lost to the environment and the larger reductions of later passes.

Comparison of roll force performance

As already outlined, the scope of this project did not include the modelling of static recovery and recrystallisation kinetics. However, since the finite element software was able to zero strain distribution at any given time, two versions of the model were formulated. The first model (version A) zeroed the strain between passes, simulating the effects of complete recovery and recrystallisation between passes. The second model (version B) retained strain between passes and thus accumulated strain for all 7 passes. It was expected that the measured roll forces would fall between those obtained by the two models. However this was not the case and roll force predictions for both models were almost identical. The close agreement of the roll forces between the two versions is understandable due to the early peak in the flow stress at high temperatures. As the simulation progresses to the later passes, the billet surface temperature fluctuates between 980 and 1070^{0}C, neither steadily rising nor steadily cooling. Because the gauge becomes thinner towards the last pass, the centre temperature drops significantly. However, the centre temperature is still well above 1100^{0}C and thus the peak stress is still found at low strains, resulting in little difference between the two versions even in later passes.

University of Cape Town

The assumption of plane strain conditions was also tested by formulating a 3-dimensional model with identical geometry and comparing the results of spread and roll force predictions, with those obtained under the 2-dimensional plane strain assumption. The spread obtained was small and made very little difference to the force predictions, even in later passes. Thus the 3D version was not used for further analysis due to its significantly longer processing times.

The force predictions correlated well with the roll forces measured at the Columbus mill for the first 4 passes and then diverged during passes 5, 7 and 7. At first, it was thought that this was probably due to excessive distortion of elements in the later passes. However, it is also known that after descaling before the first pass, the oxide layer grows in thickness during the rolling process and small flakes of oxide even detach during the rolling of later passes. For this reason a third model was formulated with a changing friction shear limit to approximate the decrease in oxide adhesion strength. This shear limit was reduced in the last three passes progressively to a value of 20 MPa in pass 7. This third model was very successful in matching the measured roll forces through all 7 passes. While the modelling of the oxide adhesion strength is lacking in experimental validation, the result does show that the roll force prediction is sensitive to this physical phenomenon in a way which could at least in part account for the discrepancy in the force predictions of the last three passes.

University of Cape Town

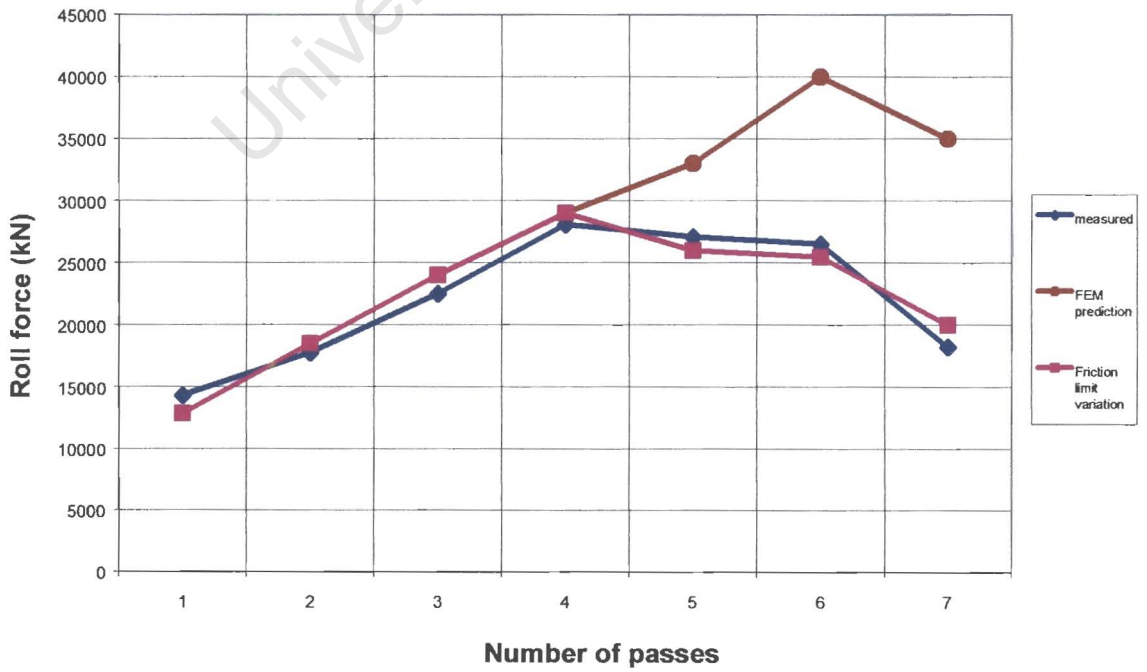

Fig 9.8: Comparison of roll force performance

Chapter10: Conclusions

The project definitely achieved its goal in providing a useful model for investigating the rolling process and for predicting the roll forces at the mill at Columbus Stainless. It also appears to have succeeded in modelling most of the heat transfer accurately. The model should prove useful in developing an understanding of the magnitude of heat loss due to various factors in the rolling process as well as gaining an appreciation of the thermal gradient and distribution through the billet and its relation to surface temperatures.

The sensitivity of the roll force prediction to many of the physical sub-models (e.g. friction and contact algorithms) and variables within the model, means that at this stage, the model is not in itself a reliably accurate tool for roll force prediction in the development of new roll schedules. However, the simulation does demonstrate an ability to accurately model the physical behaviour of the material and with further research into some of the physical phenomena affecting roll force prediction, should become a vital tool in the understanding and prediction of many aspects of the hot rolling process.

The material testing for this project has provided both the University and Columbus Stainless with the valuable knowledge of the dependence of flow stress on strain, temperature, and strain rate for 304 stainless steel in the annealed condition. The wide range and extensive nature of the training data should allow accurate interpolation within the hot working range.

The rolling simulation accesses this data directly and makes no adjustment for static recovery and recrystallisation. Thus the rolling simulation will tend to over-predict the roll forces increasingly after pass one.

University of Cape Town

Chapter 11: Recommendations for Future Work

Unfortunately the recommendations for future research in this area are both extensive and complex. The simulation makes many assumptions in the thermal and mechanical modelling. Some of these assumptions have been validated in literature, while some are merely exercising engineering judgement and are in need of experimental validation. Thus this project serves only as a foundation from which a more accurate and realistic model should be developed.

Values of the friction coefficient are of particular importance since they affect the prediction of roll forces very directly and are functions of pressure, oxide layer thickness, lubricant composition and possibly other variables such as temperature. The friction behaviour and oxide growth and properties need to be investigated further.

The cooling dynamics and heat generation by plastic work also needs to be investigated as the material is very temperature sensitive and the modelling of the temperature is very sensitive to the thermal coefficients used in the simulation. The growth and material properties of the oxide layer, and its effect on heat transfer also requires further attention.

Validation of strain could be done by inserting scribed pins in the billet material before rolling on a test mill. The billet could then be sectioned and the strain of the pins assessed and compared to the model.

Validation of the thermal gradient throughout the roughing process could be done (and has been done in the literature) by inserting thermocouples (type K) into the billet through its thickness prior to rolling on a test mill. The temperature rise and thermal distribution could then be compared to that obtained by the simulation.

Optical pyrometers could be used to take surface temperature measurements at frequent intervals and in different positions during the roughing process.

All these validation procedures should be done before the model is considered for expansion towards microstructural prediction. Only at this stage would the extensive flow stress experimental work and microstructural examination be a worthwhile addition to the research in this area.

University of Cape Town

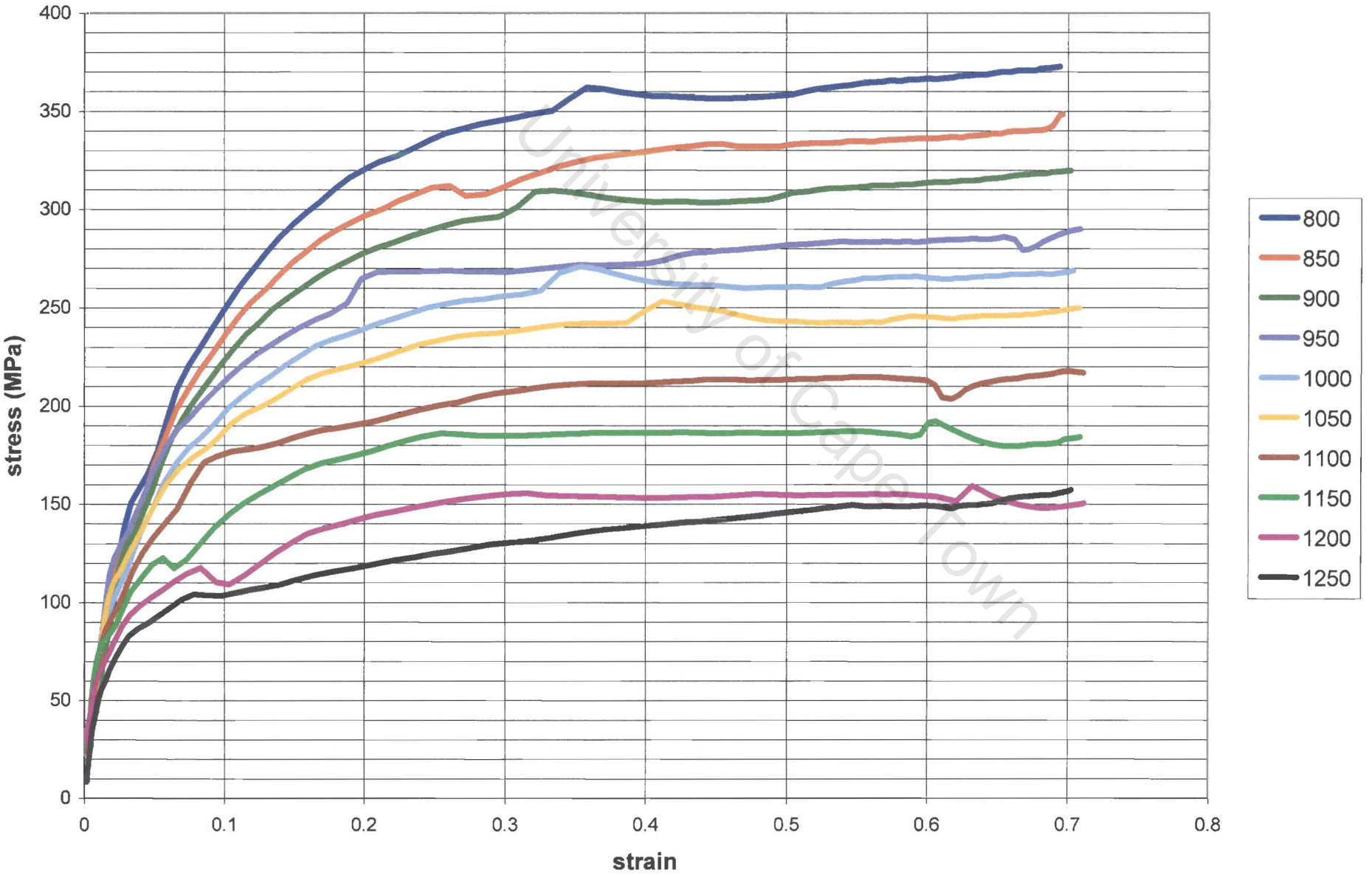

University of Cape Town

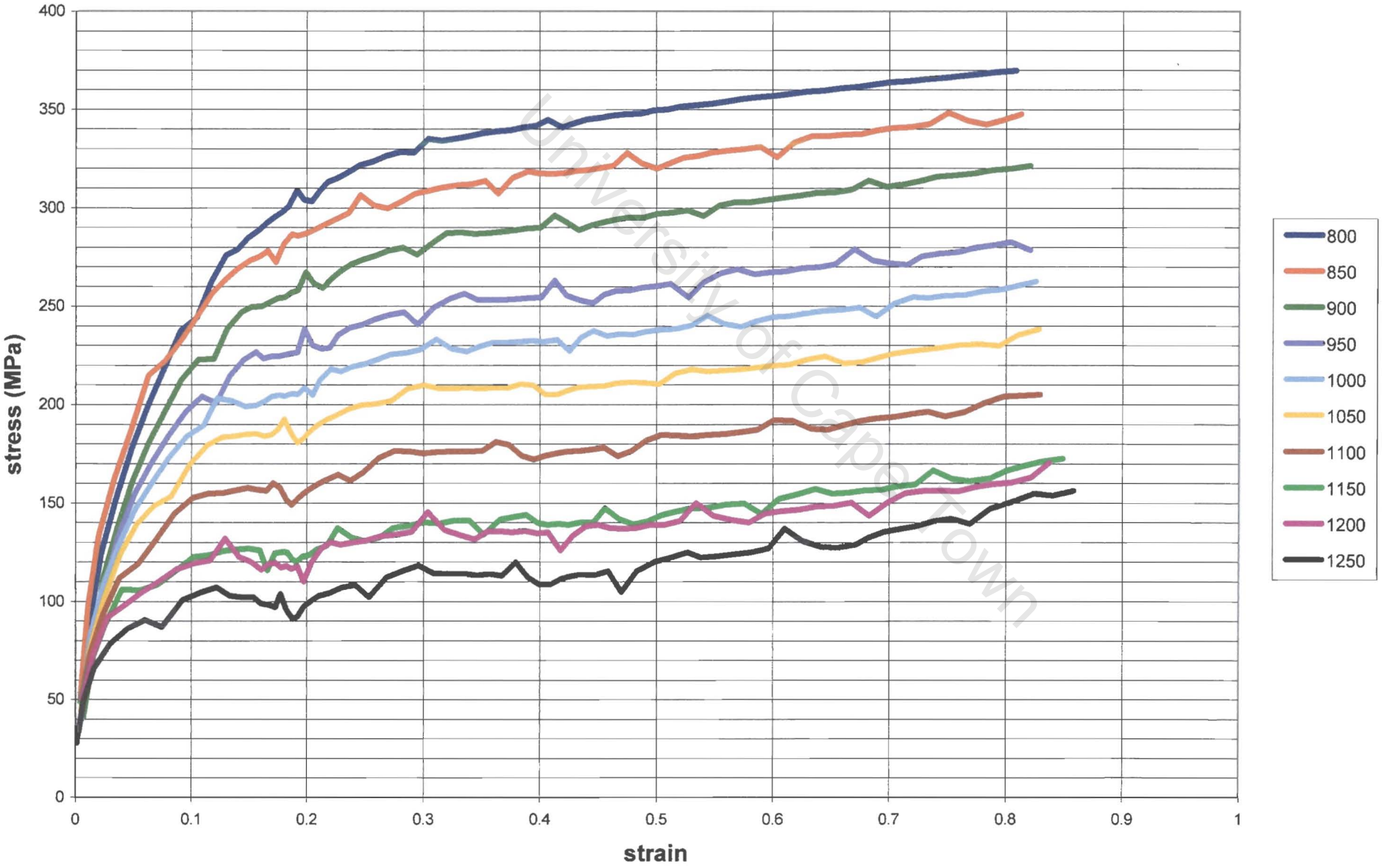

University of Cape Town

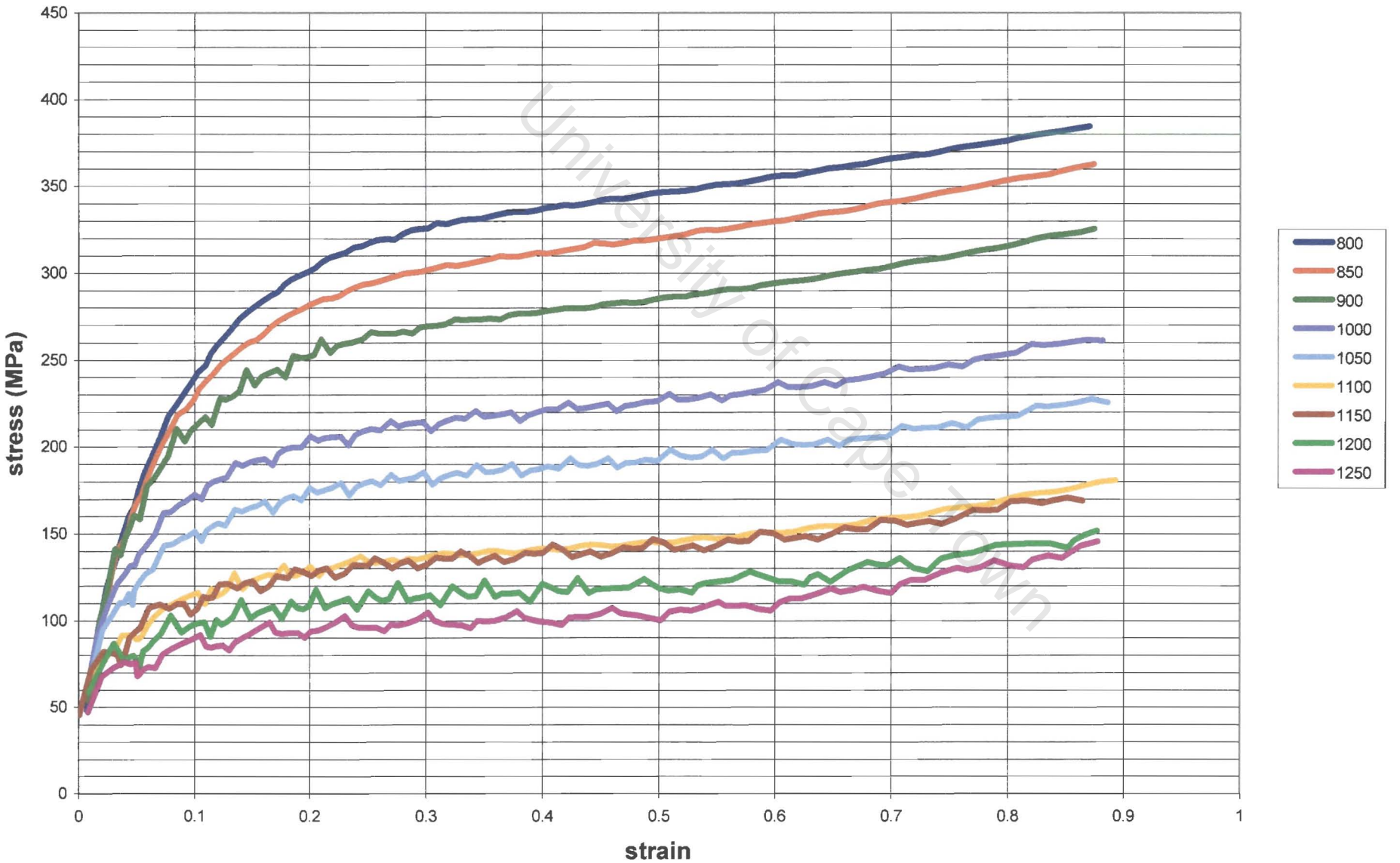

University of Cape Town

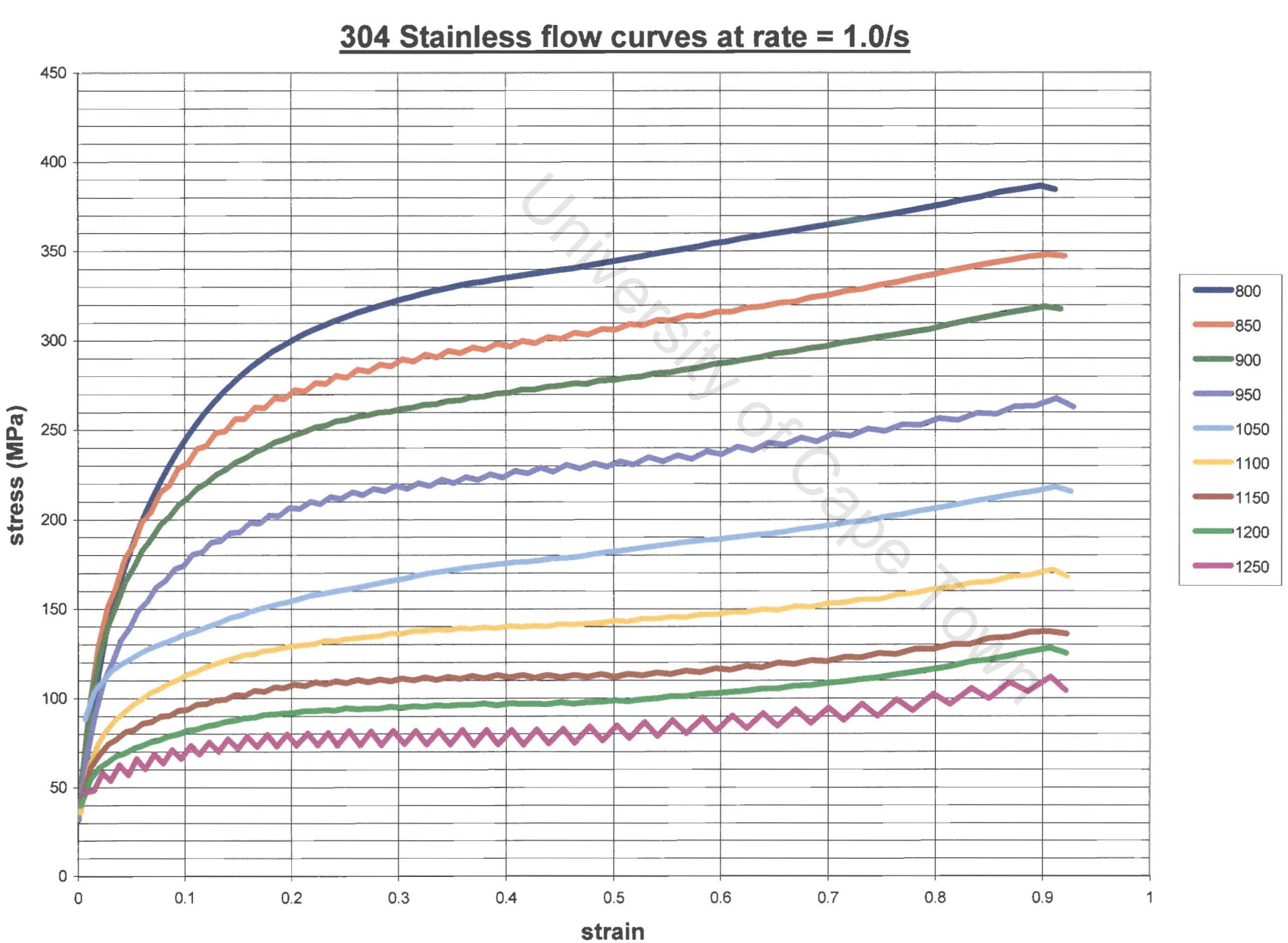

University of Cape Town

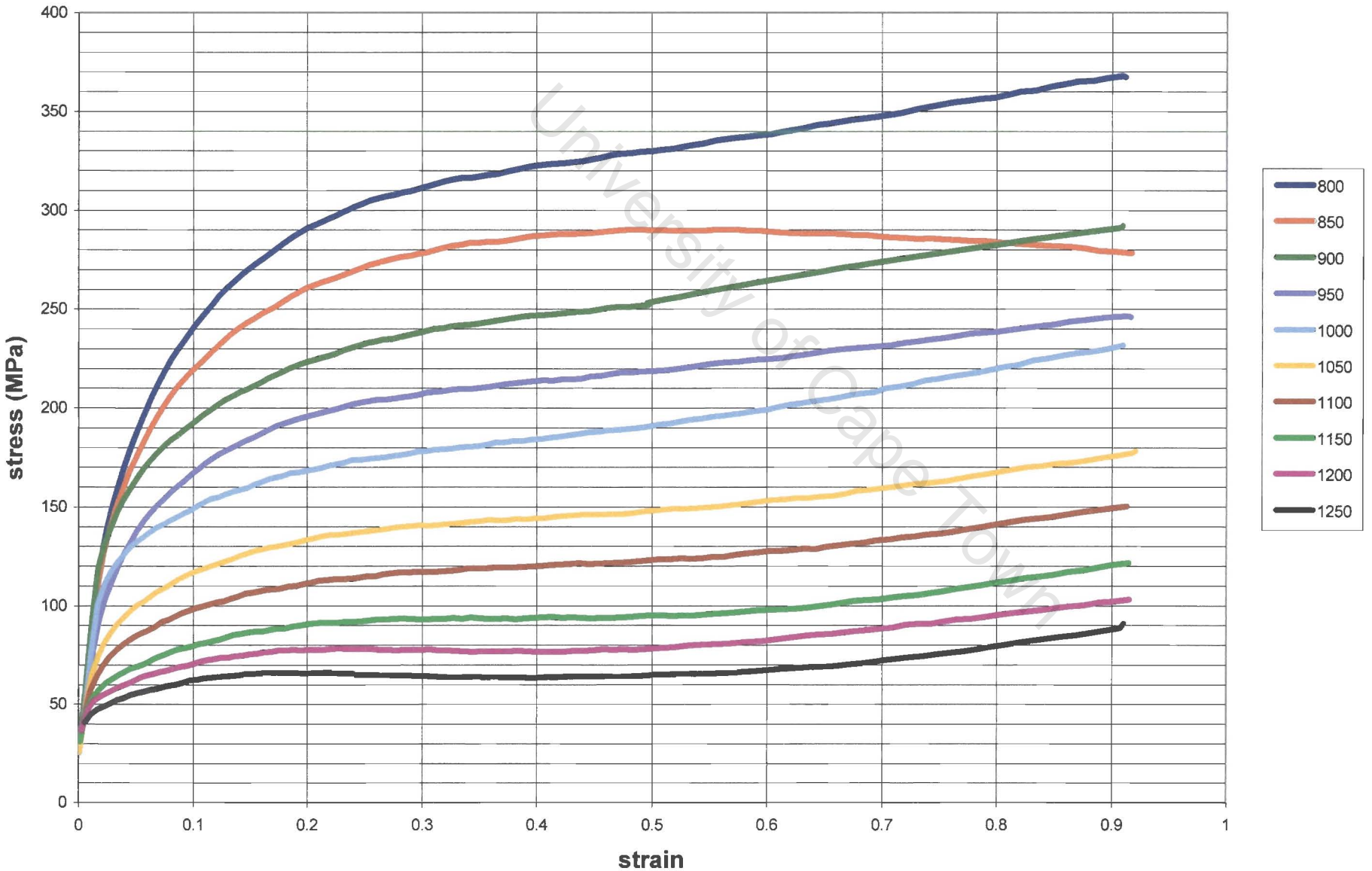

University of Cape Town

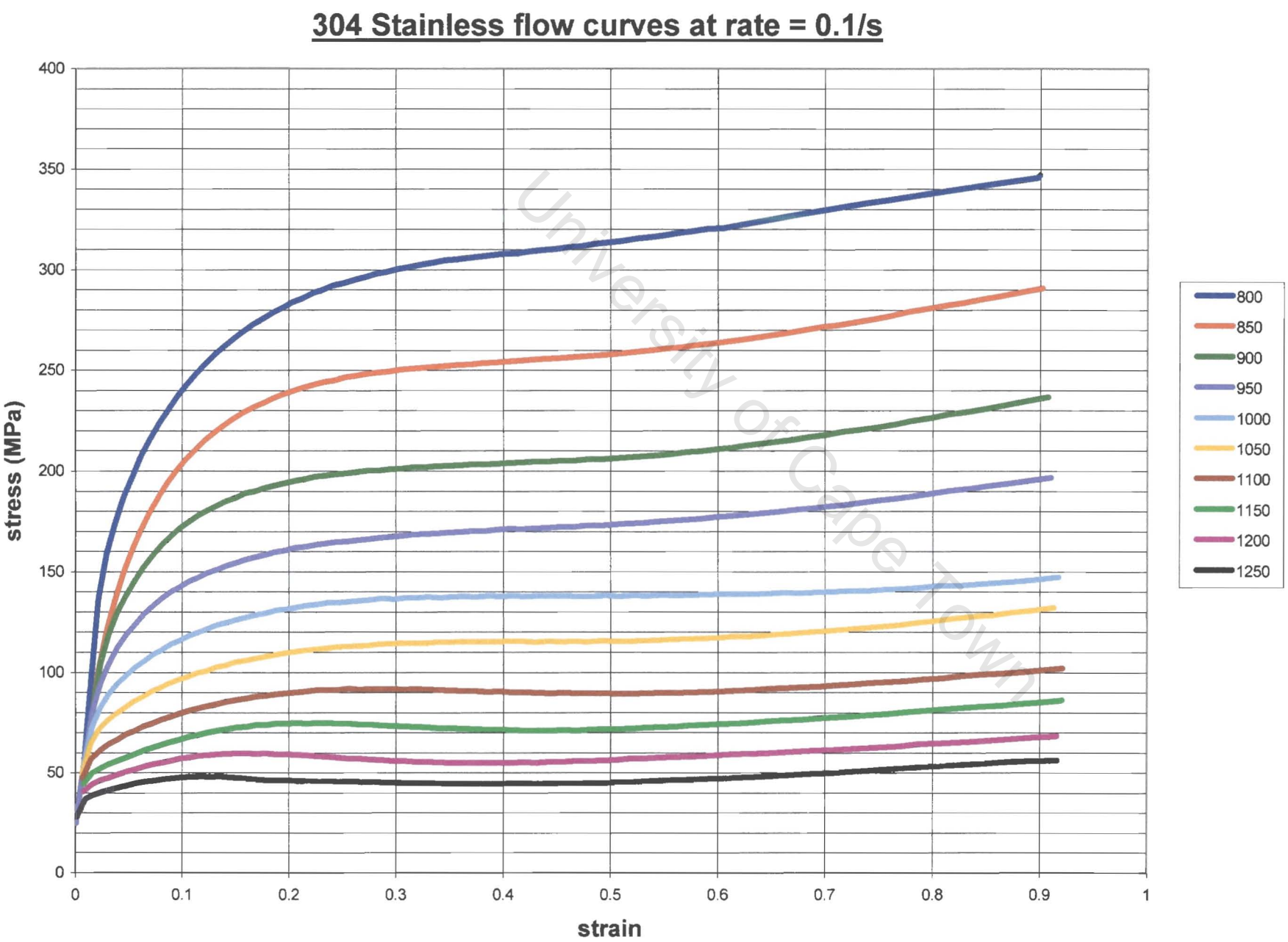

University of Cape Town

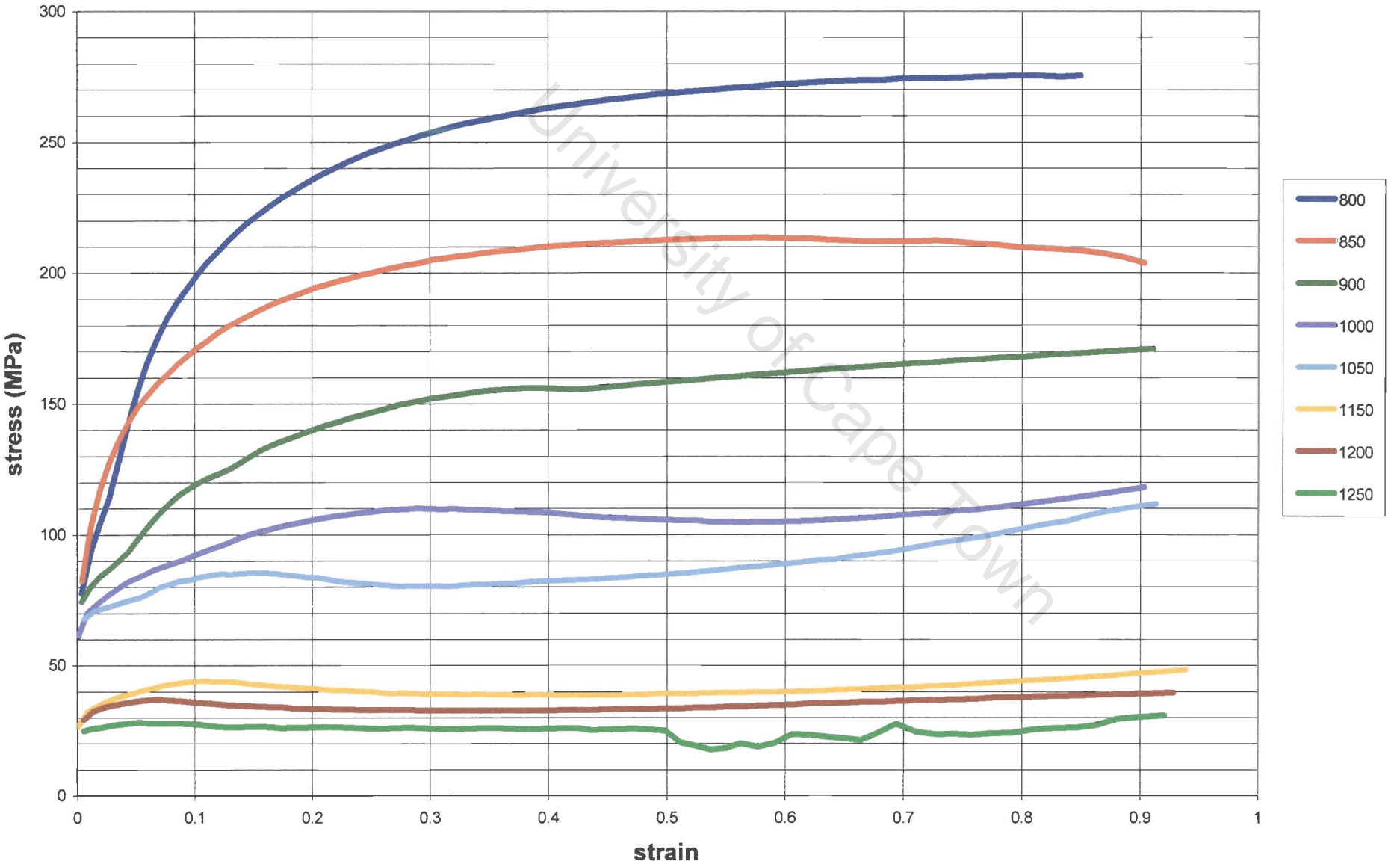

University of Cape Town

strain rate =	35	35	35	35	35	35	35	35	35	35
temperature =	800	850	900	950	1000	1050	1100	1150	1200	1250
strain	stress (Mpa)	stress (Mpa)	stress (Mpa)	stress (Mpa)	stress (Mpa)	stress (Mpa)	stress (Mpa)	stress (Mpa)	stress (Mpa)	stress (Mpa)
0.005	41.65496042	52.57341604	60.4229148	65.2034567	66.91504174	65.55766992	61.13134124	53.6360557	43.07181329	29.43861403
0.007	53.25960118	63.52030073	70.7090204	74.82576019	75.87052012	73.84330018	68.74410036	60.57292067	49.32976111	35.01462168
0.01	67.8436019	77.09875835	83.31134998	86.48137678	86.60883876	83.69373592	77.73606825	68.73583576	56.69303845	41.60767631
0.014	84.01977059	91.98200454	96.9673872	98.97591858	98.00759868	94.0624275	87.14040504	77.2415313	64.36580627	48.51322997
0.02	104.0021597	110.169013	113.4773056	113.9270375	111.5182088	106.2508193	98.12486907	87.14035817	73.29728657	56.59565426
0.026	120.7021545	125.2343996	127.0322142	126.0955984	122.4245522	116.0190756	106.8791686	95.00483114	80.3960633	63.05286505
0.03	130.5552302	134.0746684	134.9420867	133.157485	128.7208633	121.6322216	111.89156	99.49887834	84.45417675	66.75745519
0.04	151.9808148	153.1907529	151.9483443	148.253589	142.1064871	133.5070384	122.4552432	108.9511012	92.99461259	74.5857773
0.05	170.0786638	169.2371789	166.131413	160.7613663	153.1270386	143.2284299	131.0655404	116.6383699	99.94691849	80.99118614
0.06	185.791034	183.1024861	178.3258288	171.4610621	162.508186	151.4672006	138.3381058	123.1209016	105.815588	86.42216507
0.08	212.1349741	206.2260047	198.5488333	189.1034599	177.8898846	164.9081074	150.1581281	133.639947	115.3535638	95.29897871
0.1	233.6750431	225.0276899	214.8950579	203.2771472	190.1739577	175.5854894	159.5117424	141.9527167	122.9084122	102.3788289
0.12	251.7944988	240.7749378	228.5224391	215.0370028	200.3186288	184.3673171	167.1830678	148.7658808	129.1157562	108.2326939
0.14	267.3214847	254.2205568	240.1133854	224.9999704	208.8803118	191.7544097	173.6222641	154.4838749	134.3392421	113.1883658
0.17	286.8904112	271.1022807	254.6079125	237.4073064	219.5004626	200.8873809	181.5680614	161.5425042	140.8107091	119.3726762
0.2	303.010554	284.9530836	266.449513	247.4998422	228.1040711	208.2621999	187.9742285	167.240157	146.0599852	124.4337132
0.25	324.1765793	303.0544759	281.8489303	260.5599423	239.187512	217.7316393	196.1923244	174.5695671	152.8633676	131.0737257
0.3	340.0184215	316.5255714	293.241296	270.1655953	247.2984692	224.6399179	202.1899412	179.9485392	157.915712	136.0914594
0.35	351.8606366	326.5352994	301.6543098	277.2176678	253.2253734	229.6774267	206.5738275	183.914576	161.699672	139.9291157
0.4	360.564538	333.8399587	307.7493263	282.2926409	257.4699024	233.2811109	209.7262664	186.8053689	164.5184182	142.8654146
0.45	366.7266946	338.9612212	311.9804976	285.7845237	260.3732995	235.746825	211.9051003	188.8481253	166.5759	145.0884245
0.5	370.7799992	342.2763083	314.6749728	287.9759927	262.1793679	237.2850986	213.2931846	190.2036261	168.0164229	146.7315751
0.55	373.0500387	344.0680751	316.0772472	289.0775551	263.0689988	238.0515782	214.0252933	190.9901442	168.9461309	147.8932533
0.6	373.7887682	344.5548235	316.375462	289.2506837	263.1804885	238.1648765	214.2038477	191.2974021	169.4455397	148.6482605
0.65	373.1957392	343.9090379	315.7178775	288.622258	262.6221794	237.7176417	213.908645	191.1951891	169.5772742	149.0549001
0.7	371.4320738	342.2696848	314.2236566	287.2939894	261.4806831	236.7837378	213.2031533	190.7389298	169.3910673	149.1595656

strain rate =	10	10	10	10	10	10	10	10	10	10
temperature =	800	850	900	950	1000	1050	1100	1150	1200	1250
strain	stress (Mpa)	stress (Mpa)	stress (Mpa)	stress (Mpa)	stress (Mpa)	stress (Mpa)	stress (Mpa)	stress (Mpa)	stress (Mpa)	stress (Mpa)
0.005	60.34489555	64.16573417	66.09638559	66.13684983	64.28712688	60.54721674	54.91711941	47.39683489	37.98636319	26.68570429
0.007	72.70203275	75.86511529	77.13498762	76.51164976	73.9951017	69.58534343	63.28237497	55.08619631	44.99680745	33.01420839
0.01	87.75398248	89.91152192	90.20526621	88.63521535	85.20136934	79.90372818	72.74229187	63.7170604	52.82803379	40.07521202
0.014	103.9833298	104.8479468	103.9144821	101.1829358	96.65330794	90.32559844	82.19980733	72.27593462	60.55398029	47.03394436
0.02	123.5245827	122.593819	119.9832643	115.6929186	109.7227818	102.072854	92.74313513	81.73362526	69.04432435	54.67523241
0.026	139.5240769	136.958705	132.8376722	127.1609788	119.9286246	111.1406097	100.796934	88.89759762	75.44260047	60.43194259
0.03	148.8484041	145.2702253	140.2187963	133.6941169	125.6961872	116.2250072	105.2805769	92.86289633	78.97196544	63.60778425
0.04	168.8797567	162.9920778	155.8308219	147.3959889	137.687579	126.7055921	114.4500281	100.9208872	86.11816928	70.04187436
0.05	185.5831823	177.6440804	168.6194672	158.5093428	147.3137071	135.0325601	121.6659019	107.2137325	91.67605177	75.05285979
0.06	199.954138	190.167973	179.4724684	167.8676241	155.35344	141.9299162	127.5970528	112.3548496	96.20330674	79.14242416
0.08	223.8332222	210.8266357	197.230617	183.045166	168.2702827	152.9059671	136.9522192	120.4090391	103.2764266	85.55438191
0.1	243.2074196	227.4624494	211.4109701	195.0529817	178.3884842	161.4174777	144.139962	126.5559373	108.6654035	90.46836056
0.12	259.4359477	241.3187697	223.1474237	204.9219096	186.6422276	168.3083777	149.9203597	131.4781738	112.9818198	94.43129791
0.14	273.3161864	253.1176415	233.0916227	213.2381301	193.5571635	174.0487231	154.7128088	135.5494206	116.5585586	97.74022262
0.17	290.8118334	267.926086	245.5128704	223.5721866	202.1040348	181.1084148	160.5853267	140.5347704	120.9567461	101.8512536
0.2	305.2659512	280.1108638	255.6884458	231.9986974	209.0416184	186.8172088	165.3254688	144.5663982	124.5399971	105.2462655
0.25	324.3991798	296.1794594	269.0550664	243.0260008	218.0922625	194.2538515	171.5107679	149.8630117	129.3105828	109.8534813
0.3	338.9647639	308.3742968	279.171174	251.3553956	224.9269616	199.8858719	176.2321266	153.9657257	133.0866691	113.5949568
0.35	350.1428927	317.7199385	286.9201015	257.7433819	230.1897795	204.2592945	179.9519267	157.2676761	136.2065429	116.7685269
0.4	358.6908386	324.8686422	292.8591625	262.6623995	234.278353	207.7070232	182.94841	160.0025135	138.8693336	119.5488703
0.45	365.1273908	330.2643004	297.3647294	266.4286778	237.4561456	210.4471329	185.4016395	162.3196655	141.2012109	122.0462758
0.5	369.8255217	334.2242138	300.7040309	269.2649731	239.9070404	212.6302327	187.4345501	164.3199926	143.2865601	124.3342527
0.55	373.0635026	336.983922	303.0742468	271.3344771	241.7646127	214.3646538	189.1346003	166.0744522	145.1842096	126.4638724
0.6	375.0551527	338.723591	304.6253821	272.7605261	243.129023	215.7308727	190.5660752	167.6346307	146.9365389	128.4718001
0.65	375.9687507	339.5844324	305.4744246	273.6387275	244.0773409	216.7902649	191.7774995	169.0390447	148.5749004	130.3850668
0.7	375.9393949	339.6793889	305.7145134	274.0447685	244.6701542	217.5906705	192.8063175	170.317095	150.1230031	132.2240419
0.75	375.0773813	339.100349	305.4211018	274.0396399	244.9559633	218.1700719	193.6819657	171.4916447	151.599109	134.0043585
0.8	373.4740585	337.9231715	304.6562324	273.6732413	244.9741982	218.5591031	194.427956	172.5807568	153.0175057	135.7382026

strain rate =	3.5	3.5	3.5	3.5	3.5	3.5	3.5	3.5	3.5	3.5
temperature =	800	850	900	950	1000	1050	1100	1150	1200	1250
strain	stress (Mpa)	stress (Mpa)	stress (Mpa)	stress (Mpa)	stress (Mpa)	stress (Mpa)	stress (Mpa)	stress (Mpa)	stress (Mpa)	stress (Mpa)
0.005	70.92934362	70.14282679	68.24666983	65.24087275	61.12543555	55.90035821	49.56564075	42.12128316	33.56728545	23.90364761
0.007	83.708777	82.26450409	79.70756804	76.03796886	71.25570654	65.36078108	58.35319249	50.23294076	41.00002589	30.65444789
0.01	98.97744305	96.52762705	92.99456296	88.37825078	82.67869052	75.89588216	68.02982572	59.08052118	49.04796856	37.93216785
0.014	115.1404928	111.3977543	106.6374812	100.8596736	94.06433147	86.25145478	77.42104354	67.57309776	56.70761743	44.82460255
0.02	134.2654285	128.7273094	122.2899463	114.9533393	106.7174882	97.58239323	87.54805426	76.61447131	64.7816444	52.04957352
0.026	149.6973685	142.5246411	134.5768	125.8538452	116.3557768	106.0825947	95.03429888	83.21088941	70.61236626	57.23872944
0.03	158.6101602	150.4246259	141.5463885	131.9754478	121.7118038	110.7554566	99.10640623	86.76465257	73.73019567	60.00303554
0.04	177.583538	167.0885036	156.1004393	144.619345	132.6452208	120.1780667	107.2178827	93.76466867	79.81842474	65.37915087
0.05	193.2478472	180.7013899	167.8499683	154.6935826	141.2322327	127.4659185	113.3946402	99.01839766	84.33719094	69.35102002
0.06	206.6280516	192.2345312	177.7122182	163.0611125	148.2812142	133.3725233	118.3350397	103.1687634	87.87369457	72.44983305
0.08	228.6975627	211.0836209	193.6607938	176.4290814	159.3884839	142.5390011	125.8806331	109.4133799	93.13724143	77.05221776
0.1	246.4857013	226.1333756	206.2550879	186.8508382	167.9206265	149.4644527	131.4823169	113.9742191	96.9401593	80.38013745
0.12	261.3280616	238.6035282	216.6053737	195.3335984	174.7882022	154.969185	135.8765469	117.5102879	99.87040793	82.95690707
0.14	273.9971462	249.1912459	225.3384188	202.4386648	180.491984	159.4983764	139.4578419	120.3703807	102.2359926	85.05467773
0.17	289.957738	262.4646351	236.2246111	211.2376661	187.5038	165.0230128	143.7953045	123.8206752	105.0991248	87.63065339
0.2	303.1638069	273.401364	245.1521377	218.4161279	193.1933347	169.483758	147.2873978	126.6042541	107.434327	89.77761648
0.25	320.7379167	287.9108409	256.9596395	227.8843125	200.68486	175.3612818	151.9135781	130.3417488	110.6457939	92.82571346
0.3	334.2716153	299.0737928	266.0438617	235.181822	206.4876737	179.9614168	155.6030514	133.4125773	113.3899947	95.53530357
0.35	344.8428338	307.8125242	273.1858789	240.9628979	211.1435813	183.727929	158.7159411	136.1076175	115.9029583	98.10196335
0.4	353.1356675	314.7061157	278.8698276	245.6268032	214.9770425	186.9205455	161.4573122	138.5873426	118.3106367	100.6271945
0.45	359.6144599	320.1440141	283.4176347	249.4353218	218.1970753	189.7028954	163.9527819	140.9467348	120.6847542	103.1668401
0.5	364.6103849	324.4017215	287.0547303	252.5694112	220.9457642	192.1837894	166.2834866	143.244856	123.0678975	105.7526112
0.55	368.368796	327.6818599	289.9453763	255.1593452	223.3237666	194.4386405	168.5039669	145.5197458	125.4859771	108.402661
0.6	371.0770365	330.1381193	292.2131021	257.3019848	225.4047674	196.5214499	170.6520323	147.7965147	127.9548969	111.1271791
0.65	372.881712	331.8900383	293.9532221	259.0712637	227.2441628	198.4719197	172.7545341	150.0920062	130.484336	113.9315234
0.7	373.8999112	333.0325496	295.2408658	260.5248596	228.8845311	200.3198802	174.830907	152.4176114	133.0799936	116.8180533
0.75	374.2267704	333.6423825	296.136327	261.7086038	230.3592129	202.0881543	176.895428	154.781034	135.7449722	119.7872428
0.8	373.9407346	333.7824921	296.6887446	262.6594922	231.6947349	203.7944726	178.9587053	157.1874331	138.480656	122.8383739
0.85	373.1073143	333.5052083	296.9387029	263.407798	232.9124937	205.4527899	181.0286866	159.640184	141.2872818	125.9699803
0.9	371.7818296	332.8545267	296.9201135	263.9785901	234.0299565	207.0742126	183.1113586	162.1413943	144.1643198	129.180135

strain rate =	1	1	1	1	1	1	1	1	1	1
temperature =	800	850	900	950	1000	1050	1100	1150	1200	1250
strain	stress (Mpa)	stress (Mpa)	stress (Mpa)	stress (Mpa)	stress (Mpa)	stress (Mpa)	stress (Mpa)	stress (Mpa)	stress (Mpa)	stress (Mpa)
0.005	77.50045847	72.81555437	67.70510931	62.16912327	56.20759626	49.82052828	43.00791933	35.76976942	28.10607853	20.01684667
0.007	90.53525571	85.19259553	79.42137137	73.22158323	66.59323111	59.53631501	52.05083493	44.13679087	35.79418282	27.0230108
0.01	105.8531922	99.5049889	92.7576367	85.61113556	78.0654855	70.1206865	61.77673856	53.0336417	43.8913959	34.35000117
0.014	121.804836	114.1637102	106.189149	97.88115249	89.23972054	80.26485321	70.95655048	61.31481236	51.33963886	41.03102997
0.02	140.3773175	130.9408111	121.2891599	111.4223639	101.3404231	91.04333742	80.53110696	69.80373168	58.8612116	47.7035467
0.026	155.155222	144.0841074	132.9219782	121.6688344	110.3246762	98.88950341	87.36331613	75.74611433	64.03789801	52.23866717
0.03	163.6145834	151.5306619	139.4381363	127.3370067	115.2272729	103.1089351	90.98199319	78.84644721	66.70229714	54.54954298
0.04	181.45721	167.0637884	152.8614359	138.8501527	125.0299387	111.400794	97.96271842	84.71571209	71.65977499	58.7949071
0.05	196.0359675	179.5911229	163.5254132	147.8388385	132.5313988	117.603094	103.0539242	88.88388932	75.09298942	61.68122448
0.06	208.39304	190.1011323	172.3645312	155.1832366	138.5572484	122.4865669	106.9711918	92.0111232	77.60636115	63.75690561
0.08	228.6086447	207.0963156	186.4592004	166.6972991	147.8106117	129.7991383	112.6628788	96.40183327	81.01600164	66.50538395
0.1	244.7773356	220.5266226	197.4340468	175.4996082	154.7233066	135.1051422	116.645115	99.34322483	83.19947183	68.21385596
0.12	258.2023687	231.5794479	206.3670054	182.5650411	160.173555	139.1925472	119.6220176	101.4619663	84.71239319	69.37329831
0.14	269.6276366	240.923349	213.8562337	188.4262908	164.6335202	142.4779219	121.959496	103.0782424	85.8341612	70.22725229
0.17	283.997915	252.6064248	223.1521127	195.6349788	170.0550228	146.412245	124.7066453	104.9382236	87.10698008	71.21291461
0.2	295.8913912	262.230561	230.7670466	201.5008479	174.4319648	149.5603974	126.8861458	106.4092098	88.12958954	72.04728496
0.25	311.7772744	275.0518113	240.8863218	209.2808059	180.2352635	153.7496948	129.8240996	108.4584779	89.65282986	73.40715538
0.3	324.1245133	285.0283034	248.7840842	215.3918555	184.8516174	157.1633699	132.327113	110.3428467	91.21057088	74.93028569
0.35	333.911354	292.9826571	255.1417237	220.3885538	188.7231474	160.1455045	134.655625	112.2535091	92.9391567	76.71256778
0.4	341.7512873	299.4233483	260.3727721	224.5995587	192.1037082	162.8852206	136.9440958	114.2803338	94.89393476	78.78489853
0.45	348.0564954	304.6876623	264.7469948	228.234493	195.1501567	165.4939861	139.2659811	116.4661417	97.09446798	81.15095985
0.5	353.1183154	309.0112647	268.4499854	231.4344773	197.9647406	168.0407751	141.6625808	118.8301579	99.54350624	83.80262586
0.55	357.1508536	312.5655303	271.6147586	234.2985386	200.6168702	170.5697534	144.1571883	121.3791749	102.235713	86.72680286
0.6	360.3164024	315.479098	274.3397926	236.8984863	203.1551791	173.109871	146.7625619	124.113252	105.161941	89.90862921
0.65	362.7411139	317.8510529	276.6999487	239.2878013	205.6146106	175.6803768	149.4850998	127.0287795	108.3114161	93.33300948
0.7	364.5251184	319.7593696	278.7533976	241.5072025	208.0207841	178.2941426	152.3272779	130.1201901	111.672879	96.98534478
0.75	365.7493044	321.2665293	280.5461857	243.5882735	210.3927928	180.9597435	155.2891257	133.3809394	115.2351845	100.851861
0.8	366.4800088	322.423379	282.1153434	245.5559021	212.7450549	183.682802	158.3691432	136.8040787	118.9876084	104.9197323
0.85	366.772349	323.2718557	283.4910622	247.4299683	215.0885742	186.4668798	161.564885	140.38259	122.9199947	109.1770991
0.9	366.6726449	323.8469547	284.6982534	249.2265411	217.4318177	189.3140832	164.8733376	144.109581	127.0228133	113.6130345

strain rate =	0.35	0.35	0.35	0.35	0.35	0.35	0.35	0.35	0.35	0.35
temperature =	800	850	900	950	1000	1050	1100	1150	1200	1250
strain	stress (Mpa)	stress (Mpa)	stress (Mpa)	stress (Mpa)	stress (Mpa)	stress (Mpa)	stress (Mpa)	stress (Mpa)	stress (Mpa)	stress (Mpa)
0.005	77.92926979	71.31798202	64.64716378	57.91681507	51.1269359	44.27752627	37.36858616	30.40011559	23.37211455	16.28458305
0.007	90.96976342	83.70071957	76.36912224	68.97497143	61.51826715	53.99900939	46.41719815	38.77283344	31.06591524	23.29644357
0.01	106.1535613	97.87897435	89.57124898	81.23038518	72.85638295	64.44924229	56.0089632	47.53554568	39.02898973	30.48929536
0.014	121.8171842	112.2496747	102.7147404	93.21238115	83.74259704	74.30538804	64.90075416	55.52869539	46.18921174	36.88230319
0.02	139.8800635	128.5171734	117.3051491	106.2439904	95.33369739	84.57427008	73.96570847	63.50801254	53.2011823	43.04521776
0.026	154.1293518	141.1318535	128.4093511	115.9618447	103.7893343	91.89181987	80.26930143	68.92177897	57.8492525	47.05172201
0.03	162.2402947	148.2299895	134.5770908	121.2815985	108.3435125	95.76283306	83.53956	71.67369336	60.16523314	49.01417934
0.04	179.2457448	162.9259395	147.1632139	131.9575681	117.3090019	103.2175155	89.68310877	76.70578179	64.28553453	52.422367
0.05	193.0442222	174.6729939	157.046911	140.1659737	124.0301818	108.6395353	93.99403435	80.09367883	66.93846879	54.5284042
0.06	204.6772659	184.4589745	165.1620002	146.7863429	129.3320027	112.7989794	97.18727318	82.49688396	68.72781175	55.88005657
0.08	223.5952766	200.1565638	177.9590754	157.0028114	137.2877719	118.8139568	101.5813662	85.58999998	70.8398582	57.33094086
0.1	238.6358146	212.458718	187.805769	164.6769677	143.072314	122.9918079	104.4354495	87.40323871	71.89517556	57.91126005
0.12	251.0715596	222.5222552	195.7494395	170.7531126	147.5332743	126.0899249	106.4230641	88.53269213	72.41880886	58.08141434
0.14	261.6233314	230.9926602	202.3651717	175.7408661	151.1197434	128.5018035	107.8870464	89.27547215	72.66708075	58.0618722
0.17	274.8632828	241.545409	210.5307237	181.8192271	155.410919	131.3057995	109.5038686	90.00512631	72.8095726	57.91720749
0.2	285.8048883	250.2176745	217.1937868	186.7332254	158.8359902	133.5020812	110.7314984	90.52424176	72.88031134	57.79970711
0.25	300.4204043	261.7685576	226.0426949	193.2428163	163.3689218	136.4210114	112.399085	91.30314272	73.13318451	57.88921038
0.3	311.8110092	270.7884158	232.9838233	198.397232	167.0286418	138.8780526	113.9454645	92.2308775	73.73429158	58.45570674
0.35	320.8901348	278.0350542	238.6337477	202.6862151	170.1924565	141.1524719	115.5662613	93.43382478	74.75516221	59.53027364
0.4	328.2261145	283.9717918	243.3608424	206.3932664	173.0690637	143.3882344	117.3507785	94.95669586	76.20598663	61.09865075
0.45	334.1981532	288.9029364	247.4018958	209.6950312	175.7823428	145.6638305	119.3394944	96.80933436	78.07335046	63.13154268
0.5	339.0726197	293.0391854	250.9175329	212.7076621	178.4095732	148.023266	121.5487407	98.98599707	80.33503526	65.59585524
0.55	343.044168	296.532461	254.0213161	215.5107334	181.0007128	150.4912544	123.9823582	101.474024	82.96625207	68.45904225
0.6	346.2595798	299.4958917	256.7962131	218.1605442	183.5888848	153.081235	126.6375948	104.2579642	85.94234313	71.69073164
0.65	348.8324008	302.0159561	259.3044787	220.6979686	186.1964258	155.7998503	129.5082422	107.3216013	89.2399277	75.26322143
0.7	350.8523483	304.1602159	261.5938707	223.1533129	188.8385424	158.6495592	132.5863634	110.6489549	92.83733366	79.15149978
0.75	352.3915909	305.9824321	263.7017153	225.5494405	191.5256076	161.6302167	135.8632677	114.2247607	96.71469569	83.33307261
0.8	353.5090758	307.5260623	265.6576536	227.9038495	194.2646502	164.7400556	139.3300657	118.0346805	100.8539001	87.78772435
0.85	354.2535931	308.8267161	267.4855494	230.2300929	197.0603466	167.9763105	142.9779846	122.065369	105.2384635	92.49726827
0.9	354.6659954	309.9139216	269.2048471	232.5387721	199.9156965	171.3356204	146.7985437	126.3044664	109.8533885	97.44531012

strain rate =	0.1	0.1	0.1	0.1	0.1	0.1	0.1	0.1	0.1	0.1
temperature =	800	850	900	950	1000	1050	1100	1150	1200	1250
strain	stress (Mpa)	stress (Mpa)	stress (Mpa)	stress (Mpa)	stress (Mpa)	stress (Mpa)	stress (Mpa)	stress (Mpa)	stress (Mpa)	stress (Mpa)
0.005	72.38156436	65.07111906	57.89057193	50.83992297	43.91917219	37.12831959	30.46736515	23.9363089	17.53515081	11.26389091
0.007	85.18028927	77.21208788	69.37076166	61.6563106	54.06873471	46.60803398	39.27420842	32.06725801	24.98718278	18.0339827
0.01	99.99467896	91.02093449	82.20348022	73.54231617	65.03744233	56.6888587	48.49656528	40.46056208	32.58084909	24.85742631
0.014	115.1823113	104.9156443	94.87098111	85.04832163	75.44766591	66.06901395	56.91236574	47.97772128	39.26508058	30.77444364
0.02	132.5814184	120.5193708	108.7976176	97.41615864	86.37499403	75.67412376	65.31354781	55.2932662	45.61327892	36.27358596
0.026	146.2231365	132.5264806	119.2942493	106.5264426	94.22306063	82.38410324	71.00957047	60.09946233	49.65377881	39.67251992
0.03	153.9559673	139.2465045	125.0838769	111.4680843	98.39912681	85.87700436	73.90171697	62.47326464	51.59164738	41.25686517
0.04	170.094147	153.0751841	136.8027296	121.2767835	106.4973457	92.46441634	79.17799531	66.63808264	54.84467834	43.79778241
0.05	183.1159442	164.0455583	145.9097466	128.708509	112.4418455	97.10975607	82.71224077	69.24929957	56.72093247	45.12713948
0.06	194.0441386	173.1266898	153.3199866	134.624029	117.0388171	100.5643509	85.20063035	70.94765544	57.80542619	45.7739426
0.08	211.7191925	187.5813221	164.8741049	143.5975407	123.7516295	105.3363715	88.35176651	72.79781461	58.67451579	45.98187004
0.1	225.6867067	198.8104525	173.6477747	150.1986731	128.4631478	108.4411987	90.13282598	73.53802951	58.65680931	45.4891654
0.12	237.1787248	207.9302629	180.6477183	155.3310911	131.9803812	110.5955888	91.17671372	73.72375604	58.23671573	44.7155928
0.14	246.8896104	215.5597816	186.4225643	159.4779585	134.7259641	112.1665812	91.7998098	73.62564988	57.64410144	43.85516448
0.17	259.0222146	225.0051833	193.4807691	164.4489722	137.9097925	113.8632301	92.30928484	73.24795686	56.67924611	42.60315259
0.2	269.0046596	232.7182883	199.1846718	168.4038101	140.3757033	115.1003513	92.57775414	72.80791183	55.79082437	41.52649174
0.25	282.2765193	242.925515	206.6899234	173.5697446	143.5649785	116.675625	92.90168436	72.24315638	54.70004113	40.27233859
0.3	292.5704627	250.8487117	212.5343904	177.6274988	146.1280369	118.0360048	93.3514024	72.07422971	54.20448674	39.74217349
0.35	300.7449192	257.190681	217.2796456	181.0118127	148.3871825	119.405755	94.0675301	72.37250784	54.32068822	39.91207125
0.4	307.3310536	262.3775733	221.2568951	183.9690188	150.5139445	120.8916723	95.10220199	73.14553371	55.02166743	40.73060314
0.45	312.6815281	266.6871538	224.6763842	186.6492194	152.6056594	122.5457042	96.46935368	74.37660797	56.26746702	42.14193084
0.5	317.0429582	270.3103664	227.678985	189.148814	154.7198534	124.3921033	98.1655636	76.04023432	58.01611547	44.09320704
0.55	320.5948194	273.3839549	230.3630811	191.5321981	156.891306	126.4404046	100.179494	78.1085742	60.22764518	46.53670696
0.6	323.4719271	276.0090815	232.799674	193.8437048	159.1411739	128.6920811	102.4964266	80.55421025	62.86543214	49.43009226
0.65	325.7781932	278.2625909	235.0413846	196.1145743	161.4821599	131.1441414	105.1005189	83.35129236	65.89646174	52.73602706
0.7	327.5954417	280.2041517	237.1280777	198.3672196	163.9215775	133.7911513	107.9759412	86.47594695	69.2911687	56.42160642
0.75	328.9892776	281.8809613	239.0905156	200.6179405	166.463236	136.6264021	111.1074389	89.90634618	73.02312409	60.4577726
0.8	330.0131201	283.3309491	240.9528115	202.8787072	169.1086363	139.6425987	114.4805945	93.62262362	77.06868612	64.81878197
0.85	330.7110516	284.5850171	242.7341215	205.1583647	171.8577468	142.8322678	118.0819276	97.6067262	81.4066637	69.48174006
0.9	331.1198765	285.6686451	244.4498417	207.4634665	174.7095193	146.1880002	121.8989091	101.8422462	86.01801128	74.42620446

strain rate =	0.035	0.035	0.035	0.035	0.035	0.035	0.035	0.035	0.035	0.035
temperature =	800	850	900	950	1000	1050	1100	1150	1200	1250
strain	stress (Mpa)	stress (Mpa)	stress (Mpa)	stress (Mpa)	stress (Mpa)	stress (Mpa)	stress (Mpa)	stress (Mpa)	stress (Mpa)	stress (Mpa)
0.005	62.65473892	56.09888172	49.62439663	43.23128367	36.91954282	30.68917409	24.54017747	18.47255298	12.4863006	6.58142034
0.007	75.04256043	67.82894715	60.69368298	53.63676791	46.65820195	39.75798509	32.93611734	26.1925987	19.52742917	12.94060875
0.01	89.37195662	81.15280025	73.04140803	65.03777996	57.14191605	49.3538163	41.6734807	34.10090926	26.63610197	19.27905884
0.014	104.0498447	94.53776583	85.19916464	76.03404116	67.04239537	58.22422728	49.57953689	41.10832419	32.8105892	24.6863319
0.02	120.8460646	109.5386051	98.52291386	87.79899091	77.36683623	67.22644983	57.37783171	47.82098186	38.55590028	29.58258697
0.026	133.9981044	121.0560366	108.5298674	96.41959675	84.72522467	73.44675115	62.5841762	52.13749982	42.10672201	32.49184276
0.03	141.4456338	127.4907592	114.0341936	101.075937	88.61598943	76.65435085	65.19102128	54.22600071	43.75928915	33.79088659
0.04	156.9674354	140.7030606	125.1366682	110.268258	96.09783021	82.62538469	69.85092148	57.77444057	46.39594198	35.71542569
0.05	169.4677885	151.1519908	133.7222411	117.1785395	101.5208859	86.74928034	72.86372286	59.86421342	47.75075203	36.52333869
0.06	179.9386768	159.775816	140.6751749	122.6367533	105.6605513	89.746569	74.89480625	61.10526311	48.37793956	36.71283562
0.08	196.8281156	173.4448333	151.4436781	130.8246499	111.5877487	93.73297452	77.26032737	62.16980723	48.46141412	36.13514802
0.1	210.1253831	184.003717	159.5471012	136.7555356	115.6290202	96.16755508	78.37114015	62.23977543	47.77346094	34.97219667
0.12	221.0249928	192.531119	165.9546364	141.2955452	118.5538453	97.72953675	78.8226195	61.83309358	46.76095897	33.60621569
0.14	230.2000403	199.6247996	171.1936443	144.9065744	120.76359	98.76469097	78.90987739	61.19914923	45.63250649	32.20994919
0.17	241.6070457	208.3446024	177.5262503	149.1519894	123.2218196	99.73574104	78.69375364	60.09585742	43.94205237	30.2323385
0.2	250.9337981	215.4020148	182.5744604	152.4511347	125.0320378	100.3171697	78.30653036	59.00011982	42.39793805	28.49998507
0.25	263.2240422	224.6276261	189.0980965	156.6354537	127.2396975	100.910828	77.64884508	57.45374887	40.32553932	26.26421643
0.3	272.6366032	231.6694403	194.061181	159.8118254	128.9213735	101.3898253	77.21718066	56.40343973	38.94860246	24.85266887
0.35	280.0025396	237.2028896	197.9979161	162.3876193	130.371999	101.9510554	77.12478829	55.89319779	38.25628388	24.21404656
0.4	285.835879	241.6369869	201.2223706	164.5920303	131.745966	102.6841776	77.40666515	55.91342864	38.20446806	24.27978343
0.45	290.4777745	245.2379883	203.9332808	166.563652	133.1291019	103.6296305	78.06523787	56.43592392	38.74168868	24.98253214
0.5	294.1667036	248.1886999	206.2633805	168.3907455	134.5707949	104.8035287	79.08894677	57.42704926	39.81783611	26.26130733
0.55	297.0761547	250.6198783	208.3050666	170.1317196	136.0998374	106.2094199	80.46046708	58.85297904	41.38695572	28.06239714
0.6	299.336398	252.6281405	210.1247951	171.8263619	137.7328409	107.844232	82.16053528	60.68175072	43.40787832	30.33891808
0.65	301.0478056	254.2867914	211.7716472	173.5023728	139.4789684	109.7014338	84.1697691	62.8839743	45.84404938	33.04999435
0.7	302.2893853	255.6526834	213.2826715	175.1793494	141.3427172	111.7727749	86.46952257	65.43296012	48.66308758	36.15990494
0.75	303.1244616	256.7707334	214.6863497	176.8713106	143.3256161	114.0492661	89.04226061	68.30459968	51.8362833	39.63731146
0.8	303.604578	257.6769951	216.0049195	178.5883512	145.4272902	116.5217365	91.87169012	71.47715102	55.33811923	43.45459473
0.85	303.772254	258.4008077	217.2559741	180.3377533	147.6461453	119.1811501	94.94276776	74.93099817	59.14584138	47.58729738
0.9	303.6629766	258.9663333	218.453592	182.1247528	149.9798155	122.0187803	98.24164704	78.64841584	63.23908665	52.01365948

strain rate =	0.01	0.01	0.01	0.01	0.01	0.01	0.01	0.01	0.01	0.01
temperature =	800	850	900	950	1000	1050	1100	1150	1200	1250
strain	stress (Mpa)	stress (Mpa)	stress (Mpa)	stress (Mpa)	stress (Mpa)	stress (Mpa)	stress (Mpa)	stress (Mpa)	stress (Mpa)	stress (Mpa)
0.005	44.98821322	40.93242822	36.65277346	32.14924895	27.42185468	22.47059066	17.29545688	11.89645334	6.273580044	0.426836994
0.007	56.63713343	51.92359234	46.9831585	41.81583188	36.4216125	30.80050035	24.95249544	18.87759776	12.57580731	6.047124092
0.01	70.17844284	64.45935866	58.54279677	52.42875716	46.11723984	39.60824479	32.90177202	25.99782154	18.89639333	11.59748741
0.014	84.11575583	77.10374915	69.95997829	62.68444326	55.27714405	47.73808067	40.06725311	32.26466137	24.33030546	16.26418537
0.02	100.1368855	91.32949816	82.50863727	73.67430278	64.82649468	55.96521299	47.09045769	38.2022288	29.30052631	20.38535021
0.026	112.7278202	102.2858246	91.95448567	81.73380347	71.62377797	61.62440915	51.73569704	41.95764161	32.29024289	22.73350085
0.03	119.8725557	108.4177533	97.156018	86.08734987	75.21174886	64.52921499	54.03974825	43.74334864	33.64001616	23.72975082
0.04	134.7905676	121.0262651	107.6547029	94.67588125	82.0898	69.89645919	58.09585881	46.68799886	35.67287935	25.05050027
0.05	146.8231122	131.0073867	115.7724674	101.1183542	87.04504719	73.55254636	60.64085171	48.30996323	36.55988092	25.39060479
0.06	156.9074339	139.2446454	122.3388345	106.1900014	90.79814606	76.16326842	62.2853685	49.16444632	36.80050186	25.19353512
0.08	173.1648654	152.2816554	132.4753305	113.7458907	96.09333609	79.51766662	64.0188823	49.59698312	36.25196909	23.9838402
0.1	185.9355329	162.3139391	140.0521536	119.1501764	99.60800763	81.42564718	64.60309508	49.14035133	35.03741592	22.29428886
0.12	196.3650162	170.3712145	145.9895623	123.2200595	102.0627062	82.51750235	64.58444793	48.26354296	33.55478745	20.45818138
0.14	205.1021079	177.0269394	150.7906145	126.393133	103.8344952	83.11470089	64.23375014	47.19164294	31.98837929	18.62395919
0.17	215.8847323	185.1223612	156.4988394	130.014167	105.6683438	83.46136993	63.39324537	45.4639701	29.67354414	16.02196747
0.2	224.6057565	191.5740454	160.9413213	132.7075841	106.8728338	83.43707037	62.40029387	43.76250429	27.52370161	13.68388584
0.25	235.8969144	199.8005704	166.4658712	135.8928168	108.0814072	83.03164238	60.74352234	41.21704709	24.45221662	10.44903094
0.3	244.3026123	205.8355215	170.4220926	138.0623255	108.7562201	82.50377656	59.3049948	39.15987482	22.06841664	8.030620257
0.35	250.643588	210.3440102	173.3338671	139.6131587	109.1818851	82.04004609	58.18764184	37.6246723	20.35113748	6.367037361
0.4	255.4301374	213.7313174	175.5115315	140.7707797	109.509062	81.72637826	57.42272864	36.59811308	19.25253159	5.385984162
0.45	259.0024887	216.2627747	177.1528975	141.6728572	109.8226537	81.60228704	57.01175721	36.05106421	18.72020805	5.019188726
0.5	261.5994502	218.1215186	178.3910296	142.4079831	110.172379	81.68421748	56.94349843	35.95022187	18.70438781	5.205996239
0.55	263.3953999	219.4391957	179.3192143	143.0354558	110.5879201	81.97660731	57.20151736	36.26265028	19.16000605	5.893584681
0.6	264.5217268	220.3135415	180.0050264	143.5961817	111.0870072	82.47750304	57.76766915	36.95750555	20.04701223	7.036189199
0.65	265.0799884	220.8190464	180.4987325	144.1190466	111.6799887	83.18155885	58.62375699	38.00658314	21.33003731	8.594119485
0.7	265.1503648	221.0137351	180.8385535	144.6248198	112.3725342	84.08169669	59.75230716	39.38436567	22.97787221	10.53282679
0.75	264.797301	220.943645	181.0540917	145.128641	113.1672931	85.17004777	61.13690514	41.06786517	24.96292787	12.82209324
0.8	264.0733925	220.6458818	181.1686365	145.6416567	114.0649423	86.43849328	62.76230972	43.03639158	27.26073887	15.43535158
0.85	263.0221364	220.1507622	181.200759	146.1721267	115.0648653	87.87897478	64.61445523	45.2713066	29.84952889	18.3491221
0.9	261.6799234	219.4833523	181.1654414	146.7261905	116.1655999	89.48366932	66.68039893	47.75578868	32.70983858	21.54254862

Appendix C: Input Deck for Simulation

```
*HEADING
 1ST PASS ROLL -  17.2mm REDUCTION, CPE4RT
2D ELS
**
*RESTART,WRITE,NUM=6
**              BILLET DEF.
**            --------------
*NODE
1,     0.10,    0.0
501,   0.90,    0.0
3007,  0.10,    0.1012
3507,  0.90,    0.1012
**
*NGEN,NSET=BOTNDS
1,501,1
*NGEN,NSET=TOPNDS
3007,3507,1
**
*NFILL,NSET=BILNDS
BOTNDS,TOPNDS,6,501
**
*NSET, NSET=LSIDNDS, GEN
1,3007,501
*NSET, NSET=RSIDNDS, GEN
501,3507,501
*****************************************
*****
**              ELEMENT TYPE & GEN
**            --------------------
*ELEMENT,TYPE=CPE4RT
1, 1,2,503,502
**
*ELGEN,ELSET=BILELS
1, 500,1,1, 6,501,500
*ELSET, ELSET=TOPELS, GEN
2501, 3000, 1
*ELSET, ELSET=MIDELS, GEN
250, 2750, 500
**
*ELSET, ELSET=LSIDELS, GEN
1,2501,500
*ELSET, ELSET=RSIDELS, GEN
500,3000,500
*****************************************
******
**              PHYSICAL CONSTANTS
**            --------------------
*PHYSICAL CONSTANTS, ABSOLUTE ZERO=-273.15,
STEFAN BOLTZMANN=5.669E-8
**
**              BILLET MAT PROPS
**            --------------------
*SOLID SECTION,ELSET=BILELS,
 MATERIAL=SS304,CONTROL=COMB
 1.33
*SECTION CONTROLS, HOURGLASS=COMBINED,
NAME=COMB
**
*MATERIAL, RTOL=1.0, NAME=SS304
*ELASTIC
1.7E11,  0.3,  600
1.6E11,  0.3,  650
1.5E11,  0.3,  700
1.4E11,  0.3,  750
1.3E11,  0.3,  800
1.2E11,  0.3,  850
1.1E11,  0.3,  900
1.0E11,  0.3,  950
9.0E10,  0.3,  1000
8.0E10,  0.3,  1050
7.0E10,  0.3,  1100
6.0E10,  0.3,  1150
5.0E10,  0.3,  1200
4.0E10,  0.3,  1250
3.0E10,  0.3,  1300
**********************
*PLASTIC, HARDENING=ISOTROPIC, RATE=0.0

Note: *plastic data is not included here
(very long). See data sheet for these
values
***************************
*DENSITY
7865
*INELASTIC HEAT FRACTION
.9
*SPECIFIC HEAT
460.46
*CONDUCTIVITY
28.9167,  900
30.0417,  950
31.1667,  1000
32.2917,  1050
33.4167,  1100
34.5417,  1150
35.6667,  1200
36.7917,  1250
37.9167,  1300
*EXPANSION
1.E-5
```

University of Cape Town

```
**
**********************************************
******
**                    ROLLER DEFINITION
**                   ---------------------
*NODE, NSET=ROLLND
10000,  1.1377, 0.567
**
*SURFACE, TYPE=SEGMENTS, NAME=ROLL
START,  1.1377,  0.084
CIRCL,  0.6547,  0.567,  1.1377, 0.567
CIRCL,  1.1377,  1.050,  1.1377, 0.567
CIRCL,  1.6207,  0.567,  1.1377, 0.567
CIRCL,  1.1377,  0.084,  1.1377, 0.567
**
*SURFACE, TYPE=ELEMENT, NAME=TOPSURF
TOPELS, S3
LSIDELS, S4
RSIDELS, S2
*RIGID BODY, REF NODE=10000,
ANALYTICAL SURFACE=ROLL,ISOTHERMAL=YES
**
**********************************************
********
**                          INITIAL
CONDITIONS
**                         ------------------
----
*INITIAL CONDITIONS, TYPE=TEMPERATURE
BILNDS,  1300.0
10000, 100.0
**
**********************************************
******
**              STEP 1: COOLING TIME
!!!!!!!!!!
**             ---------------------
*STEP
*DYNAMIC TEMPERATURE-DISPLACEMENT, EXPLICIT
,102.5
**
*FIXED MASS SCALING, FACTOR=1E8,
ELSET=BILELS
**
**              BOUNDARY  CONDITIONS
**             ------------------------
*BOUNDARY
BOTNDS,YSYMM
10000,1,2
10000,11,11,100.
**
*BOUNDARY, TYPE=VELOCITY
10000,6,6, 2.8985
**
**                HEAT TRANSFER
**              --------------------
*FILM
  TOPELS, F3, 30.0, 10.0
*RADIATE
  TOPELS, R3, 30.0, 0.8
**
**                  SURFACE CONTACT
**                ---------------------
*CONTACT PAIR,MECHANICAL
CONSTRAINT=PENALTY,
INTERACTION=ROLL_TO_STEEL
TOPSURF,ROLL
*SURFACE INTERACTION,NAME=ROLL_TO_STEEL
*CONTACT DAMPING, DEFINITION=CRITICAL
DAMPING FRACTION
0.09
**
*GAP CONDUCTANCE
25.0E3, 0.0
15.0E3, 0.001
5.0E3,  0.01
*GAP CONDUCTANCE, PRESSURE
30.0E3, 0.0
32.0E3, 1.0E6
34.0E3, 20.0E6
*GAP RADIATION
0.8,  0.8
0.95, 0.0
0.9,  0.0001
0.8,  0.001
0.2,  0.01
*GAP HEAT GENERATION
1.0,  0.5
**
*SURFACE BEHAVIOR, PRESSURE-
OVERCLOSURE=EXPONENTIAL
1.0E-3, 20.0E6, 200.0E9
*FRICTION,TAUMAX=60.E6
 .3,
**
**                  REQUIRED OUTPUT
**                ---------------------
*OUTPUT,FIELD,NUMBER
INTERVAL=8,TIMEMARKS=YES
*ELEMENT OUTPUT
PEEQ,MISES,PE,TEMP,
*NODE OUTPUT
U,
*OUTPUT,HISTORY,FREQUENCY=100
```

University of Cape Town

```
*ELEMENT OUTPUT, ELSET=MIDELS
SP,PEP,ERV,TEMP,PEEQ
*ENERGY OUTPUT
ALLIE,ALLKE
**
*END STEP
**                    LOOPING END   !!!!!!!!!
**                ----------------------
**********************************************
******
**                STEP 2: init cond 1st pass
!!!!!
**                ---------------------------
*STEP
*DYNAMIC TEMPERATURE-DISPLACEMENT, EXPLICIT
,0.0001
**
*FIXED MASS SCALING, FACTOR=100.,
ELSET=BILELS
**
**              BOUNDARY  CONDITIONS
**            ------------------------
*BOUNDARY, TYPE=VELOCITY
BILNDS, 1,1, 1.35
10000,6,6, 2.8985
**
*OUTPUT,FIELD,NUMBER
INTERVAL=3,TIMEMARKS=YES
*ELEMENT OUTPUT
PEEQ,MISES,PE,TEMP,
*NODE OUTPUT
U,
*OUTPUT,HISTORY,FREQUENCY=20
*NODE OUTPUT, NSET=ROLLND
  RF2,
*ELEMENT OUTPUT, ELSET=MIDELS
SP,PE,ERV,TEMP
*ENERGY OUTPUT
ALLIE,ALLKE
**
*END STEP
**                      LOOPING END
!!!!!!
**                   ----------------------
**********************************************
******
**                    STEP 3: 1ST PASS
!!!!!!!!
**                   ----------------------
*STEP
*DYNAMIC TEMPERATURE-DISPLACEMENT, EXPLICIT
,0.95
**
*FIXED MASS SCALING, FACTOR=100.,
ELSET=BILELS
**
**              BOUNDARY  CONDITIONS
**            ------------------------
*BOUNDARY, OP=NEW
BOTNDS,YSYMM
10000,1,2
10000,11,11, 100.0
**
*BOUNDARY, TYPE=VELOCITY, OP=NEW
10000,6,6, 2.8985
**
*OUTPUT,FIELD,NUMBER
INTERVAL=8,TIMEMARKS=YES
*ELEMENT OUTPUT
PEEQ,MISES,PE,TEMP,
*NODE OUTPUT
U,
*OUTPUT,HISTORY,FREQUENCY=200
*NODE OUTPUT, NSET=ROLLND
  RF2,
*ELEMENT OUTPUT, ELSET=MIDELS
SP,PEP,ERV,TEMP,PEEQ
*ENERGY OUTPUT
ALLIE,ALLKE
**
*END STEP
**                      LOOPING END  !!!!!!!
**********************************************
*
**                  STEP 4: DROP ROLLER
!!!!!!
**                 ----------------------
*STEP
*DYNAMIC TEMPERATURE-DISPLACEMENT, EXPLICIT
,19.4718
**
*FIXED MASS SCALING, FACTOR=1e6.,
ELSET=BILELS
**
**              BOUNDARY  CONDITIONS
**            ------------------------
*BOUNDARY, TYPE=VELOCITY
10000,2,2,-0.000884893
*BOUNDARY, TYPE=VELOCITY
BILNDS, 1,1, 0.
**
**
*OUTPUT,FIELD,NUMBER
INTERVAL=5,TIMEMARKS=YES
```

University of Cape Town

```
*ELEMENT OUTPUT
PEEQ,MISES,PE,TEMP,
*NODE OUTPUT
U,
*OUTPUT,HISTORY,FREQUENCY=20
*NODE OUTPUT, NSET=ROLLND
  RF2,
*ELEMENT OUTPUT, ELSET=MIDELS
SP,PE,ERV,TEMP
*ENERGY OUTPUT
ALLIE,ALLKE
**
*END STEP
**                        LOOPING END   !!!!!
**                    ---------------------
*****************************************
***
**              STEP 5: init cond 2nd pass
!!!!
**             ----------------------------
*STEP
*DYNAMIC TEMPERATURE-DISPLACEMENT, EXPLICIT
,0.0001
**
*FIXED MASS SCALING, FACTOR=100.,
ELSET=BILELS
**
**              BOUNDARY  CONDITIONS
**             ------------------------
*BOUNDARY
10000,1,2
**
*BOUNDARY, TYPE=VELOCITY
BILNDS, 1,1, -1.446489
**
*OUTPUT,FIELD,NUMBER
INTERVAL=3,TIMEMARKS=YES
*ELEMENT OUTPUT
PEEQ,MISES,PE,TEMP,
*NODE OUTPUT
U,
*OUTPUT,HISTORY,FREQUENCY=20
*NODE OUTPUT, NSET=ROLLND
  RF2,
*ELEMENT OUTPUT, ELSET=MIDELS
SP,PE,ERV,TEMP
*ENERGY OUTPUT
ALLIE,ALLKE
**
*END STEP
**                        LOOPING END
!!!!!!!!
**                    ---------------------
*****************************************
***
**                      STEP 6: 2nd PASS
!!!!!!!
**                    ---------------------
*STEP
*DYNAMIC TEMPERATURE-DISPLACEMENT, EXPLICIT
,1.05
**
*FIXED MASS SCALING, FACTOR=100.,
ELSET=BILELS
**
**              BOUNDARY  CONDITIONS
**             ------------------------
*BOUNDARY, OP=NEW
BOTNDS,YSYMM
10000,1,2
10000,11,11, 100.0
**
*BOUNDARY, TYPE=VELOCITY, OP=NEW
10000,6,6, -3.10559
**
**
*OUTPUT,FIELD,NUMBER
INTERVAL=8,TIMEMARKS=YES
*ELEMENT OUTPUT
PEEQ,MISES,PE,TEMP,
*NODE OUTPUT
U,
*OUTPUT,HISTORY,FREQUENCY=200
*NODE OUTPUT, NSET=ROLLND
  RF2,
*ELEMENT OUTPUT, ELSET=MIDELS
SP,PEP,ERV,TEMP,PEEQ
*ENERGY OUTPUT
ALLIE,ALLKE
**
*END STEP
**                        LOOPING END
!!!!!!!!
**                    ---------------------
*****************************************
***
**              STEP 7: DROP ROLLER 4 3rd
pass !!!
**             ----------------------------
--
*STEP
*DYNAMIC TEMPERATURE-DISPLACEMENT, EXPLICIT
,18.99127
**
```

University of Cape Town

```
*FIXED MASS SCALING, FACTOR=1e6.,
ELSET=BILELS
**
**              BOUNDARY  CONDITIONS
**             ------------------------
*BOUNDARY, TYPE=VELOCITY
10000,2,2,-0.000907282
*BOUNDARY, TYPE=VELOCITY
BILNDS, 1,1, 0.
**
**
*OUTPUT,FIELD,NUMBER
INTERVAL=5,TIMEMARKS=YES
*ELEMENT OUTPUT
PEEQ,MISES,PE,TEMP,
*NODE OUTPUT
U,
*OUTPUT,HISTORY,FREQUENCY=20
*NODE OUTPUT, NSET=ROLLND
  RF2,
*ELEMENT OUTPUT, ELSET=MIDELS
SP,PE,ERV,TEMP
*ENERGY OUTPUT
ALLIE,ALLKE
**
*END STEP
**                        LOOPING END   !!!!!
**                     ----------------------
*****************************************
***
**              STEP 8: init cond 3rd pass
!!!!
**             ----------------------------
*STEP
*DYNAMIC TEMPERATURE-DISPLACEMENT, EXPLICIT
,0.0001
**
*FIXED MASS SCALING, FACTOR=100.,
ELSET=BILELS
**
**              BOUNDARY  CONDITIONS
**             ------------------------
*BOUNDARY
10000,1,2
**
*BOUNDARY, TYPE=VELOCITY
BILNDS, 1,1, 1.928652
**
*OUTPUT,FIELD,NUMBER
INTERVAL=3,TIMEMARKS=YES
*ELEMENT OUTPUT
PEEQ,MISES,PE,TEMP,
*NODE OUTPUT
U,
*OUTPUT,HISTORY,FREQUENCY=20
*NODE OUTPUT, NSET=ROLLND
  RF2,
*ELEMENT OUTPUT, ELSET=MIDELS
SP,PE,ERV,TEMP
*ENERGY OUTPUT
ALLIE,ALLKE
**
*END STEP
**                        LOOPING END
!!!!!!!!
**                     ----------------------
*****************************************
***
**                      STEP 9: 3rd PASS
!!!!!!!
**                     ----------------------
*STEP
*DYNAMIC TEMPERATURE-DISPLACEMENT, EXPLICIT
,1.01
**
*FIXED MASS SCALING, FACTOR=100.,
ELSET=BILELS
**
**              BOUNDARY  CONDITIONS
**             ------------------------
*BOUNDARY, OP=NEW
BOTNDS,YSYMM
10000,1,2
10000,11,11, 100.0
**
*BOUNDARY, TYPE=VELOCITY, OP=NEW
10000,6,6, 4.1407867
**
**
*OUTPUT,FIELD,NUMBER
INTERVAL=8,TIMEMARKS=YES
*ELEMENT OUTPUT
PEEQ,MISES,PE,TEMP,
*NODE OUTPUT
U,
*OUTPUT,HISTORY,FREQUENCY=200
*NODE OUTPUT, NSET=ROLLND
  RF2,
*ELEMENT OUTPUT, ELSET=MIDELS
SP,PEP,ERV,TEMP,PEEQ
*ENERGY OUTPUT
ALLIE,ALLKE
**
*END STEP
```

University of Cape Town

```
**                        LOOPING END
!!!!!!!!
**                    ----------------------
*****************************************
***
**              STEP 10: DROP ROLLER 4 4th
pass !!!
**             ------------------------------
--
*STEP
*DYNAMIC TEMPERATURE-DISPLACEMENT, EXPLICIT
,21.5562
**
*FIXED MASS SCALING, FACTOR=1e6.,
ELSET=BILELS
**
**               BOUNDARY  CONDITIONS
**              ------------------------
*BOUNDARY, TYPE=VELOCITY
10000,2,2,-0.000781642
*BOUNDARY, TYPE=VELOCITY
BILNDS, 1,1, 0.
**
**
*OUTPUT,FIELD,NUMBER
INTERVAL=5,TIMEMARKS=YES
*ELEMENT OUTPUT
PEEQ,MISES,PE,TEMP,
*NODE OUTPUT
U,
*OUTPUT,HISTORY,FREQUENCY=20
*NODE OUTPUT, NSET=ROLLND
  RF2,
*ELEMENT OUTPUT, ELSET=MIDELS
SP,PE,ERV,TEMP
*ENERGY OUTPUT
ALLIE,ALLKE
**
*END STEP
**                        LOOPING END   !!!!!
**                    ----------------------
*****************************************
***
**               STEP 11: init cond 4th pass
!!!!
**             ----------------------------
*STEP
*DYNAMIC TEMPERATURE-DISPLACEMENT, EXPLICIT
,0.0001
**
*FIXED MASS SCALING, FACTOR=100.,
ELSET=BILELS
**
**               BOUNDARY  CONDITIONS
**              ------------------------
*BOUNDARY
10000,1,2
**
*BOUNDARY, TYPE=VELOCITY
BILNDS, 1,1, -2.41278
**
*OUTPUT,FIELD,NUMBER
INTERVAL=3,TIMEMARKS=YES
*ELEMENT OUTPUT
PEEQ,MISES,PE,TEMP,
*NODE OUTPUT
U,
*OUTPUT,HISTORY,FREQUENCY=20
*NODE OUTPUT, NSET=ROLLND
  RF2,
*ELEMENT OUTPUT, ELSET=MIDELS
SP,PE,ERV,TEMP
*ENERGY OUTPUT
ALLIE,ALLKE
**
*END STEP
**                        LOOPING END
!!!!!!!!
**                    ----------------------
*****************************************
***
**                      STEP 12: 4th PASS
!!!!!!!
**                    ----------------------
*STEP
*DYNAMIC TEMPERATURE-DISPLACEMENT, EXPLICIT
,1.15
**
*FIXED MASS SCALING, FACTOR=100.,
ELSET=BILELS
**
**               BOUNDARY  CONDITIONS
**              ------------------------
*BOUNDARY, OP=NEW
BOTNDS,YSYMM
10000,1,2
10000,11,11, 100.0
**
*BOUNDARY, TYPE=VELOCITY, OP=NEW
10000,6,6, -5.175983
**
**
*OUTPUT,FIELD,NUMBER
INTERVAL=8,TIMEMARKS=YES
```

University of Cape Town

```
*ELEMENT OUTPUT
PEEQ,MISES,PE,TEMP,
*NODE OUTPUT
U,
*OUTPUT,HISTORY,FREQUENCY=200
*NODE OUTPUT, NSET=ROLLND
  RF2,
*ELEMENT OUTPUT, ELSET=MIDELS
SP,PEP,ERV,TEMP,PEEQ
*ENERGY OUTPUT
ALLIE,ALLKE
**
*END STEP
**                          LOOPING END
!!!!!!!!
**                    ----------------------
*****************************************
***
**              STEP 13: DROP ROLLER 4 5th
pass !!!
**             ------------------------------
--
*STEP
*DYNAMIC TEMPERATURE-DISPLACEMENT, EXPLICIT
,23.0886
**
*FIXED MASS SCALING, FACTOR=1e6.,
ELSET=BILELS
**
**               BOUNDARY  CONDITIONS
**              ------------------------
*BOUNDARY, TYPE=VELOCITY
10000,2,2,-0.000474346
*BOUNDARY, TYPE=VELOCITY
BILNDS, 1,1, 0.
**
**
*OUTPUT,FIELD,NUMBER
INTERVAL=5,TIMEMARKS=YES
*ELEMENT OUTPUT
PEEQ,MISES,PE,TEMP,
*NODE OUTPUT
U,
*OUTPUT,HISTORY,FREQUENCY=20
*NODE OUTPUT, NSET=ROLLND
  RF2,
*ELEMENT OUTPUT, ELSET=MIDELS
SP,PE,ERV,TEMP
*ENERGY OUTPUT
ALLIE,ALLKE
**
*END STEP
**                          LOOPING END   !!!!!
**                    ----------------------
*****************************************
***
**              STEP 14: init cond 5th pass
!!!!
**             ------------------------------
*STEP
*DYNAMIC TEMPERATURE-DISPLACEMENT, EXPLICIT
,0.0001
**
*FIXED MASS SCALING, FACTOR=100.,
ELSET=BILELS
**
**               BOUNDARY  CONDITIONS
**              ------------------------
*BOUNDARY
10000,1,2
**
*BOUNDARY, TYPE=VELOCITY
BILNDS, 1,1, 2.93197
**
*OUTPUT,FIELD,NUMBER
INTERVAL=3,TIMEMARKS=YES
*ELEMENT OUTPUT
PEEQ,MISES,PE,TEMP,
*NODE OUTPUT
U,
*OUTPUT,HISTORY,FREQUENCY=20
*NODE OUTPUT, NSET=ROLLND
  RF2,
*ELEMENT OUTPUT, ELSET=MIDELS
SP,PE,ERV,TEMP
*ENERGY OUTPUT
ALLIE,ALLKE
**
*END STEP
**                          LOOPING END
!!!!!!!!
**                    ----------------------
*****************************************
***
**                      STEP 15: 5th PASS
!!!!!!!
**                    ----------------------
*STEP
*DYNAMIC TEMPERATURE-DISPLACEMENT, EXPLICIT
,1.35
**
*FIXED MASS SCALING, FACTOR=100.,
ELSET=BILELS
**
```

University of Cape Town

```
**              BOUNDARY  CONDITIONS
**             ------------------------
*BOUNDARY, OP=NEW
BOTNDS,YSYMM
10000,1,2
10000,11,11, 100.0
**
*BOUNDARY, TYPE=VELOCITY, OP=NEW
10000,6,6, 6.211180124
**
**
*OUTPUT,FIELD,NUMBER
INTERVAL=8,TIMEMARKS=YES
*ELEMENT OUTPUT
PEEQ,MISES,PE,TEMP,
*NODE OUTPUT
U,
*OUTPUT,HISTORY,FREQUENCY=200
*NODE OUTPUT, NSET=ROLLND
  RF2,
*ELEMENT OUTPUT, ELSET=MIDELS
SP,PEP,ERV,TEMP,PEEQ
*ENERGY OUTPUT
ALLIE,ALLKE
**
*END STEP
**                       LOOPING END
!!!!!!!!
**                    ----------------------
*****************************************
***
**             STEP 16: DROP ROLLER 4 6th
pass !!!
**            -------------------------------
--
*STEP
*DYNAMIC TEMPERATURE-DISPLACEMENT, EXPLICIT
,28.50508
**
*FIXED MASS SCALING, FACTOR=1e6.,
ELSET=BILELS
**
**              BOUNDARY  CONDITIONS
**             ------------------------
*BOUNDARY, TYPE=VELOCITY
10000,2,2,-0.000249738
*BOUNDARY, TYPE=VELOCITY
BILNDS, 1,1, 0.
**
**
*OUTPUT,FIELD,NUMBER
INTERVAL=5,TIMEMARKS=YES
*ELEMENT OUTPUT
PEEQ,MISES,PE,TEMP,
*NODE OUTPUT
U,
*OUTPUT,HISTORY,FREQUENCY=20
*NODE OUTPUT, NSET=ROLLND
  RF2,
*ELEMENT OUTPUT, ELSET=MIDELS
SP,PE,ERV,TEMP
*ENERGY OUTPUT
ALLIE,ALLKE
**
*END STEP
**                       LOOPING END   !!!!!
**                     ----------------------
*****************************************
***
**             STEP 17: init cond 6th pass
!!!!
**            -----------------------------
*STEP
*DYNAMIC TEMPERATURE-DISPLACEMENT, EXPLICIT
,0.0001
**
*FIXED MASS SCALING, FACTOR=100.,
ELSET=BILELS
**
**              BOUNDARY  CONDITIONS
**             ------------------------
*BOUNDARY
10000,1,2
**
*BOUNDARY, TYPE=VELOCITY
BILNDS, 1,1, -3.44841
**
*OUTPUT,FIELD,NUMBER
INTERVAL=3,TIMEMARKS=YES
*ELEMENT OUTPUT
PEEQ,MISES,PE,TEMP,
*NODE OUTPUT
U,
*OUTPUT,HISTORY,FREQUENCY=20
*NODE OUTPUT, NSET=ROLLND
  RF2,
*ELEMENT OUTPUT, ELSET=MIDELS
SP,PE,ERV,TEMP
*ENERGY OUTPUT
ALLIE,ALLKE
**
*END STEP
**                       LOOPING END
!!!!!!!!
```

University of Cape Town

```
**                    ----------------------
*****************************************
***
**                      STEP 18: 6th PASS
!!!!!!!
**                    ----------------------
*STEP
*DYNAMIC TEMPERATURE-DISPLACEMENT, EXPLICIT
,1.65
**
*FIXED MASS SCALING, FACTOR=100.,
ELSET=BILELS
**
**               BOUNDARY  CONDITIONS
**              ------------------------
*BOUNDARY, OP=NEW
BOTNDS,YSYMM
10000,1,2
10000,11,11, 100.0
**
*BOUNDARY, TYPE=VELOCITY, OP=NEW
10000,6,6, -7.2463768
**
**
*OUTPUT,FIELD,NUMBER
INTERVAL=8,TIMEMARKS=YES
*ELEMENT OUTPUT
PEEQ,MISES,PE,TEMP,
*NODE OUTPUT
U,
*OUTPUT,HISTORY,FREQUENCY=200
*NODE OUTPUT, NSET=ROLLND
  RF2,
*ELEMENT OUTPUT, ELSET=MIDELS
SP,PEP,ERV,TEMP,PEEQ
*ENERGY OUTPUT
ALLIE,ALLKE
**
*END STEP
**                        LOOPING END
!!!!!!!!
**                    ----------------------
*****************************************
***
**              STEP 19: DROP ROLLER 4 7th
pass !!!
**            ------------------------------
--
*STEP
*DYNAMIC TEMPERATURE-DISPLACEMENT, EXPLICIT
,28.49588
**
*FIXED MASS SCALING, FACTOR=1e6.,
ELSET=BILELS
**
**               BOUNDARY  CONDITIONS
**              ------------------------
*BOUNDARY, TYPE=VELOCITY
10000,2,2,-9.98675E-5
*BOUNDARY, TYPE=VELOCITY
BILNDS, 1,1, 0.
**
**
*OUTPUT,FIELD,NUMBER
INTERVAL=5,TIMEMARKS=YES
*ELEMENT OUTPUT
PEEQ,MISES,PE,TEMP,
*NODE OUTPUT
U,
*OUTPUT,HISTORY,FREQUENCY=20
*NODE OUTPUT, NSET=ROLLND
  RF2,
*ELEMENT OUTPUT, ELSET=MIDELS
SP,PE,ERV,TEMP
*ENERGY OUTPUT
ALLIE,ALLKE
**
*END STEP
**                          LOOPING END   !!!!!
**                       ----------------------
*****************************************
***
**               STEP 20: init cond 7th pass
!!!!
**              ------------------------------
*STEP
*DYNAMIC TEMPERATURE-DISPLACEMENT, EXPLICIT
,0.0001
**
*FIXED MASS SCALING, FACTOR=100.,
ELSET=BILELS
**
**               BOUNDARY  CONDITIONS
**              ------------------------
*BOUNDARY
10000,1,2
**
*BOUNDARY, TYPE=VELOCITY
BILNDS, 1,1, 4.9705
**
*OUTPUT,FIELD,NUMBER
INTERVAL=3,TIMEMARKS=YES
*ELEMENT OUTPUT
PEEQ,MISES,PE,TEMP,
```

University of Cape Town

```
*NODE OUTPUT
U,
*OUTPUT,HISTORY,FREQUENCY=20
*NODE OUTPUT, NSET=ROLLND
  RF2,
*ELEMENT OUTPUT, ELSET=MIDELS
SP,PE,ERV,TEMP
*ENERGY OUTPUT
ALLIE,ALLKE
**
*END STEP
**                          LOOPING END
!!!!!!!!
**                    ---------------------
*****************************************
***
**                       STEP 21: 7th PASS
!!!!!!!
**                    ---------------------
*STEP
*DYNAMIC TEMPERATURE-DISPLACEMENT, EXPLICIT
,1.25
**
*FIXED MASS SCALING, FACTOR=100.,
ELSET=BILELS
**
**               BOUNDARY  CONDITIONS
**              ------------------------
*BOUNDARY, OP=NEW
BOTNDS,YSYMM
10000,1,2
10000,11,11, 100.0
**
*BOUNDARY, TYPE=VELOCITY, OP=NEW
10000,6,6, 10.35196687
**
**
*OUTPUT,FIELD,NUMBER
INTERVAL=8,TIMEMARKS=YES
*ELEMENT OUTPUT
PEEQ,MISES,PE,TEMP,
*NODE OUTPUT
U,
*OUTPUT,HISTORY,FREQUENCY=200
*NODE OUTPUT, NSET=ROLLND
  RF2,
*ELEMENT OUTPUT, ELSET=MIDELS
SP,PEP,ERV,TEMP,PEEQ
*ENERGY OUTPUT
ALLIE,ALLKE
**
*END STEP
**                          LOOPING END
!!!!!!!!
**                    ---------------------
*****************************************
***
```

University of Cape Town

Appendix D: List of References

1 P. Hartley, C. E. N. Sturgess, C. Lui and G. W. Rowe – Experimental and Theoretical Studies of Workpiece Deformation, Stress and Strain during Flat Rolling.
International Material Reviews, 1989, Vol 34, No. 1, pp19-34.

2 Martha P. Guerrero, Carlos R. Flores, Antonio Pérez, Rafael Colás – Modelling Heat Transfer in Hot Rolling Work Rolls.
Journal of Materials Processing Technology, 94 (1999) pp. 52-59.

3 Mechanical Working of Metals – Theory and Practice.
By J.N. Harris - Hoon Higher Institute, Libya
Volume 36, International Series on Materials Science and Technology.
Pergamon Press Ltd 1983

4 T.L. Zaharoff, R.E. Johnson and M.E. Karabin – Spread in Sheet Rolling: A Comparison using Experiments, Analytical Solutions and Numerical Methods.
Alcoa Laboritories, Alcoa Center, USA and University of Illinois, Urbana, USA.
Int. J. Mech. Sci. Vol. 34, No5, pp. 435-443

5 Z.Y. Jiang and A.K. Tieu - 3-D Finite Element Modelling of Ribbed Strip Rolling
Department of Mechanical Engineering, Faculty of Engineering, University of Wollongong, Australia.
International Journal of Machine Tools and Manufacture 40 (2000) pp. 2139-2154.

6 S. Nishino, H. Narazaki, A. Kitamura, Y. Morimoto and K. Ohe – An Adaptive Approach to Improve the Accuracy of a Rolling Load Prediction Model for a Plate Rolling Process.
ISIJ International, Vol. 40 (2000), No.12, pp.1216-1222.

7 D. Raabe – Texture and Microstructure Evolution during Cold Rolling of a Strip Cast and of a Hot Rolled Stainless Steel.
Instutut für Metallkunde und Metallphysik, RWTH Aachen, Kopernikusstr, Aachen, Germany.
Acta mater. Vol. 45, No. 6 pp.1137-1151, 1997.

University of Cape Town

8 R.P Tavares and R.I.L. Guthrie – Computational Fluid Dynamics Applied to Twin Roll Casting.
McGill Materials Processing Centre, McGill University, Montreal Quebec, Canada.
Canadian Metallurgical Quarterly, Vol. 37, No. 3-4, 1998, pp. 241-250.

9 R.I.L. Guthrie and R.P Tavares – Mathematical and Physical Modelling of Steel Flow and Solidification in Twin-roll/Horizontal Belt Thin-strip Casting.
McGill Materials Processing Centre, McGill University, Montreal Quebec, Canada.
Applied Mathematical Modelling, 22 (1998), pp. 851-872.

10 J.J.M. Too - On Numerical Modelling of Hot Rolling of Metals.
Metals Technology Laboratories, CANMET, Energy, Mines and Resources,
Ottawa, Canada.
International Journal for Numerical Methods in Engineering. Vol. 30 (1990)

11 H. P. Cherukuri #, R. E. Johnson # and R. E. Smelser * – A Rate Dependent Model for Hot Rolling.
The University of North Carolina, Department of Mechanical Engineering and Engineering Sciences, U.S.A. and * University of Idaho, Mechanical Engineering Department, Moscow, Idaho, USA.
Int. J. Mech. Sci. Vol. 39, No. 6 pp.705-727, 1997.

12 C. Devadas, D. Baragar, G. Ruddle, I.V. Samarasekera and E.B.Hawbolt - The Thermal and Metallurgical State of Steel Strip during Hot Rolling: Part 2. Factors Influencing Rolling Loads.
Centre for Metallurgical Process Engineering, University of British Columbia.
Metallurgical Transactions A, Volume 22A, February 1991

13 C. Devadas, I.V. Samarasekera and E.B.Hawbolt - The Thermal and Metallurgical State of Steel Strip during Hot Rolling: Part 1. Characterisation of Heat Transfer.
Centre for Metallurgical Process Engineering, University of British Columbia.
Metallurgical Transactions A, Volume 22A, February 1991

University of Cape Town

14 Anne Bettina Richelsen – Viscoplastic Analysis of Plane Strain Rolling using Different Friction Models.
Department of solid mechanics, The Technical University of Denmark, Lyngby, Denmark.
Int. J. Mech. Sci. Vol33, No. 9 pp.761–774, 1991.

15 L.M. Galantucci and L. Tricarico - Thermo-mechanical Simulation of a Rolling Process with an FEM Approach.
Journal of Materials Processing Technology, 92-93 (1999) pp. 494-501.

16 Zone-Ching Lin and Chi-Chih Shen – A Coupled Finite Element Method for a Three Dimensional Analysis of the Flat Rolling of Aluminium with Different Reductions.
Department of Mechanical Engineering, National Taiwan University of Science and Technology, Taipei, Taiwan
Journal of Materials Processing Technology, 110 (2001) pp. 10-18.

17 Martín Torres and Rafael Colás – A Model For Heat Conduction through the Oxide Layer of Steel during Hot Rolling.
Journal of Materials Processing Technology, 105 (2000) pp. 258-263.

18 Ashok Kumar, I.V. Samarasekera and E.B.Hawbolt – Roll-bite deformation during the hot rolling of steel strip.
Centre for Metallurgical Process Engineering, University of British Columbia.
Journal of Materials Processing Technology, vol. 30 (1992)

19 R.I. Nepershin – Plane Strain Hot Rolling of Slab and Strip.
Department of Theoretical Mechanics, Moscow State Acadamy of Instrument Engineering and Informatics, Moscow, Russia.
Int. J. Mech. Sci., 41 (1999), pp.1401-1421.

20 Laila S. Bayoumi – Edge Stresses in Wide Strip Hot Rolling.
Department of Mechanical Design and Production, Faculty of Engineering, Cairo University, Egypt.
Int. J. Mech. Sci. Vol. 39, No. 4 pp.397-408, 1997.

University of Cape Town

21 T. Anglov and A. Nedev – Finite Element Analysis of a Hot Rolling Problem with Nonlinear Friction.
Institute of Mechanics, Bulgarian Academy of Sciences, Sofia, Bulgaria.
Advances in Engineering Software, Vol. 28 (1997), pp.555-561.

22 J.H. Beynon, P.R. Brown, S.I.Mizban, A.R.S. Ponter and C.M. Sellers – An Eulerian Finite Element Method for the Thermal and Visco Plastic Deformation of Metals in Industrial Hot Rolling.
Department of Engineering, University of Leicester, U.K. and Department of Metallurgy, University of Sheffield, U.K.
Presented at STRUCMAT '87, in Cachan, France. 8-11 Sept 1987

23 P.D. Hodgson, L.X. Kong, C.H.J. Davies – The prediction of the hot strength in steels with an integrated phenomenological and artificial neural network model. School of Engineering and Technology, Deakin University, Australia
Journal of Materials Processing Technology, vol. 87 (1999)

24 Miguel A. Cavaliere, Gonzalo Gomez, Javier I. Gazzarri, Teresa Perez and Eduardo N. Dvorkin – Experimental Procedure for Determining "True Stress – True Strain" Curves for Steels in the High Temperature Range and under Controlled Deformation Rate.
Centre for Industrial Research, FUDETEC, Buenos Aires, Argentina.

25 D.L. Baragar - The High Temperature and High Strain Rate Behaviour of a Plain Carbon and an HSLA Steel.
Physical Metallurgy Research Laboratories, Energy, Mines and Resources, Ottawa, Ontario, Canada.
Journal of Mechanical Working Technology, 14 (1987) pp.295 - 307

26 Dynamic Systems Inc. (D.S.I.) GLEEBLE SYSTEMS Application note 1 (APN001) – Axisymmetric Uniaxial Compression Testing Using ISO-T Anvils on Gleeble Systems.
http//www.gleeble.com
P.O. Box 1234, route 355, Poekstenkill, New York 12140 USA

University of Cape Town

27 Dynamic Systems Inc. (D.S.I.) GLEEBLE SYSTEMS Application note 2 (APN002) – Flow Stress Correction in Uniaxial Compression Testing.
http//www.gleeble.com
P.O. Box 1234, route 355, Poekstenkill, New York 12140 USA

28 A. Laasraoui and J.J. Jonas – Prediction of steel Flow Stresses at High Temperatures and Strain Rates.
Department of Metallurgical Engineering, McGill University, Montreal, Canada.
Metallurgical Transactions A, Vol. 22A, July 1991, pp. 1545-1558.

29 I. Schindler and E. Hadisik – A New Model Describing the Hot Stress-strain Curves of HSLA Steel at High Deformation.
Journal of Materials Processing Technology, 106 (2000) pp. 131-135.

30 H.J. McQueen and N.D. Ryan – Constitutive Analysis in Hot Working.
Mech. Eng., Concordia University, Montreal, Canada H3G 1M8

31 H.J. McQueen*, E. Evangelista# and N.D. Ryan* – Hot and Cold Working of Austenitic Stainless Steels.
*Mech. Eng., Concordia University, Montreal, Canada H3G 1M8
#Mechanics, Univ. Ancona, 60131 Ancona, Italy

32 Jong-Jin Park – Prediction of the Flow Stress and Grain Size of Steel during Thick Plate Rolling.
Department of Mechanical and System Design Engineering, Hong-Ik University, Seoul, South Korea.
Journal of Materials Processing Technology, 113 (2001) pp. 581-586.

33 Sung-Il Kim and Yeon-Chul Yoo – Dynamic Recrystallization Behaviour of AISI 304 Stainless Steel.
Department of Material Science and Engineering, Inha University, Inchon, South Korea.
Materials Science and Engineering, A311 (2001) pp. 108-113.

University of Cape Town

34 P. Korczak and H. Dyja – Investigation of Microstructure Prediction during Experimental Thermo-mechanical Plate Rolling.
Faculty of Metallurgy and Material Engineering, Czestochowa Technical University, Czestochowa, Poland.
Journal of Materials Processing Technology, 109 (2001) pp. 112-119.

35 M. Fishkis and J.C. Lin – Formation and Evolution of a Subsurface Layer in a Metalworking Process.
Aluminium Company of America, Alcoa Technical Center, Philadelphia, U.S.A.
Wear. No. 206 (1997) pp. 156-170.

36 F. Czerwinski, A. Brodtka, J.Y. Cho, A. Zielinska-Lipiec, J.H. Sunwoo, J.A. Szpunar – A Role of Ferrite in Edge Crack Formation During Hot Rolling of Austenitic Stainless Steels
Department of Metallurgical Engineering, McGill University, Montreal Quebec, Canada.
Scripta Materialia, Vol. 37, No. 8 (1997), pp. 1231-1235.

37 H. Dyja and P. Korczak – The Thermal-mechanical and Microstructural Model for the FEM Simulation of Hot Plate Rolling.
Czestochowa Technical University, Armii Krajowej 19, 42200 Czestochowa, Poland.
Journal of Materials Processing Technology, 92-93 (1999) pp. 463-467.

38 B.K.Chen, P.K.Thomson, S.K.Choi – Temperature distribution in the roll-gap during hot flat rolling.
Journal of Materials Processing Technology, vol. 30 (1992)

39 M. Pietrzyk and J.G. Lenard – A Study of Boundary Conditions in Hot/Cold Flat Rolling.
Department of Mechanical Engineering, University of Waterloo, Canada.

40 Amnon Shirizly, John G. Lenard – The Effect of Scaling and Emulsion Delivery on Heat Transfer during the Hot Rolling of Steel Strips.
Department of Mechanical Engineering, University of Waterloo, Canada.
Journal of Materials Processing Technology, 101 (2000) pp. 250-259.

University of Cape Town

41 José Rivallin and Stéphane Viannay – General Principles of Controlled Water Cooling for Metallurgical on-line Hot Rolling Processes: Forced Flow and Sprayed Surfaces with Film Boiling Regime and Rewetting Phenomena.
Bertin Technologies Company, France.
Int. J. Therm. Sci. (2001) 40, pp. 263-272

42 J. Horski, M. Raudensky, P. Kotrbá_ek – Experimental Study of Long Product Cooling in Hot Rolling.
Technical University of Brno, Technická 2, Brno, Czech Republic.
Journal of Materials Processing Technology, 80-81 (1998) pp. 337-340.

43 Amnon Shirizly, John G. Lenard – The Effect of Lubrication on Mill Loads during Hot Rolling of Low Carbon Steel Strips.
Department of Mechanical Engineering, University of Waterloo, Canada.
Journal of Materials Processing Technology, 97 (2000) pp. 61-68.

44 Per A. Munther and John G. Lenard – The Effect of Scaling on Interfacial Friction in Hot Rolling of Steels.
Department of Mechanical Engineering, University of Waterloo, Canada.
Journal of Materials Processing Technology, 88 (1999) pp. 105-113.

45 Jonas Lagergren – Friction Evaluation in Hot Strip Rolling by Direct Measurement in the Roll Gap of a Model Duo Mill.
Department of Metal Forming, The Royal Institute of Technology, Stockholm, Sweden.
Journal of Materials Processing Technology, 70 (1997) pp. 207-214.

46 M.J. Grimble and G. Hearns – LQG Controllers for State Space Systems with Pure Transport Delays: Application to Hot Strip Mills.
Industrial Control Centre, University of Strathclyde, Glasgow, U.K.
Automatica. Vol. 34, No. 10, (1998) pp. 1169-1184.

47 M. Okada, K. Murayama, A. Urano, Y. Iwasaki, A. Kawano, H. Shiomi – Optimal Control System for Hot Strip Finishing Mill.
Mizushima Works, Kawasaki Steel Corperation, Mizushima Kurashiki 712, Japan
Control Engineering Practice Vol. 6, (1998) pp. 1029-1034.

University of Cape Town

48 Heat Transfer, by J.P. Holman
8th Edition, Copyright 1997 McGraw Hill Publishing.

University of Cape Town